



HAL
open science

Radio-oxidation mechanisms of polyethylene and the role of antioxidants: atomic scale simulations

Yunho Ahn

► **To cite this version:**

Yunho Ahn. Radio-oxidation mechanisms of polyethylene and the role of antioxidants: atomic scale simulations. Materials Science [cond-mat.mtrl-sci]. Université Paris-Saclay, 2022. English. NNT: 2022UPASP167 . tel-03962227

HAL Id: tel-03962227

<https://theses.hal.science/tel-03962227v1>

Submitted on 30 Jan 2023

HAL is a multi-disciplinary open access archive for the deposit and dissemination of scientific research documents, whether they are published or not. The documents may come from teaching and research institutions in France or abroad, or from public or private research centers.

L'archive ouverte pluridisciplinaire **HAL**, est destinée au dépôt et à la diffusion de documents scientifiques de niveau recherche, publiés ou non, émanant des établissements d'enseignement et de recherche français ou étrangers, des laboratoires publics ou privés.

Radio-oxidation mechanisms of
polyethylene and the role of antioxidants:
atomic scale simulations
*Mécanismes de radio-oxydation du polyéthylène et rôle des
antioxydants : simulations à l'échelle atomique*

Thèse de doctorat de l'université Paris-Saclay

École doctorale n° 564 Physique en Île-de-France (EDPIF)
Spécialité de doctorat : Physique
Graduate School : Physique, Référent : Faculté des Sciences d'Orsay

Thèse préparée dans le **Service de Recherches de Métallurgie Physique**
DES/ISAS/DMN (Université Paris-Saclay, CEA),
sous la direction de **Guido ROMA**, Directeur de Recherche au CEA-Saclay,
et la co-direction de **Xavier COLIN**, Professeur à l'ENSAM Paris.

Thèse soutenue à Paris-Saclay, le 14 décembre 2022, par

Yunho AHN

Composition du jury

Membres du jury avec voix délibérative

Benoît GERVAIS

Directeur de recherche CEA, CIMAP/CEA-Ganil

Marialore SULPIZI

Professeure, Université de la Ruhr, Bochum, Allemagne

Véronique LACHET

Chercheur, IFP Énergies Nouvelles

Pascal WONG-WAH-CHUNG

Professeur, Université de Aix-Marseille

Président & Rapporteur

Rapporteur & Examinatrice

Examinatrice

Examineur

Titre: Mécanismes de radio-oxydation du polyéthylène et rôle des antioxydants : simulations à l'échelle atomique

Mots clés: polymères, radio-oxydation, théorie de la fonctionnelle de la densité, ab initio, cinétique, polyéthylène

Résumé:

Le polyéthylène (PE) est l'un des polymères les plus abondamment fabriqués pour diverses applications. Parmi ces applications, le PE a été largement utilisé comme isolant de câbles électriques dans les centrales nucléaires (NPP). Cependant, étant donné que les isolants en polymères constituent le maillon le plus vulnérables de la globalité du câble sous des conditions de haute température ou d'irradiation (par exemple, les rayons γ), la compréhension des mécanismes cinétiques de dégradation est essentielle pour assurer une durée de vie la plus longue possible de ce composant en conditions opérationnelles. L'étude menée dans

cette thèse, basée sur la théorie fonctionnelle de la densité (DFT), vise à élucider les mécanismes de dégradation du polyéthylène résultant principalement de l'oxydation sous irradiation, ou radio-oxydation, qui joue un rôle crucial dans le déclenchement du vieillissement des câbles. Par ailleurs, les antioxydants sont couramment utilisés comme additifs afin de ralentir le processus de vieillissement. Le rôle des antioxydants et leur mécanisme d'action sont soigneusement étudiés. Les résultats attendus pourraient trouver une application dans divers domaines, de l'isolation des câbles électriques dans les centrales nucléaires aux plastiques utilisés dans la vie quotidienne.

Title: Radio-oxidation mechanisms of polyethylene and the role of antioxidants: atomic scale simulations

Keywords: polymers, radio-oxidation, density functional theory, ab initio, kinetics, polyethylene

Abstract:

Polyethylene (PE) is one of the most abundantly manufactured polymers for various applications. Among the various them, PE has been widely used as insulation of electrical cables in nuclear power plants (NPPs). However, because cable insulators consisting of polymers are most vulnerable in cable structures under high temperature or irradiation conditions (e.g., γ -rays), understanding the kinetic mechanisms involved in the polymer degradation is essential to ensure their long operation lifetime.

This thesis study, based on density functional theory (DFT), aims to elucidate the degradation mechanisms of polyethylene mainly resulting from oxidation under irradiation, the so-called radio-oxidation process, that crucially triggers the aging of cables. Besides, antioxidants are commonly used as additives in order to slow down the aging process. The role of antioxidants and their action mechanism are carefully studied. The insight that is expected might find application in various fields, from electrical cable insulation in nuclear power stations to plastics used in everyday life.

Acknowledgements

Studying abroad has been quite challenging as a foreigner without experience living outside Korea. Everything should be set up from scratch to stay in France: learning languages (English & French), understanding cultures, administrative processes, finding a house, making friends, etc. However, something unconscious in my mind brought me to France without hesitation. Fortunately, I could start with a master degree due to the dual master program between the department of information display at Kyung Hee University and the LPICM (Laboratoire de Physique des Interfaces et des Couches Minces) at École Polytechnique. I firstly want to thank two professors, Yvan BONNASSIEUX (Polytechnique) and Jin JANG (Kyung Hee University), who organized this program and gave me a special opportunity to study in France. This program consists of one year in Korea and one year and a half in France. In Korea, I was a member of the OEML team (Organic Electronic Materials Laboratory) under Prof. Min Chul SUH. I could study the photochemistry of organic materials and perovskite light-emitting diodes. After coming to France, many Korean friends (Thomas/Sang Hyuk, Hee Ryung, Yongjeong, Seonyong, Hyeonseok, Junha, Minjin) have helped me to adapt.

During the first internship, I could change my research field from experiments to simulations by studying organic field effect transistors (OFET) in the LPICM team. Thank you (Yvan, Gilles HOROWITZ, Sungyeop JUNG, Yongjeong) for supervising and teaching me. During this period, I was attracted to the simulation field, which can predict the device properties with numerical or analytical methods. Furthermore, while I took the lecture on "Materials Design" (Silke BIERMANN, Thierry GACOIN, Jong Wook KIM), I could study the characterization of materials and ab-initio approach and further felt attracted to the simulations. Finally, I have decided to be a researcher in these fields.

For the second internship, I contacted Guido ROMA, my thesis director, at CEA (Commissariat à l'Énergie Atomique et aux Énergies Alternatives). I am deeply grateful for his understanding, guidance, and a lot of patience. It was my first time diving into the ab initio calculations, so there would be many stupid questions, but he never got bothered with them and had the enthusiasm to supervise me. Besides, he allowed me to keep studying as a PhD student, which led to me becoming a researcher and growing scientific insight. I also thank Xavier COLIN, co-director of my thesis, for giving me proper guidance when I was stuck in finding chemical reactions and developing studies. During my thesis, I learned many things from my co-directors: how to approach, solve, and analyze the subjects, which led us to have significant scientific results in two publications, as well as the attitude as a researcher. I also thank other members (Muriel FERRY, Morgane BROUDIN, Adeline PAUL) of «TeaM Cables», European project: European tools and methodologies for an efficient aging management of nuclear power plant cables. Thank you all jury members (Benôit GERVAIS, Marialore SULPIZI, Véronique LACHET, Pascal WONG-WAH-CHUNG, Xavier COLIN, Guido ROMA) for coming to my defense and accepting my studies.

I would also like to thank all members of the SRMP team (Service de Recherches de Métallurgie Physique). Thank you, Jean-Luc BÉCHADE, the head of the team, for his warm welcome and kindness and for taking care of the students. His leadership was incredible, even during the tough period of COVID-19. Thank the other students in the lab (Ivan, Océane, Savneet, Liangzhao, Thomas, Clovis, Martin, Orane, Quentin, Pamela, Xixi, Daphné, Charbel, Kajal, Émile). They helped me a lot to adapt and came to me to talk. I also thank my other Korean friends (Junbum, Jinhyeok, Jihye, Yeonsoo, Myeongseop, Jisoo), who also came to France as part of the dual master program and are now PhD students. We have shared

our difficulties, valuable time, dreams, and life. I hope that they will finish their journey well and safely in Europe.

I hope I did not miss anyone and thank all of you again!

Contents

Résumé étendu en français	v
Bibliography	ix
1 Introduction	1
1.1 General description of polyethylene	1
1.2 Electrical cables in nuclear power plants	5
1.3 From the basic auto-oxidation scheme by Bolland-Gee	9
1.4 Open issues	10
1.4.1 Formation of Hydroperoxides and their role	10
1.4.2 Chain scission and crosslinking	13
1.5 Impact of humidity	14
1.6 Survey of previous ab initio calculations related to the problem	15
1.7 Role of antioxidants	18
1.8 Motivations and approach	20
Bibliography	24
2 Methodology	37
2.1 Introduction	37
2.2 Background of DFT	37
2.2.1 Several functionals	38
2.2.2 Self-consistent calculations	39
2.2.3 Equilibrium structures	40
2.2.4 Energy cut-off	41
2.2.5 k-point convergence	43
2.3 Nudged Elastic Band (NEB) Calculation	45
2.4 Formation energy	46
2.5 Calculation details	47
2.6 Ab initio molecular dynamics (AIMD)	48
Bibliography	50
3 Oxidation of PE: from the initiation step to ketones	53
3.1 Initiation step	53
3.2 Formation of hydroperoxides	55
3.2.1 Peroxy radical	55
3.2.2 Conventional pathways	55
3.2.3 Alternative pathways	59
3.3 Formation of ketones	62
3.4 Summary and Conclusions	69
Bibliography	72

4	The role of alkoxy radicals	77
4.1	Formation of alkoxy radicals	79
4.1.1	From hydroperoxides	79
4.1.2	From peroxy radicals	81
4.2	Crosslinking reactions	83
4.3	Chain scission reactions	87
4.4	Termination through alcohol and ketone groups	90
4.5	Summary and Conclusions	92
	Bibliography	93
5	Antioxidants	97
	Bibliography	104
6	Conclusion & Perspectives	107
	Appendices	110
A	Modelling polyethylene structure	113
B	Diffusion in a polymer matrix: a few case studies	117
B.1	Oxygen kinetics in a PE matrix	117
B.2	Diffusion of radical species	120
C	A list of reactions	123
D	Molecular dynamics: a few case studies	135
D.1	Oxygen in crystalline PE	136
D.2	Hydroperoxide decomposition by a hydroxyl radical	138
D.3	Formation of alkoxy radicals	140
D.4	From alkoxy radicals: crosslinking from different starting configurations	141
	Bibliography	145

Résumé étendu en français

Le polyéthylène est un des polymères dont la production est plus importante, pour des applications variées. Selon le type d'application, son usage et les procédures de production sont différentes. Par exemple, quand il est utilisé pour des objets en plastique d'usage courant, il doit pouvoir être facilement broyé pour être recyclé, ou, selon le type de polymère, être biodégradable. Pour cette raison, en phase de production, on rajoute certains groupes polaires (par exemple des cétones) aux chaînes du polymère pour réduire sa persistance dans l'environnement [1]. Au contraire, pour des applications comme les isolants des câbles électriques utilisés dans les bâtiments réacteurs des centrales nucléaires, le but est celui d'assurer la plus longue durée de vie possible dans des conditions plus sévères de température et irradiation (typiquement des γ en fonctionnement nominal) [2, 3, 4]. Dans ces conditions, pour assurer le maintien des propriétés fonctionnelles d'isolation, ainsi que pour améliorer ses propriétés mécaniques, le polymère subit un processus de réticulation (XLPE) et on y ajoute des antioxydants, des charges et parfois des nanocomposites tels Al_2O_3 , TiO_2 ou SiO_2 pour augmenter la stabilité en température [5, 6, 7, 8, 9]. Il est donc essentiel, indépendamment de l'application visée, de comprendre les mécanismes cinétiques qui pilotent la dégradation du matériau en différentes conditions pour en connaître les limites d'utilisation et les exploiter jusqu'à la fin de leur durée de vie. Dans cette thèse nous étudions les mécanismes à l'échelle atomiques qui contribuent à la dégradation du polyéthylène en conditions de radio-oxydation. Ce sont ces mécanismes qui pilotent le vieillissement des câbles et, finalement, en déterminent la durée de vie en conditions opérationnelles. L'oxydation du polyéthylène finit par causer des fractures suite à la chemicristallisation et la formation de différents types de défauts carbonyles peut mener à des échauffements locaux et modifier les propriétés diélectriques jusqu'au claquage diélectrique [5, 10]. Pour éviter ces évolutions néfastes, des antioxydants phénoliques sont incorporés dans le polymère [11, 12, 13]. Au moins deux mécanismes d'action des antioxydants ont été évoqués en littérature: le premier fait référence aux transferts d'énergies, selon lequel l'absorption préférentielle des photons par les noyaux aromatiques, agissant comme puits d'énergie, limiterait la formation de radicaux alkyl qui sont à l'origine de la chaîne de réactions oxydatives. En d'autres termes, un transfert d'énergie ayant lieu entre parties aromatique et aliphatique permettrait de distribuer de façon plus uniforme l'énergie des photons absorbés par la fonction phénolique lors de la désexcitation non-radiative et donc d'éviter la rupture de liaisons C-H. Le deuxième mécanisme repose sur la capacité des antioxydants, via leur fonction phénolique, de participer à une réaction de transfert d'hydrogène qui permet d'éliminer certains radicaux et donc de bloquer la propagation de la réaction et/ou l'étape de ramification de chaîne.

Les outils utilisés pour cette étude sont essentiellement ceux de la théorie de la fonctionnelle de la densité (DFT), qui a été utilisée en particulier en combinaison avec la méthode NEB (ou méthode de la bande élastique), qui permet d'explorer des paysages énergétiques complexes; nous l'utilisons pour prédire les énergies d'activations des réactions chimiques ayant lieu dans le polymère. Dans certains cas nous avons utilisé d'autres méthodes, comme des séries de relaxations avec contraintes ou de la dynamique moléculaire ab initio de type Car-Parrinello. Les détails des méthodes et approximations utilisées (notamment la fonctionnelle d'échange et corrélation choisie, qui assure une description fiable des interactions de van der Waals) et des études de convergence sont exposés dans le chapitre 2. Ce chapitre introduit également les modèles atomiques utilisés, qui vont de simples molécules d'alcanes en phase gaz à un modèle plus

développé d'interface entre lamelles cristallines et zone amorphe. Cette dernière structure permet de simuler des réactions chimiques ayant lieu sur la surface des lamelles cristallines, donc, si l'on veut, à l'interface entre et les zones cristalline et amorphe.

Nous avons considéré la globalité du chemin cinétique d'oxydation à partir de l'étape d'initiation à celle de terminaison avec les méthodes mentionnées, en calculant les barrières d'énergie et les enthalpies de chacune des réactions considérées.

Notre étude se focalise sur les réactions qui impliquent deux principaux produits d'oxydation, intermédiaires et finaux : les cétones et les radicaux alcoyle. La méthode NEB permet de calculer l'énergie totale et l'enthalpie de réaction, y compris le point de selle et les images le long de la coordonnée de réaction, de sorte que les chemins de réaction favorables, ceux qui présentent une énergie d'activation suffisamment basse, peuvent effectivement être sélectionnées pour élucider le mécanisme de dégradation en support à une étude cinétique.

Pour certaines réactions nous avons aussi effectué des simulations de dynamique moléculaire Car-Parrinello (CPMD) pour vérifier que les réactions en question ont bien lieu à la température ambiante dans un temps très court, accessible à ce type de simulations, ce qui pourrait être empêché par une contribution entropique importante, négligée dans les calculs NEB.

Un autre point à souligner, dans ce travail de thèse, est la prise en compte de la microstructure du PE, ce qui n'est pas le cas dans la plupart des études théoriques. En effet, la plupart des calculs DFT ou de chimie quantique qui ont abordé la question des constantes de réaction sont des calculs sur de petites molécules, et où les réactions sont supposées se produire en phase gazeuse. Il convient de souligner que le PE est un polymère semi-cristallin comprenant des régions cristallines, amorphes et d'interface, et que ces environnements locaux affectent potentiellement les différentes vitesses de réaction. Les calculs présentés ici considèrent ces différents environnements, tels que cristallins ou la surface des lamelles, où la zone amorphe séparant les lamelles cristallines, ce qui nous permet une analyse plus détaillée des paramètres pouvant influencer la cinétique d'oxydation.

Sur la base de ces stratégies, les chemins de réaction conventionnels qui mènent à la formation de cétones, qui constituent, selon les études expérimentales, la majorité des produits d'oxydation, sont d'abord considérés pour revisiter les réactions à l'échelle atomique et vérifier l'explication générale de la dégradation oxydative. C'est le but du chapitre 3 de cette thèse. Les chemins de réaction classiques correspondent au schéma d'auto-oxydation de base (BAS), développé par Bolland, Gee et leurs collègues. D'après les profils énergétiques calculés, le goulot d'étranglement critique est la formation et la décomposition des hydroperoxydes. Dans ce schéma, la formation des hydroperoxydes est expliquée par un radical peroxyde qui arrache un atome d'hydrogène à une chaîne de polymère voisine. Cependant, l'énergie d'activation pour cette réaction est d'environ 0,7 eV, et la réaction est clairement endothermique. Par conséquent, d'autres voies alternatives sont envisagées :

1. une double liaison adjacente ($-C=C-$), qui présente une liaison π , peut stabiliser un électron non apparié sur le produit final en formant une structure de résonance,
2. la réaction n'est pas une réaction d'abstraction d'hydrogène sur une chaîne voisine, mais sur un radical hydroperoxyde ($^{\circ}OOH$),
3. les réactions oxydatives contournent l'étape de formation d'hydroperoxydes.

La première voie permet de diminuer légèrement l'énergie d'activation, mais elle reste relativement élevée (0,48 eV à la surface des lamelles). Concernant la deuxième option proposée, un radical hydroperoxyde peut, en effet, transférer spontanément un atome d'hydrogène, mais des études complémentaires pour élucider l'origine des radicaux hydroperoxydes sont nécessaires. La dernière possibilité envisage des réactions qui se révèlent, également des, spontanées. Ces processus seront discutés plus tard. Néanmoins, même si nous supposons que les hydroperoxydes sont produits par les chemins de réaction défavorables que nous avons montrés, les réactions qui suivent dans les schémas cinétiques habituels, qui les réactions de décomposition des hydroperoxydes, ne sont pas non plus plausibles. Par exemple, sans espèces radicalaires voisines des hydroperoxydes, la barrière minimale pour la décomposition est de 0,91 eV, et avec des radicaux alkyles, la barrière diminue à 0,46 eV à la surface des lamelles, ce qui implique que la présence d'espèces radicalaires affecte l'énergie d'activation, mais que la barrière reste relativement élevée. Dans le cas des radicaux hydroxyle, ils extraient spontanément un atome d'hydrogène au niveau du site primaire ou tertiaire des hydroperoxydes. En particulier, lorsqu'un atome d'hydrogène est retiré au niveau du site tertiaire, la liaison O-O du radical α -alkyl-hydroperoxyde est spontanément décomposée en formant une cétone et un radical hydroxyle, ce qui déclenche d'autres réactions. Par conséquent, les radicaux hydroxyle décomposent efficacement les hydroperoxydes sans barrières et provoquent une grave dégradation du PE. Cependant, comme pour les radicaux hydroperoxyde, les mécanismes expliquant la formation d'un radical hydroxyle dans les conditions habituelles de radio-oxydation ne sont pas clairement identifiés jusqu'à présent et doivent donc être examinés dans une étude future.

Comme la décomposition des hydroperoxydes n'est pas un processus très probable à l'ambient, le dernier chemin réactionnel, celui qui contourne l'étape des hydroperoxydes, pourrait être envisagé. C'est ce chemin qui est analysé et discuté au chapitre 4, qui se focalise sur les réactions qui impliquent la présence de radicaux alcoxy. Une réaction possible, parmi les nombreuses testées pour expliquer la présence des alcoxy, est la décomposition bimoléculaire de deux radicaux peroxy, qui conduit à deux radicaux alcoxy et une molécule d'oxygène. Comme cette réaction présente un profil énergétique sans barrière et est exothermique, elle est beaucoup plus favorable que l'absorption de H par les radicaux peroxy. Cependant, les réactions qui s'en suivent sont complexes car le chemin réactionnel impliquant des radicaux alcoxy peut également se ramifier en de nombreuses réactions telles que la réticulation, la scission de chaîne et la production d'alcools et de défauts carbonyles. Ces réactions entrent en compétition à des positions spécifiques sur la surface de la lamelle en fonction de l'encombrement stérique. La concentration des espèces radicalaires affecte également le poids relatif de ces réactions car, si la scission de chaîne peut être déclenchée par un seul radical alcoxy, les autres réactions nécessitent la présence de deux espèces radicalaires proches. En outre, quatre configurations de départ différentes de deux radicaux alcoxy dans le même environnement local (c'est-à-dire sur la surface de la lamelle) donnent lieu, selon nos calculs, à divers produits d'oxydation, avec des énergies d'activation différentes.

Deux radicaux peroxy forment spontanément, pour toutes les dispositions proches que nous avons testées, des radicaux alcoxy. Ces réactions ont également été examinées par CPMD à température ambiante. Les résultats montrent que deux radicaux peroxy produisent deux radicaux alcoxy, comme prévu par les calculs NEB. Cependant, à partir des radicaux alcoxy issus de ces réactions, on peut obtenir des produits finaux différents, que nous n'avons pas tous envisagés lors de nos calculs NEB. Les réactions oxydatives pourraient donc se révéler encore plus complexes.

D'autre part, ces chemins cinétiques contrôlant la dégradation du polymère impliquent que les espèces

quantitative du schéma réactionnel menant à l'oxydation du polyéthylène. Les nombreuses barrières d'énergie et enthalpies de réaction calculées constituent une base de données qui peut être utilisée pour nourrir les simulations de cinétique chimique homogène ou les simulation de Monte Carlo cinétique pour décrire le vieillissement du polyéthylène.

De façon plus qualitative, les résultats principaux de ce travail mènent à une vision globale du processus de radio-oxydation du polyéthylène qui peut être résumé dans la figure 1. Dans cette représentation en blocs de principales espèces entrant en jeu, les flèches en couleur distinguent les réactions qui peuvent avoir lieu à température ambiante de celles qui sont pratiquement impossibles ou plutôt rares. Même si cette classification est quelque peu arbitraire, du fait du choix des limites des barrières d'énergie définissant les trois plages considérées, elle permet d'un coup d'œil de comprendre les chemins préférentiels.

La stratégie utilisée dans ce travail de doctorat peut également être appliquée à d'autres types de polymères, tels que le polypropylène, par exemple, ou l'oxyde d'éthylène. L'étude peut être approfondie en considérant la dégradation photochimique, en considérant les réactions de Norrish (de type I et II), dans lesquelles des états excités sont impliqués.

À cet égard, l'étude des propriétés optiques est importante, puisque les excitations électroniques sur les produits d'oxydation peuvent donner lieu à photoluminescence mais aussi à une désexcitation non-radiative qui peut potentiellement mener à des scissions de chaîne. En outre, cela peut également s'appliquer aux antioxydants, où la question du transfert d'énergie entre partie aromatique et chaînes aliphatiques est liée au canaux de désexcitation des excitons localisés non seulement sur l'antioxydant vierge, mais aussi sur ses produits de dégradation, comme les quinones méthydes. L'absorption optique et ses modes de désexcitation radiative et non-radiative pourraient donc faire l'objet d'études futures.

Les appendices de ce manuscrit contiennent des informations diverses, importantes, mais parfois encore partielles ou qui auraient risqué, si insérées dans les chapitres du manuscrit, de gêner le déroulement des arguments.

L'appendice A) décrit en détail les modèles atomiques utilisés et dans quelle mesure ils sont capables de décrire le matériau réel. La suivante (appendice B.1) discute des résultats obtenus concernant la diffusion de l'oxygène moléculaire dans le polyéthylène; mais aussi la diffusion des radicaux alkyle et des vinylènes (doubles liaisons). Une liste complète de toutes les réactions étudiées au cours de la thèse a été compilée en appendice C. Enfin, la dernière appendice (D) traite de quelques réactions (ou processus de diffusion) étudiées à l'aide de simulations de dynamique moléculaire *ab initio* (Car-Parrinello); cela inclut la diffusion de la molécule O₂ dans le cristal, la formation d'hydroperoxydes à l'aide de radicaux hydroxyle et des réactions variées impliquant des radicaux alcoxyles. Les résultats suggèrent que la dynamique moléculaire *ab initio* est un outil précieux pour mieux comprendre la variété de produits finaux pour des réactions présentant des barrières très faibles ou nulles.

Bibliography

- [1] Maximilian Baur, Fei Lin, Tobias O Morgen, Lukas Odenwald, and Stefan Mecking. Polyethylene materials with in-chain ketones from nonalternating catalytic copolymerization. *Science*, 374(6567):604–607, 2021.

(Cited on page v)

- [2] Zhi Wang, Ruichao Wei, Xiaoyao Ning, Tian Xie, and Jian Wang. Thermal degradation properties of ldp insulation for new and aged fine wires. *Journal of Thermal Analysis and Calorimetry*, 137(2):461–471, 2019.
(Cited on pages v and 5)
- [3] Tadao Seguchi, Kiyotoshi Tamura, Hisaaki Kudoh, Akihiko Shimada, and Masaki Sugimoto. Degradation of cable insulation material by accelerated thermal radiation combined ageing. *IEEE Transactions on Dielectrics and Electrical Insulation*, 22(6):3197–3206, 2015.
(Cited on pages v and 5)
- [4] Christian Decker and Frank R Mayo. Aging and degradation of polyolefins. ii. γ -initiated oxidations of atactic polypropylene. *Journal of Polymer Science: Polymer Chemistry Edition*, 11(11):2847–2877, 1973.
(Cited on pages v, 14, 18 and 21)
- [5] Ilona Pleșa, Petru V Noțingher, Cristina Stancu, Frank Wiesbrock, and Sandra Schlögl. Polyethylene nanocomposites for power cable insulations. *Polymers*, 11(1):24, 2018.
(Cited on pages v, 4 and 5)
- [6] Jan Pospíšil. Mechanistic action of phenolic antioxidants in polymers—a review. *Polymer Degradation and Stability*, 20(3):181–202, 1988. *Polymer Additives in Stabilisation: Performance and Mechanisms*.
(Cited on pages v and 18)
- [7] YG Hsuan and RM Koerner. Antioxidant depletion lifetime in high density polyethylene geomembranes. *Journal of Geotechnical and Geoenvironmental Engineering*, 124(6):532–541, 1998.
(Cited on pages v and 18)
- [8] Zhonglei Li and Boxue Du. Polymeric insulation for high-voltage dc extruded cables: challenges and development directions. *IEEE Electrical Insulation Magazine*, 34(6):30–43, 2018.
(Cited on page v)
- [9] Simin Peng, Jinliang He, Jun Hu, Xingyi Huang, and Pingkai Jiang. Influence of functionalized mgo nanoparticles on electrical properties of polyethylene nanocomposites. *IEEE Transactions on Dielectrics and Electrical Insulation*, 22(3):1512–1519, 2015.
(Cited on page v)
- [10] Len A Dissado and John C Fothergill. *Electrical degradation and breakdown in polymers*, volume 9. Iet, 1992.
(Cited on page v)
- [11] Anne Xu, Sébastien Roland, and Xavier Colin. Physico-chemical analysis of a silane-grafted polyethylene stabilised with an excess of irganox 1076®. proposal of a microstructural model. *Polymer Degradation and Stability*, 183:109453, 2021.
(Cited on page v)

- [12] Anne Xu, Sébastien Roland, and Xavier Colin. Thermal ageing of a silane-crosslinked polyethylene stabilised with an excess of irganox 1076[©]. *Polymer Degradation and Stability*, 189:109597, 2021.
(Cited on pages v, 5, 18, 20, 97 and 103)
- [13] M Ferry, E Bessy, H Harris, PJ Lutz, J-M Ramillon, Y Ngonon-Ravache, and E Balanzat. Irradiation of ethylene/styrene copolymers: Evidence of sensitization of the aromatic moiety as counterpart of the radiation protection effect. *The Journal of Physical Chemistry B*, 116(6):1772–1776, 2012.
(Cited on pages v, 20 and 97)

1 - Introduction

1.1 . General description of polyethylene

Polyethylene (PE) is the polymer with the simplest chemical structure among polyolefins. It is made by polymerization of ethylene (C_2H_4 , monomer) and consists of consecutive $-CH_2CH_2-$ units. During polymerization, the monomer (ethylene) breaks its double bond and creates an extra single bond with another ethylene molecule. Although the simplest unit is $-CH_2-$, it is conventional to define repeating units as monomer structure. $-CH_2-$ is referred to as the base unit. Thus, PE, which forms large polymers with consecutive $-CH_2CH_2-$ units, has the following chemical structure.

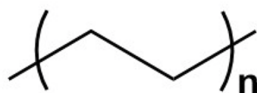


Figure 1.1 – Chemical structure of PE

This simple structure, in which single chain molecules are repeated thousands of times, plays an important role in determining the density, the properties and the structure of PE depending on the type of chains formed. The long chain molecules, in which hydrogen atoms are linked to a carbon backbone, can be divided into linear, branched, or crosslinked forms. Each structure affects the molecular weight (g/mol) or density (g/cm^3) of polyethylene. Linear versions (Fig.1.2a) could be efficiently packed together because there is no branch along the chains. They are of two types: high-density polyethylene (HDPE) and ultrahigh-molecular-weight polyethylene (UHMWPE). In low-density polyethylene (LDPE)(1.2b), the branches interrupt the efficient packing of the chains modulating the space into the polymer matrix. In crosslinked polyethylene (1.2c), the chains are chemically connected to each other, which enhances heat and chemical resistance.

Polyethylene can be chemically modified by replacing hydrogen with specific atom groups or copolymerized with other monomers to produce various types of vinyl polymers. For example, there is chlorinated polyethylene (CPE), where chlorine is substituted for some of the hydrogen atoms. Ethylene can also be copolymerized with vinyl acetate and vinyl alcohol, referred to as ethylene-vinyl acetate (EVA) and ethylene vinyl alcohol (EVOH), respectively.

As an industrial polymer, PE has been commercialized in many fields in different forms, such as bags, fiber, adhesives, coatings, and electric cable insulation and jacket. In the case of plastics [1], its world consumption has increased dramatically since the 1950s, and recently in 2019, around 368 million tons of plastics were produced worldwide. In particular, PE has a wide range of applications depending on its density (unit: g/cm^3). Types and major uses are summarized in Table1.1.

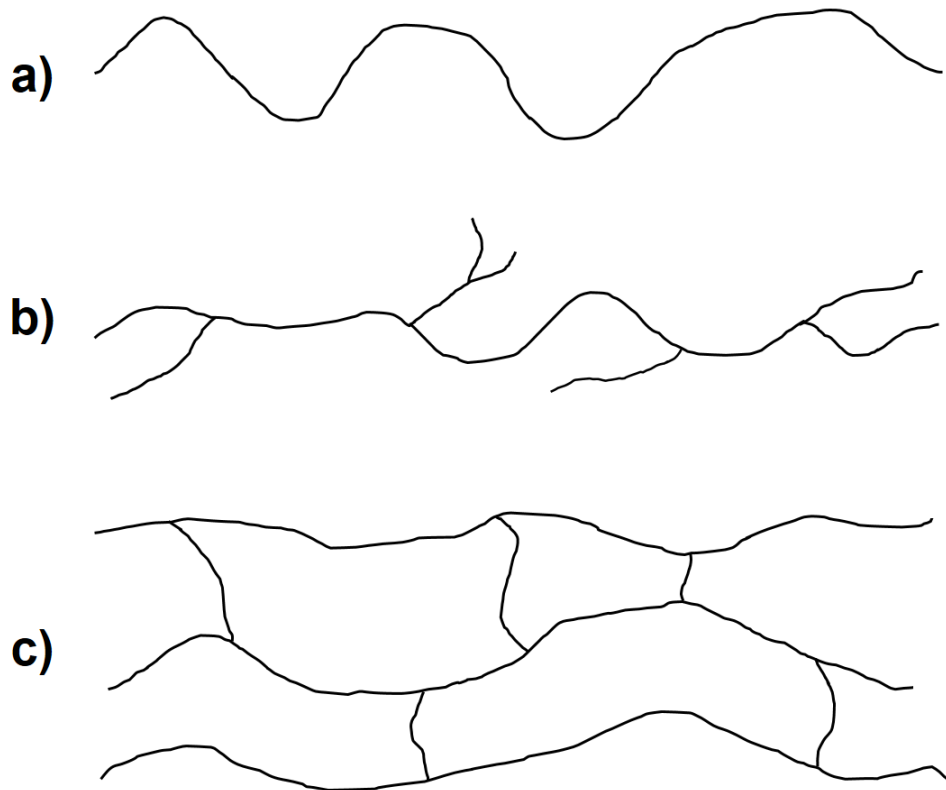


Figure 1.2 – Schematic structure of PE. (a) linear, (b) branched, and (c) crosslinked

Looking at the structure of PE from a microscale point of view, long-chain molecules can assume an ordered structure of polymer chains through regular and repeated folding, a crystallized form called a lamella. The structure can be obtained by slowly cooling the molten polymer, which promotes crystal growth. The amorphous phase fills regions other than the crystallized polyethylene and provides the deformability and impact resistance of PE by connecting the lamellar structures [3]. They constitute the polymer matrix as described in Fig.1.3.

Table 1.1 – Classification of PE and its applications [2]

Type	Abbreviation	Density [g/cm ³]	Major Uses
Ultra-high-molecular-weight polyethylene	UHMWPE	0.930 – 0.935	Articular portions of implants, fiber ...
High-density polyethylene	HDPE	> 0.941	Bottles, pipe, wire and cable insulation ...
Medium-density polyethylene	MDPE	0.926 – 0.940	Gas pipe and fittings, packaging, sacks ...
Linear low-density polyethylene	LLDPE	0.915 – 0.925	Cable covering, lids, containers, pipe ...
Low-density polyethylene	LDPE	0.910 – 0.940	Packaging film, wire and cable insulation, plastic bag ...
Very-low-density polyethylene	VLDPE	0.880 – 0.915	Hose and tubing, food packaging and stretch wrap ...

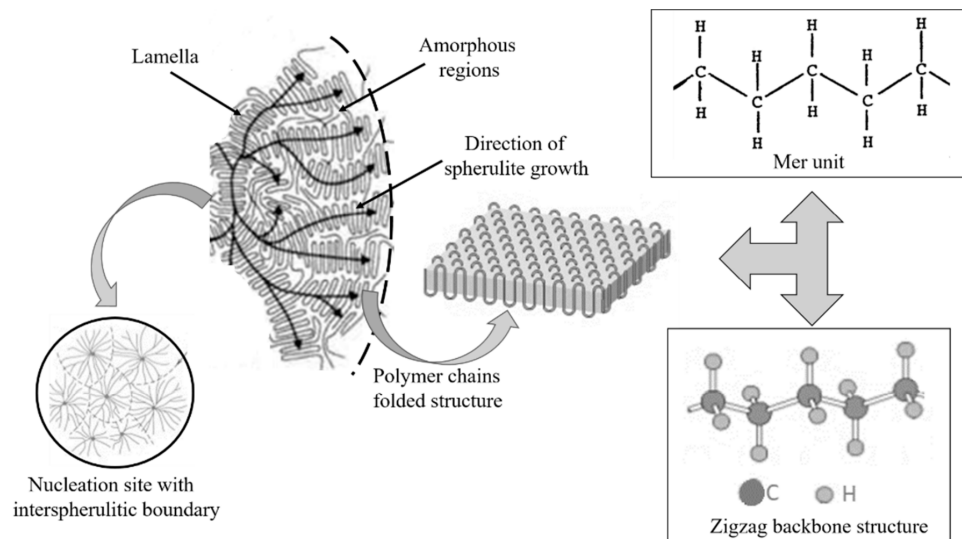


Figure 1.3 – PE structure (taken from Ref. [4])

1.2 . Electrical cables in nuclear power plants

Among the various applications, PE has been widely used as electrical cable insulation in nuclear power plants (NPPs) because of its easy fabrication, low cost, low permittivity, high electrical breakdown strength, and suitable material performance for a wide range of operating voltages [4, 5]. In particular, PE exhibits excellent insulating properties due to its high energy band gap of about 8-9 eV and enables high power loss protection, making it an adequate material for various types of electrical cables [6, 7, 8].

Due to the growing demand for sustainable energy development to meet current and future energy supplies, the lifespan of NPPs is expected to extend to 80 years potentially. Electrical, mechanical, and thermal stresses are the main factors in general insulation aging in daily life, but when electrical cables are used in NPPs, additional environmental stresses such as temperature, radiation, and oxygen for the aging of insulation must also be considered. Under normal operation conditions, the dose rate is typically in the range of 10^{-2} to 10^{-1} Gy h⁻¹ and the temperature is about 30-50 °C, but in severe accident conditions, the dose rate and temperature can reach up to 10^5 Gy h⁻¹ and 150 °C, respectively [9, 10]. Therefore, to ensure the control and safety of NPPs under both normal and accidental conditions is important to determine the long-term resistance from radio-thermal ageing of polymer insulation.

On the other hand, in order to stably operate the NPP for a long time, the management and inspection of all the components that make up the NPP must be carefully carried out, including the normal and abnormal states (all scenarios of accidents). For electrical cables where the PE type is used (e.g., XLPE), it is important to ensure the qualification, condition monitoring, and aging management, as there are about 1500 km of cables per NPP unit [11, 12]. PE constitutes the insulation and jacket, which are the most vulnerable to aging degradation among cable structures (Fig.1.4). In particular, since PE is sensitive to high temperature, radiation, and electrical stress and the degradation of the insulation determines the lifetime of the electrical cables, a lot of research has been done on the degradation mechanism of PE [13, 14, 15, 16, 17].

Oxidation is the most critical mechanism for the aging of PE under these stresses [18, 19]. In particular, the loss of insulating properties is often attributed to the formation of more polar species (i.e., oxidation products such as carbonyl groups) and increased water absorption [20, 21]. The general lifetime prediction of PE is summarized in Fig.1.5 [22].

At first, some amount of antioxidants (AOs) (typically less than 1 wt%) are incorporated to delay the oxidation process by stabilizing the polymer matrix. After the consumption of AOs, the oxidation process is initiated by the reaction of oxygen with an alkyl radical resulting from the breaking of C-C and C-H bonds. Their dissociation energies are typically 342 and 393 kJ/mol (or 3.76 and 4.32 eV), respectively, in the saturated chains [22]. The alkyl radicals are formed under

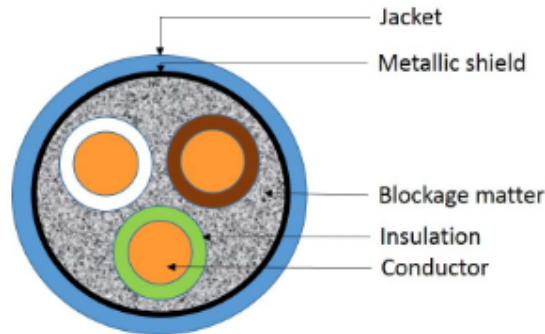


Figure 1.4 – The general structure of electrical cables.

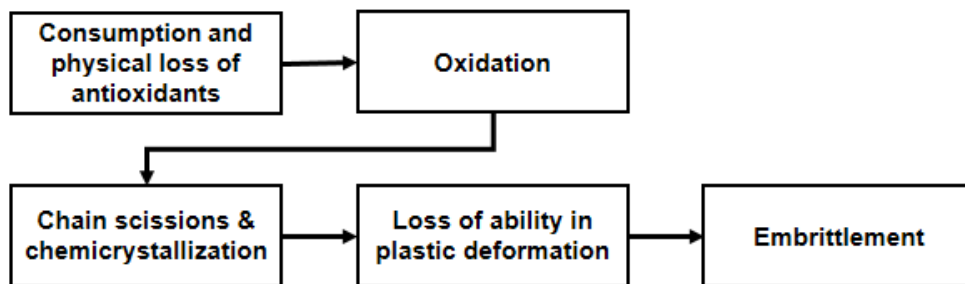


Figure 1.5 – The lifetime prediction of PE

the combined effects of irradiation (e.g., γ -rays, electrons, and rapid heavy ions) and temperature as the initiation steps. For example, the conventional radiothermo-oxidation mechanism is composed of two main initiation steps, and Fig.1.6 shows the summarized degradation mechanisms of both types of oxidation [23, 24, 25]. During oxidation, chain scissions cause chemicrystallization and lead to PE embrittlement (cracking) [22].

Several techniques have been used in experiments to track the oxidative degradation of PE, such as Fourier transform infrared (FTIR) spectroscopy, iodometry, and differential scanning calorimetry (DSC) [22, 26, 27, 28, 29]. More recently, electron spin resonance (ESR) and dielectric spectroscopy have been identified as attractive techniques to investigate radical species such as alkyl, allylic, peroxy radicals, and defect sites (i.e., impurities) [30, 31, 32, 33, 34].

These measurements provide evidence for analyzing many types of oxidation products by observing the concentrations of final or intermediate oxidation products whose lifetime is long enough to be detected and building a kinetic model despite the complexity of oxidation mechanisms. For example, measurements by FTIR spectroscopy confirmed that ketones accumulate during thermal oxidation and are produced in the highest amount of other carbonyl defects. Under photooxidation conditions, ketones are decomposed by Norrish I and II reactions, leading to carboxylic acids or other products such as vinyls [35, 23, 36, 37]. In the case of DSC measurement, the oxidation induction time (OIT) at which oxidation begins

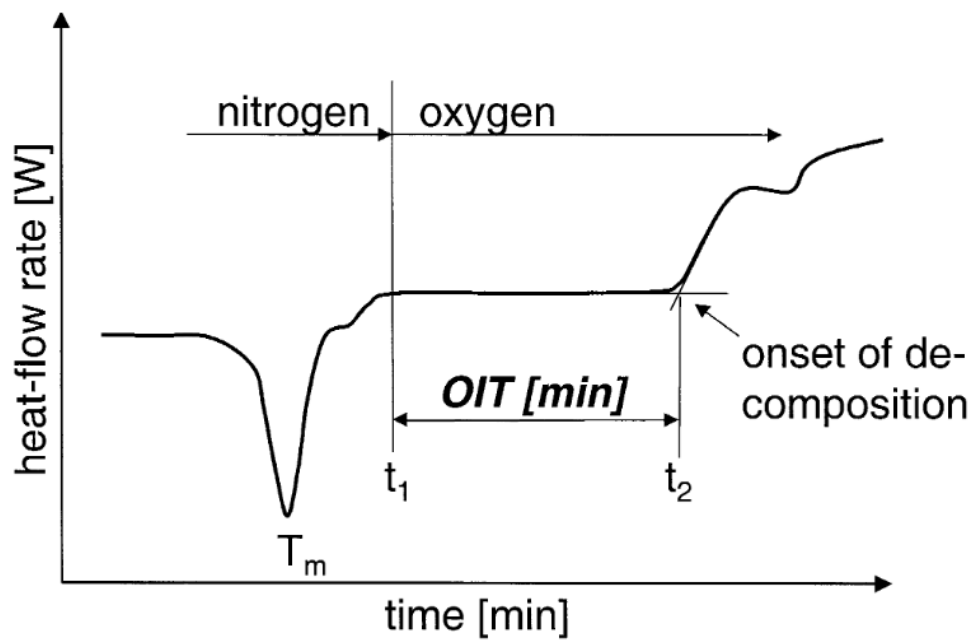


Figure 1.7 – Schematic diagram of DSC measurement for determining oxidation induction time adapted from [26]

1.3 . From the basic auto-oxidation scheme by Bolland-Gee

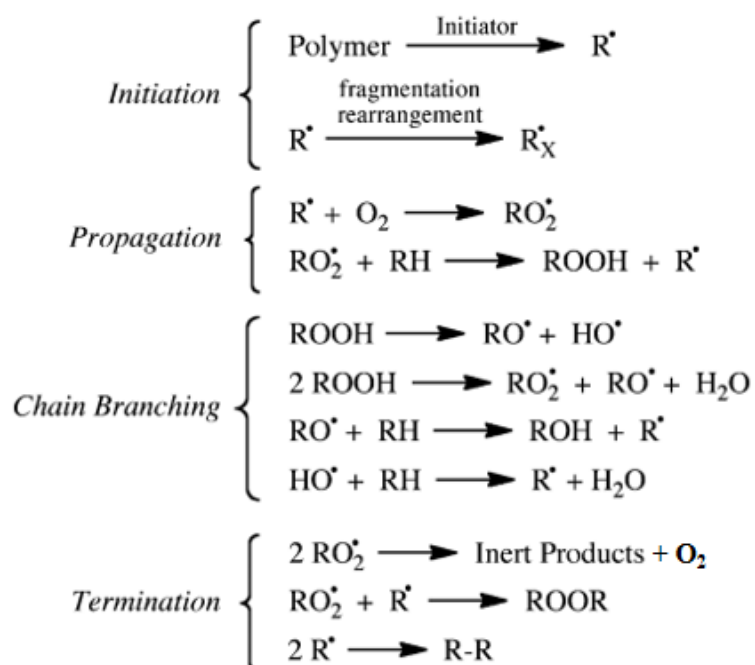


Figure 1.8 – Basic auto-oxidation scheme adapted from Ref. [43]

As the applications and demand for PE increase, the study of the stability and degradation mechanism of polyethylene becomes more and more important. In order to understand the degradation mechanism of PE, it is essential to study the kinetics of oxidative degradation to find out and prevent critical reactions that cause severe degradation of PE among those pathways. As part of these studies, Bolland and co-workers developed the oxidative degradation mechanism of PE called the basic auto-oxidation scheme in 1946, which represents the free radical chain reactions on which many modern polymer studies of the degradation mechanism are based, as shown in Fig.1.8 [38, 39, 40, 41, 42]. This process describes the overall polymer oxidation process of rubbers such as ethyl linoleate and ethyl linolenate through initiation, chain propagation, chain branching, and termination steps.

In the initiation step, high energy is usually applied to break the C-H bond of polyethylene, extracting the H to create a carbon-centered radical in the polymer chain (R^\bullet). Considering that the C-H bond and C-C bond energies are in the range of 293–440 kJ/mol and 250–375 kJ/mol respectively, high irradiation energies (e.g., γ -rays, electrons, and swift heavy ions) mostly produce alkyl radicals during electrical cable operation [44, 45, 46, 47].

When a carbon-centered radical is formed, it reacts rapidly with nearby O_2 to produce a peroxy radical (ROO^\bullet). The formed peroxy radicals then subsequently abstract H atoms from the C-H bonds of the same or surrounding alkyl chains to form hydroperoxide (ROOH) and new carbon-centered radicals. Then, hydroperoxide breaks the O-O bond and forms new radical species such as alkyl, alkoxy, and peroxy radicals through unimolecular or bimolecular reactions in the chain branching step (Fig.1.8). The produced radicals repeatedly contribute to the oxidative degradation process, accelerating the whole process. That is, as oxidation itself proceeds as an autocatalytic reaction, the formation of radicals is accelerated. Then PE matrix subsequently undergoes the termination steps, such as crosslinking reactions, whose products do not undergo further reactions.

However, although BAS was developed for oxidation processes on rubber and lipids, it has been used very extensively to elucidate degradation mechanisms for all types of polymers. This does not adequately account for some reactions in which the extracted alkyl radical center is unstable from a kinetic and/or thermodynamic point of view for some types of polymers. For example, for some small saturated alkyl groups, bond dissociation energies for the R-H range from 400.4 to 422.2 kJ/mol, which is larger than for the corresponding ROO-H bond (344.0 to 370.3 kJ/mol), implying that the H-abstraction reaction by a peroxy radical is thermodynamically unfavorable [48]. The activation energy also exhibits high energy of 73 kJ/mol [22, 49].

1.4 . Open issues

Since BAS was constructed to elucidate the oxidation mechanisms of rubber and lipids, efforts are underway to revise and improve oxidation schemes for other types of polymers. In particular, the formation and the decomposition of hydroperoxides in the propagation steps in Fig.1.8 require understanding and improvement of the reactions for polyethylene because some of those considered are endothermic reactions and show high activation energies. This section is devoted to open issues related to specific reactions, particularly those related to the formation and decomposition of hydroperoxides, as well as chain scission and crosslinking reactions triggered by radical species; the latter two processes might be in competition with one another.

1.4.1 . Formation of Hydroperoxides and their role

A general explanation of hydroperoxide formation is most commonly given by the H-abstraction reaction, in which a peroxy radical abstracts a hydrogen atom in the propagation step (Fig.1.8). However, studies of polyethylene and other types of polymers have raised questions about this reaction from various perspectives. Gryn'ova *et al.* [43] compared the enthalpies of the reaction with various types of polymers based on the bond dissociation energy (BDE) of HOO-H and R-H. From the study, polymers with saturated hydrocarbon chain structures showed mostly

thermodynamically unfavorable Gibbs free energies ($\Delta G > 0$). In the case of PE, the value was 43.5 kJ/mol. They suggested that the produced alkyl radical center as the final product must be stabilized by double bonds or strong captodative effects for a thermodynamically favorable reaction. Chen *et al* [50] also suspected the conventional reactions explaining the formation of hydroperoxide produced by the reaction between peroxy radicals and hydrogen atoms from other alkyl chains, due to the high endothermic reactions and the slow reaction rates of the intermolecular H-transfer reaction, including intramolecular H-transfer reactions of ROO° [51]. To solve this problem, they proposed a modified scheme for the formation of hydroperoxides produced between ROO° and HOO° according to atmospheric chemistry [52, 53].

Later, in a comprehensive paper, Smith *et al.* proposed an improved scheme of BAS by including the results of these two papers and summarizing the research results on peroxy radicals (Fig.1.9) [54]. In their paper, they considered not only hydroperoxyl radicals but also hydroperoxides formed by other atmospheric species, such as ozone and hydroxyl radicals. They also mentioned the termination step of the reaction from two peroxy radicals and the formation of alkoxy radicals as an alternative reaction pathway instead of the H-transfer reaction. However, while they considered all reactions from a thermodynamic point of view, the activation energies associated with kinetic studies were not considered for possible reaction pathways. Moreover, the modified scheme focused only on the propagation and termination steps; in particular, the chain branching step for the decomposition of hydroperoxides, which are largely attributed to radical-generating auto-oxidation processes, was not considered. More recently, De Keer *et al.* [55] developed the reaction scheme with kinetic Monte Carlo modeling by calculating rate coefficients. Peroxy radicals can bypass the formation of hydroperoxides and lead to the termination step. Moreover, the reported O–O bond cleavage energy of hydroperoxide is highly endothermic ($\Delta G_{gas} = 134.9 \text{ kJ/mol}$) and supports this revised reaction scheme. It means that the formation of radical species through the decomposition of hydroperoxides may also be difficult, and therefore the reaction should be thoroughly re-considered as in the propagation step. For activation energy, the dissociation energy of RO-OH experimentally ranges from 67 to 160 kJ/mol [56, 57, 58, 59]. This is because the experimental environment and polymer type can affect activation energy. For example, Chen *et al.* reported that the RO-OH bond of polyethylene oxide (PEO) in aqueous solution is easily broken even under mild conditions [60]. On the other hand, Costa *et al.* reported that the RO-OH bond of UHMWPE is stable at room temperature and begins to decompose at temperature above 80 °C [61]. Theoretical calculations indicate higher energy than the experimentally reported values at around 188 kJ/mol [51, 62, 63]. Therefore, in order to review the viability of the overall oxidation mechanism for a specific polymer, it is important to study the reaction considering the properties of each corresponding polymer.

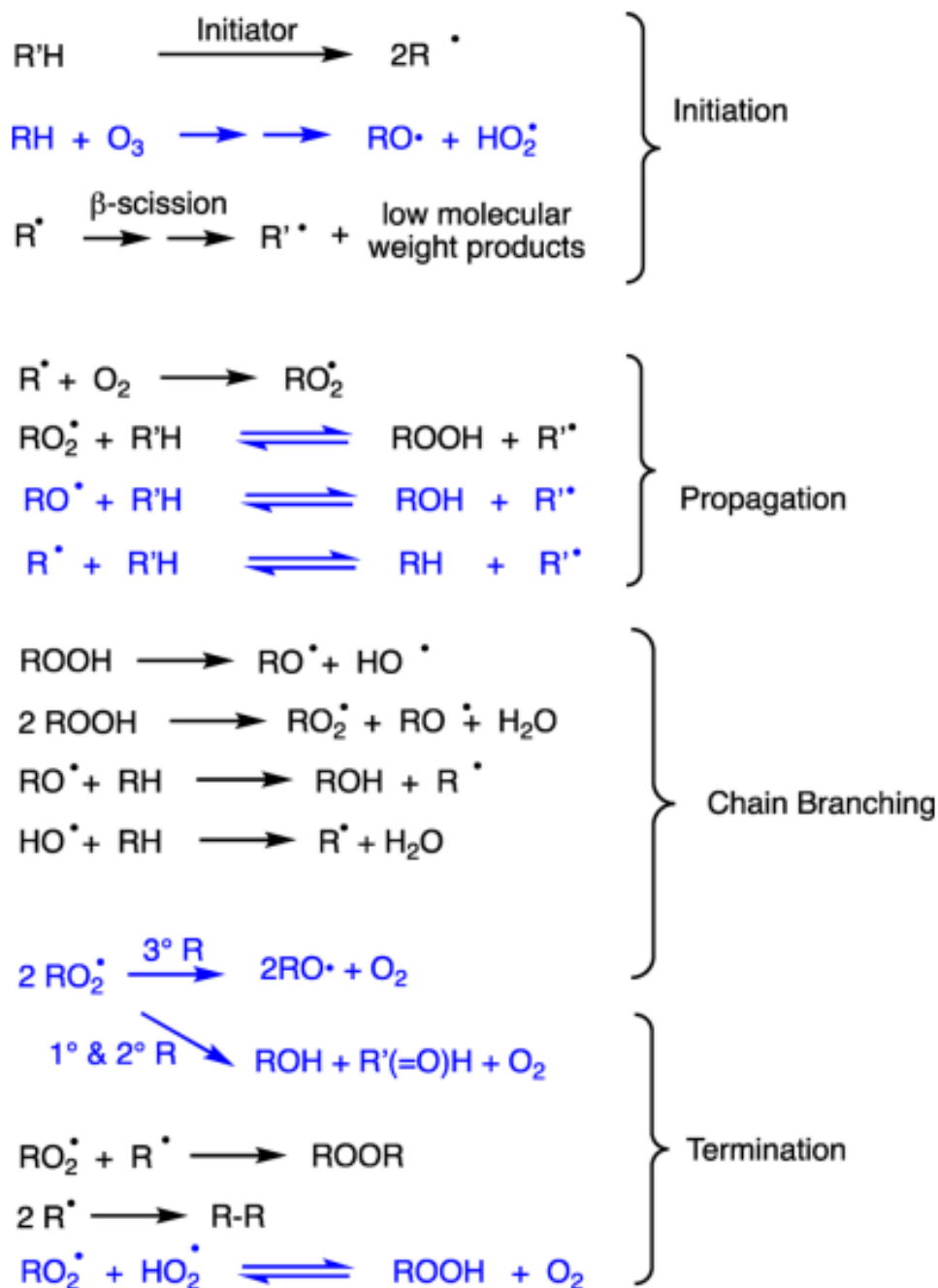


Figure 1.9 – Basic auto-oxidation scheme revised by Smith, et al. [54]

1.4.2 . Chain scission and crosslinking

While oxidation proceeds and radical species accumulate through the chain branching step, chain scission and crosslinking reactions can be competitive at certain points in time. For example, alkoxy radicals disappear by forming aldehydes and primary alkyl radicals through β -scission reactions or lead to crosslinking reactions that bind other radical species, such as alkyl and alkoxy radicals. Since the crosslinking reaction always requires two kinds of radicals, the reaction takes place in the condition of a high concentration of radicals or locally trapped radicals. Therefore, the chain scission reaction, which can only react with a single chain, will be dominant at the beginning of the oxidation process.

Chain scission and crosslinking reactions can be compared by monitoring the weight and number of average molecular masses (i.e., M_w and M_n). This is because chain scissions usually decrease the masses, and crosslinking reactions increase them. Fayolle *et al.* [64] described the mechanism of embrittlement from oxidative degradation with the chain scission reactions. The reactions generate mobile short chain fragments in the lamellar surface region and induce them to chemicrystallization. Rodriguez *et al.* investigated the chemo-mechanical aspects of oxidative embrittlement under irradiation conditions [65]. They observed transient strengthening, chemical cracking, and radiation-induced cavitation and visualized schematic scenarios of UV-induced cracking without mechanical loading, as shown in Fig.1.10. They proposed a second lamellar structure with chemicrystallization to account for the predominant chain scission reactions without changing the crystallinity ratio. As UV radiation is further increased (in the range of 48 - 96h), chemicrystallization stops, and thus the chain scission reactions causing embrittlement become the dominant reactions.

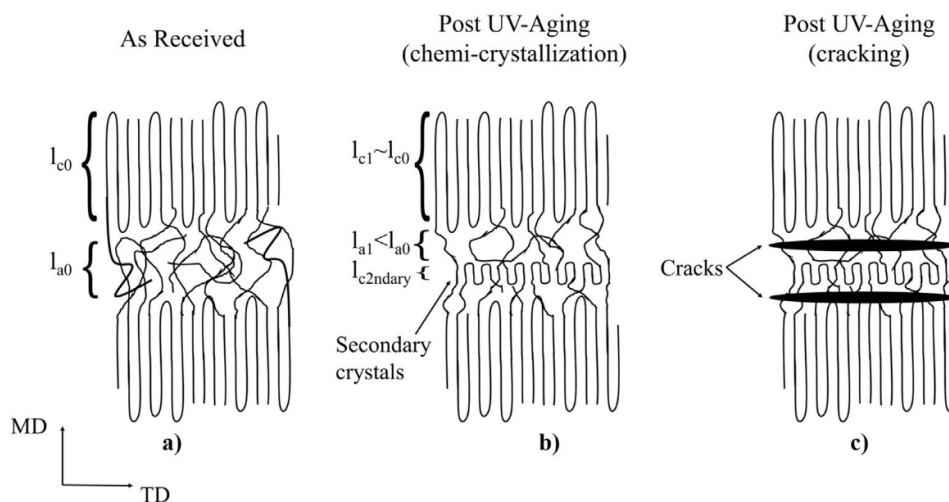


Figure 1.10 – schematic scenario of UV-induced cracking without mechanical loading [65]

Da Cruz *et al.* observed the macromolecular structural behavior of PE by

monitoring M_w , and M_n [22]. They exposed the samples at high temperatures between 100 °C and 140 °C and observed a trend towards the asymptotic value 2 of the polydispersity index (PDI). They concluded that these results were caused by a pure chain scission process from alkoxy radicals (β -scission) through a comparison of the concentration of oxidation products (i.e., aldehydes and carboxylic acids).

Crosslinking reactions under irradiation have also been extensively studied under inert atmosphere or in air [66, 67, 68, 69, 70, 71, 72]. Crosslinking reactions are the dominant process when polyethylene is irradiated under inert atmosphere; however, when it is irradiated in air, oxidative degradation takes place. Within radio-oxidation chain scission tends to dominate at low dose rate of gamma irradiation, but at high dose rate, crosslinking reactions become the dominant process again [73, 74]. Singh *et al.* [70] consider three possible radiation effects: cationic reactions, crosslinking reactions in the crystalline region, and excitation energy transfer by following suggestions in the literature. They re-visited several reactions related to irradiation and suggested possible reactions expected to occur, such as the formation of superoxide anions, hydroperoxy radicals and hydroperoxides, cationic condensation reactions, and excitation energy transfer to peroxides and hydroperoxides. Hsu *et al.* [75] studied photo-oxidative degradation of PE to investigate embrittlement. They showed similar results with ref. [64] showing the reduction of interlamellar distance and chemicrystallization. The study without irradiation but focusing on the thermal condition was also reported [72]. The LDPE films were at 70°C in the dark and underwent degradation. They exhibit increased crystallinity from 35 to 55 wt % according to aging time. This corresponds to the secondary crystallization of mobile short chain segments coming from the oxidative cleavage of macromolecules explained by chemicrystallization. It seems obvious that the chemicrystallization takes place after chain scission. However, as the difficulties in measuring the concentration of the second crystalline molecular weight, further consideration of different structural scales (i.e., from molecular to macroscopic scale) is required. Nevertheless, studies of elementary molecular processes responsible for chain scission and chemicrystallization, which help to establish the most realistic mechanistic scheme and inform kinetic studies for the oxidation rate, are rarely reported.

1.5 . Impact of humidity

As polyethylene (PE) photodegrades more rapidly in air than in an inert environment, not only the temperature and irradiation, but monitoring other factors, such as humidity (i.e., water vapor partial pressure) which also affect the degradation of PE, should also be considered. CO₂ partial pressure is an important parameter because the amount of CO₂ generated increases with humidity [76, 77, 78]. Fernando *et al.* observed CO₂ photogeneration of biaxially oriented polypropylene (BOPP) films [76]. They compared two different oxygen conditions in order to

1.6. Survey of previous ab initio calculations related to the problem 15

monitor photodegradation affected by humidity. One is 'dry oxygen,' which is further dried by silica gel, and the other is 'wet oxygen,' which passes through two water bubblers. As a result, irradiation of BOPP films with 'dry oxygen' exhibited an induction time of around 60 min, whereas with 'wet oxygen,' it eliminated the induction time and increased the rate of CO₂ formation.

Most studies with many types of polymers, such as poly(vinyl chloride) (PVC) and poly(ethylene terephthalate) (PET), incorporate TiO₂ as a stabilizer, but sometimes it is postulated that the stabilizer increases the rate of carbon dioxide generation due to enhanced photocatalysis with the formation of hydroxyl radicals [76, 77, 78]. However, it is also observed that increasing humidity raises the rate of oxidation in unpigmented PE matrix [78]. The main reactions come from the decomposition of hydroperoxides, β -scission, and Norrish type I reaction, and therefore acetic acid and acetone are also mainly observed as well as carbon dioxide [79, 80]. In contrast to thermo-oxidation, where ketones are the main oxidative products, Norrish type I reaction decomposes ketones and produces many acid types products [35]. Therefore, the impact of humidity can also be studied by kinetic studies by comparing the reaction pathways.

1.6 . Survey of previous ab initio calculations related to the problem

Theoretical calculations such as ab initio and molecular dynamics simulations are used for various reasons to reinforce or verify the experimental results. These studies calculate optical, electrical, and transport properties and can target some specific oxidative products or reactions. We summarized several remarkable studies on the oxidation of PE from a physical and/or chemical point of view and various materials structures.

Table 1.2 – *Summary of papers devoted to the study of reactions at the atomic scale [8, 43, 46, 51, 62, 81, 82, 83, 84]*

Representative reactions	Method	Structure used	Ref.
Evolution of a trapped exciton*	ab initio molecular dynamics (Car-Parrinello), BLYP/plane-wave	polyethylene crystal & lamella surface	[8]
Enthalpies of H-abstraction reaction	ab initio (G3(MP2)-RAD), DFT, B3LYP33,34/6-31G(d), GAUSSIAN09	gas- and solution-phase	[43]
H-isomerization*	DFT, 3LYP/6-311+G** and/or B3LYP/6-31G**, GAUSSIAN03	molecules	[46]
Oxidation of PEO*	DFT, B3P86/6-31++G(d,p), GAUSSIAN03	molecules	[51]
Oxidation of PE*	DFT, PBE/DNP (double numerical plus polarisation), DMol ³ package	PE(100) surface,	[62]
H-Atom transfer reactions*	DFT, composite ab initio (G3MP2B3), B3LYP/6-31G(d), GAUSSIAN03	molecules	[81]
Dissociation and recombination of chain scission reaction*	first-principles molecular dynamics, B3LYP/6-31g(d), GAUSSIAN03	molecules	[82]
Chain scission*	ab initio, molecular dynamics, Perdew and Wang(1992)/plane-wave, VASP	polyethylene chain (in periodic boundary conditions)	[83]
Gas-phase reaction of OH radicals with ketones	Car-Parrinello molecular dynamics, BLYP/plane-wave	molecules	[84]

*: Activation energy is calculated

1.6. Survey of previous ab initio calculations related to the problem 17

For example, Kysel *et al.* studied reaction barriers of H-isomerisation such as alkoxy, alkylperoxy, and alkyl radicals for small molecules and compared intramolecular H-shifts and intermolecular H-transfer [46]. The decrease of activation energies was observed with increasing transition state (TS) ring size. Intermolecular H-transfer reactions exhibited smaller activation energies than respective intramolecular reactions. Hayes *et al.* also reported similar results that 1,5- and 1,6-H-transfers have smaller barriers than the others in the case of alkyl radicals. Some interesting reactions are also observed from intramolecular H-shifts by a peroxy radical. When a hydrogen atom is abstracted from α positions, which is the nearest position to the peroxy radical, the alkyl radical with a hydroperoxyl substituent (α -alkyl-hydroperoxy radical) is very unstable, and it spontaneously leads to the dissociation of O-O bond by forming a ketone and a hydroxyl radical [85]. The observed time by experiments is less than 20 μ s, which is consistent with the simulation results [86, 87]. The calculated activation energy for this reaction is from 144 to 209 kJ/mol, which is high [51, 88]. The generated hydroxyl radical ($^{\circ}\text{OH}$) from the O-O dissociation of α -alkyl-hydroperoxy radical can easily abstract a hydrogen atom by forming an alkyl radical and water. In case of *i*-butane, the calculated barrier for the abstraction is only 0.03 eV obtained by BHandHLYP and MP2 calculations using the 6-311G(d,p) basis set [89]. Therefore, these small radicals, such as hydroxyl and hydroperoxyl radicals, are important as initiators for creating alkyl radicals and accelerating the oxidative degradation of polymers. On the other hand, when a hydrogen atom abstracted moves far from a peroxy radical at γ -position, the activation energy decreases in a range from 85 to 94 kJ/mol [51, 46]. In the case of an alkoxy radical, the activation energy of H-isomerisation strongly decreases from 122.6 to 23.9 kJ/mol by increasing the transition state (TS) ring size.

The activation energies of oxidation reactions are calculated by small molecules or the surface of lamellæ structures. de Sainte Claire *et al.* presented quantitative kinetic data of activation energies and rate constants for polyethylene oxide (PEO) [51]. Oluwoye *et al.* also reported the reaction pathway for thermo-oxidation of crystalline PE to elucidate the degradation mechanism of PE [62] by using Perdew-Burke-Ernzerhof (PBE) xc-functional with linear synchronous and quadratic synchronous transit approaches (LST/QST). The structure was built by a vacuum slab along the [100] Miller index to represent a PE {100} surface. The benefits of crystalline PE structures are that they can consider the activation energy of intermolecular reactions as well as intramolecular ones with optimized structures and the results can be compared with small molecules. Intermolecular reactions in the amorphous phase are expected to show a gaussian distribution of activation energies according to the distance and orientation. Nevertheless, the amorphous phase is studied by isolated molecules or molecular dynamics. For example, Frank *et al.* investigated the reactions between hydroperoxyl radicals and ketones using Car-Parrinello (CP) molecular dynamics [84]. The reaction could be affected by

the direction and kinetic energy of a hydroperoxyl radical by forming different ring sizes. Ceresoli *et al.* also studied by *ab initio* molecular dynamics the evolution of an exciton trapped on ketones, double bonds, and carboxylic acids situated on the top of a PE lamellar surface [8]. They found that excitons can be trapped at the carbonyl defects and make radiative recombination, whereas nonradiative electron-hole recombination takes place by the vinyl and carboxyl groups, and sometimes it weakens chemical bonds. When the reactions have high activation energies, which cannot be overcome by temperature (i.e., molecular dynamics at temperatures below the melting point) and they are intermolecular reactions, calculations aimed at obtaining energy barriers in crystalline PE would be needed. Although bimolecular reactions are rarely studied in crystalline PE, various kinetic models of reaction pathways have been developed and could also be verified in other environments, such as a surface of crystalline lamellæ (i.e., the amorphous-crystalline interface). Therefore, further studies would be essential to elucidate the degradation mechanism of PE as follows: i) comparing the energy barriers of intramolecular reactions between isolated molecules and crystalline PE, ii) calculating the energy barriers of intermolecular reactions in crystalline PE, and iii) elucidating alternative reaction pathways, which were hardly explained by intramolecular reactions, e.g., formation of alkoxy radicals.

1.7 . Role of antioxidants

Oxidation of PE occurs at all stages involved in the lifetime of the material. It comes with irreversible changes in chemical composition and has a serious impact on polymer degradation. To retard this oxidation process and increase the lifetime of electric cables, typically low concentrations of antioxidants (AOs) are incorporated into the polymer matrix. Many types of antioxidants have been developed to prevent the oxidation of polymers effectively.

In general, AOs can be divided into two types according to the polymer stabilization mechanism which depends on the chemical structure of the functional groups. The first type is constituted by free radical scavengers (e.g., hindered phenols), also called "primary antioxidants" or "chain-breaking antioxidants" [90, 91]. The main role of the primary antioxidants is to prevent the auto-oxidation of polyethylene by reacting with peroxy radicals or other radical species formed in the propagation step and increase the termination rate to block radical chain propagation effectively [92, 93, 94, 95]. Their stabilization mechanism leads to the termination of the peroxy radicals (POO°) generated by the propagation step by donating the H atoms in the phenol function to radical species through the H-transfer reaction of AO (Fig. 1.12(a)) [10, 92, 96]. For example, Fig.1.13 shows that butylated hydroxytoluene (BHT) incorporated in polypropylene (PP) decreases the amounts of oxygen reacted with increasing concentration of antioxidants [69].

The second type is a hydroperoxide decomposer called a "secondary antioxi-

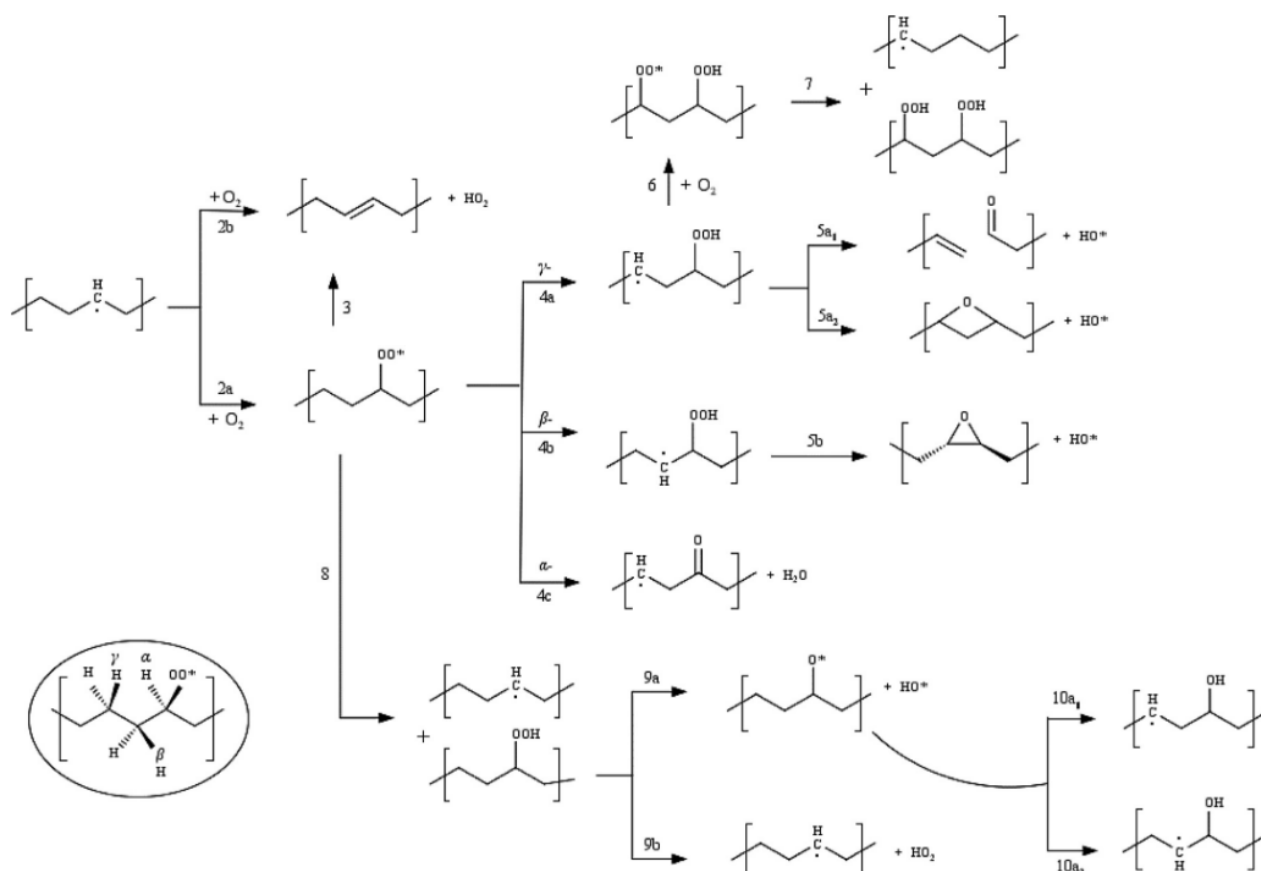


Figure 1.11 – Reaction pathway for thermo-oxidation of crystalline polyethylene as proposed in Ref. [62].

tant." They are responsible for converting hydroperoxide into alcohol, a relatively non-reactive and thermally stable product. In other words, the hydroperoxide decomposer prevents the decomposition of hydroperoxides into alkoxy and hydroxyl radicals, a commonly known decomposition reaction. Alkoxy and hydroxy radicals are highly reactive and act to accelerate PE degradation. Therefore, the key is to retard the auto-oxidation in PE efficiently by converting hydroperoxide to a non-radical product and reducing the initiation rate coming from hydroperoxides. They are often combined with primary antioxidants to provide a synergistic stabilizing effect.

Among secondary antioxidants, structures containing a thioether functional group (denoted as -S- for simplicity) are widely used. In particular, distearyl thiodipropionate (DSTDP) has been shown to be effective for polyolefins during the BAS cycle by reducing hydroperoxides as shown in Fig.1.12(b) [97]. For both the first and second types of antioxidants, the mechanism retarding the oxidation of PE is explained by chemical reactions, and their effectiveness could slightly differ due to the different structures that they contain. Because antioxidants are

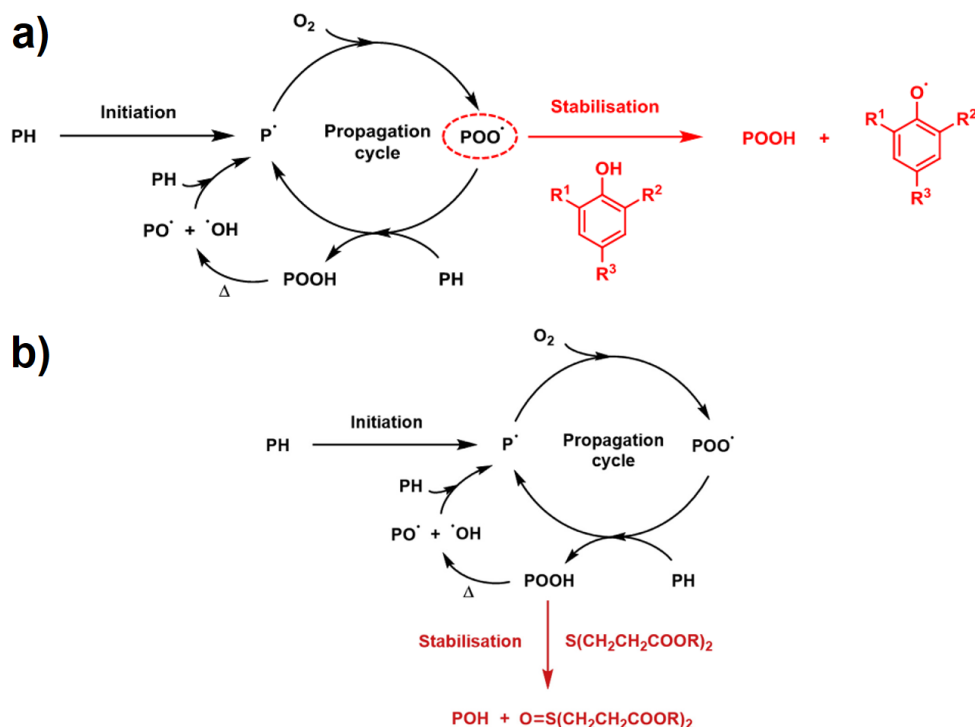


Figure 1.12 – Simplified mechanistic scheme for a polyolefin stabilised by (a) a hindered phenol antioxidant, and (b) thiodipropionate antioxidant. Taken from Refs. [10, 97]

relatively polar compared to PE, they cannot be dissolved in large amounts, and typically less than 1 wt% of antioxidants are included in semi-crystalline polymers.

Antioxidants are also effective to protect polymer matrix from radiation effect [98]. When polymer chains are submitted to ionizing radiations, excitation and ionization take place, and radicals can come from the evolution of the excited chains by excitation transfer such as Dexter and Förster processes. When antioxidants are incorporated, especially with aromatic (benzene) rings of primary antioxidants, the energy transfer takes place from the aliphatic moiety to the aromatic one, which means aromatic rings bear the excitation energy along the polymer chains as an energy sink [99]. However, because most studies are reported under inert atmosphere or vacuum, the mechanisms of energy transfer in the presence of oxygen should also be studied.

1.8 . Motivations and approach

Due to the nature of the operation of nuclear power plants, electrical cables employed here undergo radiation aging. In particular, electrical cable insulation is composed of polymers and are typically degraded by γ -ray or other possible

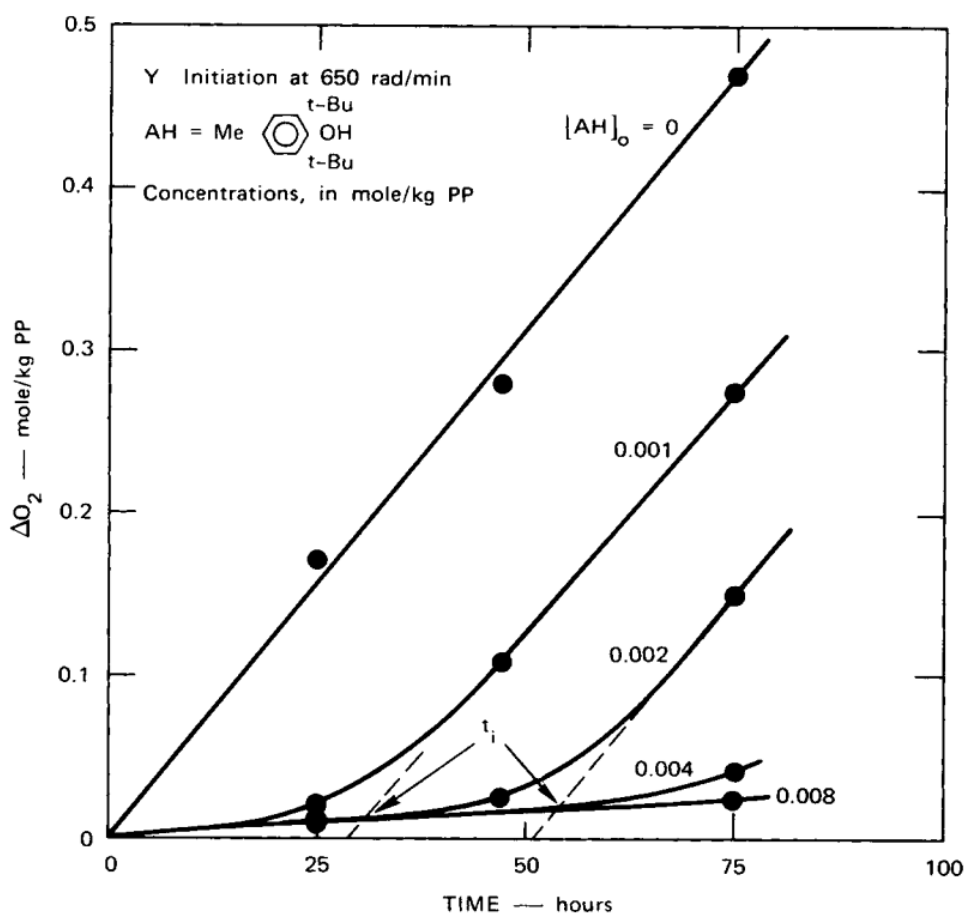


Figure 1.13 – BHT antioxidant retards the oxidation of PP under irradiation condition (650 rad/min, 45 °C). It is efficient with increasing concentration of antioxidants.
 Taken from Ref. [69]

environments (electrons and neutrons), and degradation is accelerated by reaction with oxygen (i.e., radio-oxidation). This degradation should be seriously taken as it determines the lifetime of the cable. When the polymer is exposed to high energy irradiation, electron excitation initiates oxidation by generating alkyl radicals. Such radical species spontaneously capture oxygen and form peroxy radicals.

Although there is a global consensus as far as the mechanism explaining the formation of peroxy radicals is concerned, the oxidation kinetic pathway from propagation to termination is complex, and various possible routes starting from peroxy radicals explain the overall degradation mechanism of PE.

Among them, many types of polymers, including PE, were studied following the basic auto-oxidation scheme developed by Bolland, Gee, and co-workers in order to describe the oxidation pathways. However, as mentioned in section 1.4 explaining several reactions involving important intermediates such as hydroperoxides, this

scheme is problematic from both kinetic and thermodynamic points of view (i.e., high activation energy and positive reaction enthalpy). This is because the basic scheme was originally developed for rubbers and lipids, not for polyolefins. In the case of PE, having saturated carbon chains, the reaction leading to the formation of hydroperoxides needs overcoming an energy barrier of 0.7 eV, and the reaction enthalpy is positive and almost as high. Even assuming that hydroperoxides are produced, the subsequent reaction (decomposition of hydroperoxides) also exhibits high activation energies. Therefore, an overall review of the oxidation mechanism is strongly required, and a careful examination of the energy profile for each reaction should be carried out. An alternative reaction pathway that does not go through hydroperoxide proceeds through the formation of alkoxy radicals from two peroxy radicals. This reaction does not require high activation energy on the lamellar surface and efficiently generates alkoxy radicals. The produced alkoxy radicals can then lead to several reaction pathways, such as chain scission, crosslinking, and formation of ketones. Therefore, many possible reactions involving alkoxy radicals will be discussed in this thesis as these reactions could be competitive with respect to the accepted basic oxidation scheme.

On the other hand, several additives are included in the polymer matrix to protect electrical cable insulation from radio-oxidation. In particular, antioxidants such as those of the Irganox family are widely used and are believed to delay OIT by removing reactive radical species or acting as an energy sink of excitation energy. Therefore, it is necessary to discuss how antioxidants operate within the polymer matrix. The activation energy for the H-transfer reaction between antioxidants and radical species could be calculated (chemical reaction), and the optical properties such as absorption/emission cross section calculation according to the energy band-gap of pure PE, defects, and antioxidants could also be studied. In this thesis, we mainly deal with chemical reactions.

This thesis aims to re-visit the overall oxidative reactions resulting in the degradation of PE and study several competitive or controversial reactions. Based on the oxidative degradation mechanism, the role of antioxidants can be deduced and can help understand when they are necessary or which reactions should be blocked by antioxidants to delay OIT. In order to study the oxidative degradation mechanism of PE, we take for granted the initiation steps, which create alkyl radicals, and then focus on several crucial oxidation products. First, we investigate reaction pathways leading to a ketone because it is the majority product and thermodynamically stable on polyethylene chains. Furthermore, ketones are good candidates to study, because thermo- and photo-oxidation degradation are explained by similar kinetic pathways except that, for the latter, further reactions take place after the formation of ketones, so-called Norrish type reactions. The formation of hydroperoxides will also be taken into account, as they have been considered an important intermediate product. Besides, since alkoxy radicals are involved in many reactions, such as the formation of hydroperoxides, chain scissions, and crosslinking

reactions, elucidating the role of alkoxy radicals is also important. Therefore, we investigate the formation of alkoxy radicals from the decomposition of hydroperoxides or peroxy radicals. Alkoxy radicals also lead to termination steps, which are stable defects such as ketones and crosslinks. However, comparing the activation energies is required because all these reactions are in competition. As for antioxidants, hindered phenol function of primary antioxidants is envisaged. H-transfer reactions create hydroperoxides but can also give a hydrogen atom to other radical species, such as alkoxy and alkyl radicals. The reactions are examined mostly with butylated hydroxytoluene (BHT).

Another point is the microstructure of PE, which is a semicrystalline polymer, including crystalline, amorphous and interface regions. In order to elucidate the degradation mechanism of PE and the role of antioxidants, we constructed material structures reflecting various local environments: i) a molecular model, ii) a solid, crystalline model, and iii) a lamellar surface model. We approach them through density functional theory (DFT) to calculate formation energy, energy barriers, and a trajectory in configuration space. The detailed methodology is explained in the following chapter. We believe that these results, obtained from calculations at the atomic scale, can be used as a useful database of the energetics of relevant reactions to estimate the lifetime of electrical cables operated in NPPs. The schematic summary of our approach is shown in Fig.1.14.

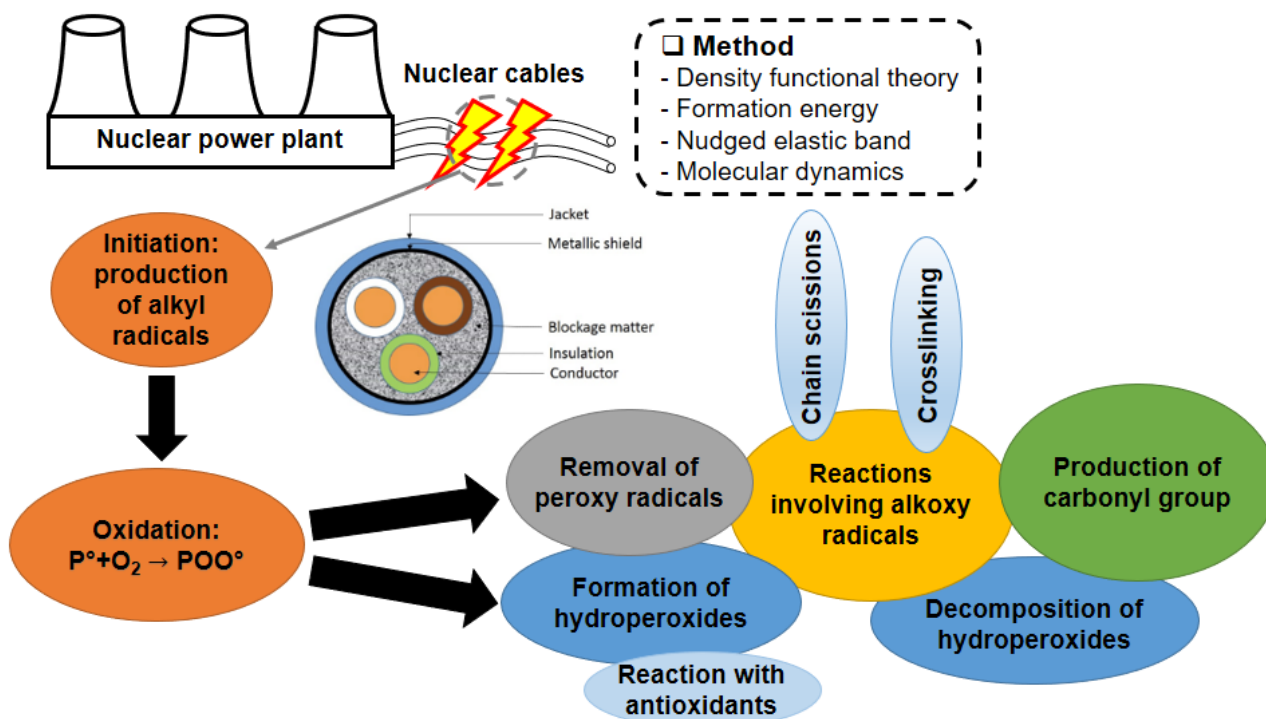


Figure 1.14 – Study approach to investigate the degradation mechanism of PE and role of antioxidants

Bibliography

- [1] <https://www.plasticsoupfoundation.org/en/plastic-facts-and-figures/{#}productie>. Accessed: 2022-10-03.
(Cited on page 1)
- [2] Malcolm P Stevens. entitled “polymer chemistry, an introduction” third edition, 1999.
(Cited on page 3)
- [3] Leo Mandelkern, R. G. Alamo, and M. A. Kennedy. The interphase thickness of linear polyethylene. *Macromolecules*, 23(21):4721–4723, 1990.
(Cited on page 2)
- [4] Ilona Pleșa, Petru V Noțingher, Cristina Stancu, Frank Wiesbrock, and Sandra Schlögl. Polyethylene nanocomposites for power cable insulations. *Polymers*, 11(1):24, 2018.
(Cited on pages v, 4, and 5)
- [5] Diaa-Eldin A. Mansour, Nagat M. K. Abdel-Gawad, Adel Z. El Dein, Hanaa M. Ahmed, Mohamed M. F. Darwish, and Matti Lehtonen. Recent advances in polymer nanocomposites based on polyethylene and polyvinylchloride for power cables. *Materials*, 14(1), 2021.
(Cited on page 5)
- [6] Masamichi Fujihira and Hiroo Inokuchi. Photoemission from polyethylene. *Chemical Physics Letters*, 17(4):554–556, 1972.
(Cited on page 5)
- [7] Ken Barber and Graeme Alexander. Insulation of electrical cables over the past 50 years. *IEEE Electrical Insulation Magazine*, 29(3):27–32, 2013.
(Cited on page 5)
- [8] Davide Ceresoli, Erio Tosatti, Sandro Scandolo, G Santoro, and S Serra. Trapping of excitons at chemical defects in polyethylene. *The Journal of chemical physics*, 121(13):6478–6484, 2004.
(Cited on pages 5, 16, 18, and 48)
- [9] Jonathan W Martin, Rose Ann Ryntz, Joannie Chin, and Ray Dickie. *Service life prediction of polymeric materials: global perspectives*. springer science & business media, 2008.
(Cited on page 5)
- [10] Anne Xu, Sébastien Roland, and Xavier Colin. Thermal ageing of a silane-crosslinked polyethylene stabilised with an excess of irganox 1076[©]. *Polymer Degradation and Stability*, 189:109597, 2021.

(Cited on pages v, 5, 18, 20, 97, and 103)

- [11] *Assessing and Managing Cable Ageing in Nuclear Power Plants*. Number NP-T-3.6 in Nuclear Energy Series. INTERNATIONAL ATOMIC ENERGY AGENCY, Vienna, 2012.

(Cited on page 5)

- [12] HW Bock, R Burgis, J Eiler, HM Hashemian, KH Kim, AI Kononenko, S Manners, K Thoma, and T Yamamoto. Management of life cycle and ageing at nuclear power plants: Improved i&c maintenance. report prepared within the framework of the technical working group on nuclear power plant control and instrumentation. Technical report, IAEA-TECDOC-1402, 2004.

(Cited on page 5)

- [13] Zhi Wang, Ruichao Wei, Xiaoyao Ning, Tian Xie, and Jian Wang. Thermal degradation properties of lDpe insulation for new and aged fine wires. *Journal of Thermal Analysis and Calorimetry*, 137(2):461–471, 2019.

(Cited on pages v and 5)

- [14] Tadao Seguchi, Kiyotoshi Tamura, Hisaaki Kudoh, Akihiko Shimada, and Masaki Sugimoto. Degradation of cable insulation material by accelerated thermal radiation combined ageing. *IEEE Transactions on Dielectrics and Electrical Insulation*, 22(6):3197–3206, 2015.

(Cited on pages v and 5)

- [15] K. Anandakumaran and D. J. Stonkus. Determination of pvc cable insulation degradation. *Journal of Vinyl Technology*, 14(1):24–28, 1992.

(Cited on page 5)

- [16] E.F. Steennis and F.H. Kreuger. Water treeing in polyethylene cables. *IEEE Transactions on Electrical Insulation*, 25(5):989–1028, 1990.

(Cited on page 5)

- [17] G. Mazzanti, G.C. Montanari, and J.M. Alison. A space-charge based method for the estimation of apparent mobility and trap depth as markers for insulation degradation-theoretical basis and experimental validation. *IEEE Transactions on Dielectrics and Electrical Insulation*, 10(2):187–197, 2003.

(Cited on page 5)

- [18] A. Garton, S. Bamji, A. Bulinski, and J. Densley. Oxidation and water tree formation in service-aged xlpe cable insulation. *IEEE Transactions on Electrical Insulation*, EI-22(4):405–412, 1987.

(Cited on page 5)

- [19] JH Adams. Analysis of the nonvolatile oxidation products of polypropylene i. thermal oxidation. *Journal of Polymer Science Part A-1: Polymer Chemistry*, 8(5):1077–1090, 1970.
(Cited on page 5)
- [20] Dirk Willem Van Krevelen and Klaas Te Nijenhuis. *Properties of polymers: their correlation with chemical structure; their numerical estimation and prediction from additive group contributions*. Elsevier, 2009.
(Cited on page 5)
- [21] E. Linde, L. Verardi, D. Fabiani, and U.W. Gedde. Dielectric spectroscopy as a condition monitoring technique for cable insulation based on crosslinked polyethylene. *Polymer Testing*, 44:135–142, 2015.
(Cited on page 5)
- [22] Manuela Da Cruz, Laetitia Van Schoors, Karim Benzarti, and Xavier Colin. Thermo-oxidative degradation of additive free polyethylene. part i. analysis of chemical modifications at molecular and macromolecular scales. *Journal of Applied Polymer Science*, 133(18), 2016.
(Cited on pages 5, 6, 7, 10, 14, and 77)
- [23] Mélanie Gardette, Anthony Perthue, Jean-Luc Gardette, Tünde Janecska, Enikő Földes, Béla Pukánszky, and Sandrine Therias. Photo-and thermal-oxidation of polyethylene: comparison of mechanisms and influence of unsaturation content. *Polymer Degradation and Stability*, 98(11):2383–2390, 2013.
(Cited on page 6)
- [24] A Rivaton, S Cambon, and J-L Gardette. Radiochemical ageing of epdm elastomers. 3. mechanism of radiooxidation. *Nuclear Instruments and Methods in Physics Research Section B: Beam Interactions with Materials and Atoms*, 227(3):357–368, 2005.
(Cited on page 6)
- [25] Anne Xu. *Impact de la distribution des antioxydants sur la stabilisation des isolants PE de câbles électriques de centrale nucléaire*. Theses, HESAM Université, March 2021.
(Cited on pages 6 and 7)
- [26] Manfred Schmid and Samuel Affolter. Interlaboratory tests on polymers by differential scanning calorimetry (dsc): determination and comparison of oxidation induction time (OIT) and oxidation induction temperature (OIT*). *Polymer Testing*, 22(4):419–428, 2003.
(Cited on pages 6, 7, and 8)

- [27] J.V Gulmine, P.R Janissek, H.M Heise, and L Akcelrud. Polyethylene characterization by ftir. *Polymer Testing*, 21(5):557–563, 2002.
(Cited on page 6)
- [28] A. Valadez-Gonzalez, J.M. Cervantes-Uc, and L. Veleza. Mineral filler influence on the photo-oxidation of high density polyethylene: I. accelerated uv chamber exposure test. *Polymer Degradation and Stability*, 63(2):253–260, 1999.
(Cited on page 6)
- [29] VS Savost'yanov, DA Kritskaya, and AN Ponomarev. Investigation of formation of peroxides in γ -irradiated polyethylene by the method of iodometry. *Khimiya Vysokikh Ehnergij*, 20(2):153–158, 1986.
(Cited on page 6)
- [30] Masayuki Kuzuya, Junji Niwa, and Hideki Ito. Nature of plasma-induced surface radicals of powdered polyethylene studied by electron spin resonance. *Macromolecules*, 26(8):1990–1995, 1993.
(Cited on page 6)
- [31] Masayuki Kuzuya, Shin-ichi Kondo, Masami Sugito, and Tomoyuki Yamashiro. Peroxy radical formation from plasma-induced surface radicals of polyethylene as studied by electron spin resonance. *Macromolecules*, 31(10):3230–3234, 1998.
(Cited on page 6)
- [32] Anthony J. Bur. Dielectric properties of polymers at microwave frequencies: a review. *Polymer*, 26(7):963–977, 1985.
(Cited on page 6)
- [33] Kichinosuke Yahagi. Dielectric properties and morphology in polyethylene. *IEEE Transactions on Electrical Insulation*, EI-15(3):241–250, 1980.
(Cited on page 6)
- [34] X. Wang, H.Q. He, D.M. Tu, C. Lei, and Q.G. Du. Dielectric properties and crystalline morphology of low density polyethylene blended with metal-locene catalyzed polyethylene. *IEEE Transactions on Dielectrics and Electrical Insulation*, 15(2):319–326, 2008.
(Cited on page 6)
- [35] Luigi Costa, MP Luda, and Luigi Trossarelli. Ultra high molecular weight polyethylene—ii. thermal-and photo-oxidation. *Polymer Degradation and Stability*, 58(1-2):41–54, 1997.
(Cited on pages 6 and 15)

- [36] Mario Salvalaggio, Roberto Bagatin, Marco Fornaroli, Sergio Fanutti, Stefano Palmery, and Ezio Battistel. Multi-component analysis of low-density polyethylene oxidative degradation. *Polymer degradation and stability*, 91(11):2775–2785, 2006.
(Cited on page 6)
- [37] ZS Fodor, M Iring, F Tüdös, and T Kelen. Determination of carbonyl-containing functional groups in oxidized polyethylene. *Journal of Polymer Science: Polymer Chemistry Edition*, 22(10):2539–2550, 1984.
(Cited on page 6)
- [38] JL Bolland. Kinetic studies in the chemistry of rubber and related materials. i. the thermal oxidation of ethyl linoleate. *Proceedings of the Royal Society of London. Series A. Mathematical and Physical Sciences*, 186(1005):218–236, 1946.
(Cited on pages 7, 9, and 62)
- [39] JL Bolland and Geoffrey Gee. Kinetic studies in the chemistry of rubber and related materials. ii. the kinetics of oxidation of unconjugated olefins. *Transactions of the Faraday Society*, 42:236–243, 1946.
(Cited on pages 7 and 9)
- [40] JL Bolland and Geoffrey Gee. Kinetic studies in the chemistry of rubber and related materials. iii. thermochemistry and mechanisms of olefin oxidation. *Transactions of the Faraday Society*, 42:244–252, 1946.
(Cited on pages 7 and 9)
- [41] JL Bolland and P Ten Have. Kinetic studies in the chemistry of rubber and related materials. v. the inhibitory effect of phenolic compounds on the thermal oxidation of ethyl linoleate. *Discussions of the Faraday Society*, 2:252–260, 1947.
(Cited on pages 7 and 9)
- [42] L Bateman. Olefin oxidation. *Quarterly Reviews, Chemical Society*, 8(2):147–167, 1954.
(Cited on pages 7 and 9)
- [43] Ganna Gryn'ova, Jennifer L Hodgson, and Michelle L Coote. Revising the mechanism of polymer autooxidation. *Organic & biomolecular chemistry*, 9(2):480–490, 2011.
(Cited on pages 9, 10, 16, 53, and 59)
- [44] KU Ingold. Inhibition of the autoxidation of organic substances in the liquid phase. *Chemical Reviews*, 61(6):563–589, 1961.
(Cited on pages 9 and 54)

- [45] F. Gugumus. Physico-chemical aspects of polyethylene processing in an open mixer. discussion of hydroperoxide formation and decomposition. *Polymer Degradation and Stability*, 68(3):337–352, 2000.
(Cited on page 9)
- [46] Ondrej Kysel', Šimon Budzák, Miroslav Medved', and Pavel Mach. A dft study of h-isomerisation in alkoxy-, alkylperoxy-and alkyl radicals: Some implications for radical chain reactions in polymer systems. *Polymer degradation and stability*, 96(4):660–669, 2011.
(Cited on pages 9, 16, 17, 53, and 78)
- [47] Yu-Ran Luo. *Handbook of bond dissociation energies in organic compounds*. CRC press, 2002.
(Cited on pages 9 and 53)
- [48] YR Luo. *Handbook of bond dissociation energies in organic compounds* crc. New York, page 61, 2003.
(Cited on page 10)
- [49] N Khelidj, X Colin, L Audouin, J Verdu, C Monchy-Leroy, and V Prunier. Oxidation of polyethylene under irradiation at low temperature and low dose rate. part ii. low temperature thermal oxidation. *Polymer degradation and stability*, 91(7):1598–1605, 2006.
(Cited on pages 10 and 81)
- [50] Liang Chen, Shogo Yamane, Tomohiro Sago, Hideaki Hagihara, Shuzo Kutsuna, Tadafumi Uchimaru, Hiroyuki Suda, Hiroaki Sato, and Junji Mizukado. Experimental and modeling approaches for the formation of hydroperoxide during the auto-oxidation of polymers: Thermal-oxidative degradation of polyethylene oxide. *Chemical Physics Letters*, 657:83–89, 2016.
(Cited on pages 11 and 60)
- [51] Pascal de Sainte Claire. Degradation of peo in the solid state: A theoretical kinetic model. *Macromolecules*, 42(10):3469–3482, 2009.
(Cited on pages 11, 16, 17, 63, 66, 67, 77, 78, and 87)
- [52] Roger Atkinson. Kinetics and mechanisms of the gas-phase reactions of the hydroxyl radical with organic compounds under atmospheric conditions. *Chemical Reviews*, 86(1):69–201, 1986.
(Cited on pages 11 and 60)
- [53] Phillip D Lightfoot, RA Cox, JN Crowley, M Destriau, GD Hayman, ME Jenkin, GK Moortgat, and F Zabel. Organic peroxy radicals: kinetics, spectroscopy and tropospheric chemistry. *Atmospheric Environment. Part A. General Topics*, 26(10):1805–1961, 1992.
(Cited on pages 11 and 60)

- [54] Leesa M Smith, Heather M Aitken, and Michelle L Coote. The fate of the peroxy radical in autoxidation: how does polymer degradation really occur? *Accounts of chemical research*, 51(9):2006–2013, 2018.
(Cited on pages 11 and 12)
- [55] Lies De Keer, Paul Van Steenberge, Marie-Françoise Reyniers, Ganna Gryn'Ova, Heather M Aitken, and Michelle L Coote. New mechanism for autoxidation of polyolefins: kinetic monte carlo modelling of the role of short-chain branches, molecular oxygen and unsaturated moieties. *Polymer Chemistry*, 13(22):3304–3314, 2022.
(Cited on pages 11, 78, 81, and 135)
- [56] Pieter Gijsman, Jan Hennekens, and Jef Vincent. The mechanism of the low-temperature oxidation of polypropylene. *Polymer Degradation and Stability*, 42(1):95–105, 1993.
(Cited on pages 11, 63, and 77)
- [57] B Fayolle, J Verdu, M Bastard, and D Piccoz. Thermooxidative ageing of polyoxymethylene, part 1: chemical aspects. *Journal of applied polymer science*, 107(3):1783–1792, 2008.
(Cited on pages 11, 63, and 77)
- [58] Frédéric Fraisse, Sandrine Morlat-Therias, J-L Gardette, J-M Nedelec, and Mohamed Baba. In situ kinetics study of the accelerated aging of poly (ethylene oxide) using photodisc. *The Journal of Physical Chemistry B*, 110(30):14678–14684, 2006.
(Cited on page 11)
- [59] Jacqueline L Henry, Ascencion L Ruaya, and Andrew Garton. The kinetics of polyolefin oxidation in aqueous media. *Journal of Polymer Science Part A: Polymer Chemistry*, 30(8):1693–1703, 1992.
(Cited on pages 11, 63, and 77)
- [60] Liang Chen, Qin Guo, Shuzo Kutsuna, and Junji Mizukado. Determination of the mechanism of polymer thermolysis at low temperatures using spin trap electron spin resonance. *Polymer*, 203:122747, 2020.
(Cited on page 11)
- [61] Luigi Costa, I Carpentieri, and Pierangiola Bracco. Post electron-beam irradiation oxidation of orthopaedic uhmwpe. *Polymer Degradation and Stability*, 93(9):1695–1703, 2008.
(Cited on page 11)

- [62] Ibukun Oluwoye, Mohammednoor Altarawneh, Jeff Gore, and Bogdan Z Dlugogorski. Oxidation of crystalline polyethylene. *Combustion and Flame*, 162(10):3681–3690, 2015.
(Cited on pages 11, 16, 17, 19, 63, 77, and 78)
- [63] John M Simmie, Gráinne Black, Henry J Curran, and John P Hinde. Enthalpies of formation and bond dissociation energies of lower alkyl hydroperoxides and related hydroperoxy and alkoxy radicals. *The Journal of Physical Chemistry A*, 112(22):5010–5016, 2008.
(Cited on pages 11, 63, and 77)
- [64] Bruno Fayolle, Emmanuel Richaud, Xavier Colin, and Jacques Verdu. Degradation-induced embrittlement in semi-crystalline polymers having their amorphous phase in rubbery state. *Journal of materials science*, 43(22):6999–7012, 2008.
(Cited on pages 13, 14, and 78)
- [65] AK Rodriguez, B Mansoor, G Ayoub, Xavier Colin, and AA Benzerga. Effect of uv-aging on the mechanical and fracture behavior of low density polyethylene. *Polymer Degradation and Stability*, 180:109185, 2020.
(Cited on pages 13 and 78)
- [66] Arthur Charlesby. *Atomic radiation and polymers: international series of monographs on radiation effects in materials*. Elsevier, 2016.
(Cited on page 14)
- [67] ADOLPHE Chapiro. Radiation chemistry of polymeric systems. interscience publ. Inc.(New York), 1962.
(Cited on page 14)
- [68] Walter J Chappas and Joseph Silverman. The radiation chemistry of crystalline alkanes. *Radiation Physics and Chemistry (1977)*, 16(6):437–443, 1980.
(Cited on page 14)
- [69] Christian Decker and Frank R Mayo. Aging and degradation of polyolefins. ii. γ -initiated oxidations of atactic polypropylene. *Journal of Polymer Science: Polymer Chemistry Edition*, 11(11):2847–2877, 1973.
(Cited on pages v, 14, 18, and 21)
- [70] Ajit Singh. Irradiation of polyethylene: Some aspects of crosslinking and oxidative degradation. *Radiation Physics and chemistry*, 56(4):375–380, 1999.
(Cited on page 14)

- [71] RA Jones, GA Salmon, and IM Ward. Radiation-induced crosslinking of polyethylene in the presence of acetylene: A gel fraction, uv-visible, and esr spectroscopy study. *Journal of Polymer Science Part B: Polymer Physics*, 31(7):807–819, 1993.
(Cited on page 14)
- [72] Salem F Chabira, Mohamed Sebaa, and Christian G'sell. Oxidation and crosslinking processes during thermal aging of low-density polyethylene films. *Journal of applied polymer science*, 124(6):5200–5208, 2012.
(Cited on page 14)
- [73] Malcolm Dole. Free radicals in irradiated polyethylene. *The radiation chemistry of macromolecules*, 1:335, 1972.
(Cited on page 14)
- [74] Yongxiang Feng and Zueteh Ma. Crosslinking of wire and cable insulation using electron accelerators. In *Radiation processing of polymers*. 1992.
(Cited on page 14)
- [75] Yu-Chieh Hsu, Michael P Weir, Rowan W Truss, Christopher J Garvey, Timothy M Nicholson, and Peter J Halley. A fundamental study on photo-oxidative degradation of linear low density polyethylene films at embrittlement. *Polymer*, 53(12):2385–2393, 2012.
(Cited on page 14)
- [76] Sudesh S Fernando, Paul A Christensen, Terry A Egerton, and Jim R White. Humidity dependence of carbon dioxide generation during photodegradation of biaxially oriented polypropylene in oxygen. *Polymer Degradation and Stability*, 94(1):83–89, 2009.
(Cited on pages 14 and 15)
- [77] PA Christensen, A Dilks, TA Egerton, and J Temperley. Infrared spectroscopic evaluation of the photodegradation of paint part i the uv degradation of acrylic films pigmented with titanium dioxide. *Journal of Materials Science*, 34(23):5689–5700, 1999.
(Cited on pages 14 and 15)
- [78] Changqing Jin, PA Christensen, TA Egerton, EJ Lawson, and JR White. Rapid measurement of polymer photo-degradation by ftir spectrometry of evolved carbon dioxide. *Polymer Degradation and Stability*, 91(5):1086–1096, 2006.
(Cited on pages 14 and 15)
- [79] Patrick Delprat, Xavier Duteurtre, and Jean-Luc Gardette. Photooxidation of unstabilized and hals-stabilized polyphasic ethylene-propylene polymers. *Polymer degradation and stability*, 50(1):1–12, 1995.
(Cited on page 15)

- [80] Jean-Louis Philippart, Fabrice Posada, and Jean-Luc Gardette. Mass spectroscopy analysis of volatile photoproducts in photooxidation of polypropylene. *Polymer degradation and stability*, 49(2):285–290, 1995.
(Cited on page 15)
- [81] Carrigan J Hayes and Donald R Burgess Jr. Kinetic barriers of h-atom transfer reactions in alkyl, allylic, and oxoallylic radicals as calculated by composite ab initio methods. *The Journal of Physical Chemistry A*, 113(11):2473–2482, 2009.
(Cited on pages 16 and 78)
- [82] Yuji Higuchi, Takeshi Ishikawa, Nobuki Ozawa, Laurent Chazeau, Jean-Yves Cavaillé, and Momoji Kubo. Different dynamic behaviors of the dissociation and recombination reactions in a model calculation of polyethylene by first-principles steered molecular dynamics simulation. *Chemical Physics*, 459:96–101, 2015.
(Cited on page 16)
- [83] JCL Hageman, GA De Wijs, RA De Groot, and Robert J Meier. Bond scission in a perfect polyethylene chain and the consequences for the ultimate strength. *Macromolecules*, 33(24):9098–9108, 2000.
(Cited on pages 16, 53, 54, and 87)
- [84] Irmgard Frank, Michele Parrinello, and Andreas Klamt. Insight into chemical reactions from first-principles simulations: the mechanism of the gas-phase reaction of oh radicals with ketones. *The Journal of Physical Chemistry A*, 102(20):3614–3617, 1998.
(Cited on pages 16 and 17)
- [85] Luc Vereecken, Thanh Lam Nguyen, Ive Hermans, and Jozef Peeters. Computational study of the stability of α -hydroperoxyl-or α -alkylperoxyl substituted alkyl radicals. *Chemical physics letters*, 393(4-6):432–436, 2004.
(Cited on page 17)
- [86] Ghanshyam L Vaghjiani and AR Ravishankara. Kinetics and mechanism of oh reaction with ch₃ooh. *J. phys. Chem*, 93(5):1948–1959, 1989.
(Cited on pages 17 and 67)
- [87] F Gugumus. Thermolysis of polyethylene hydroperoxides in the melt: 1. experimental kinetics of hydroperoxide decomposition. *Polymer degradation and stability*, 69(1):23–34, 2000.
(Cited on pages 17 and 64)

- [88] Wai-To Chan, IP Hamilton, and Huw O Pritchard. Self-abstraction in aliphatic hydroperoxyl radicals. *Journal of the Chemical Society, Faraday Transactions*, 94(16):2303–2306, 1998.
(Cited on page 17)
- [89] Graciela Bravo-Pérez, J Raúl Alvarez-Idaboy, Annia Galano Jiménez, and Armando Cruz-Torres. Quantum chemical and conventional tst calculations of rate constants for the OH^+ alkane reaction. *Chemical physics*, 310(1-3):213–223, 2005.
(Cited on page 17)
- [90] Tadao Seguchi, Kiyotoshi Tamura, Akihiko Shimada, Masaki Sugimoto, and Hisaaki Kudoh. Mechanism of antioxidant interaction on polymer oxidation by thermal and radiation ageing. *Radiation Physics and Chemistry*, 81(11):1747–1751, 2012.
(Cited on page 18)
- [91] S. Al-Malaika, S. Riasat, and C. Lewucha. Reactive antioxidants for peroxide crosslinked polyethylene. *Polymer Degradation and Stability*, 145:11–24, 2017. Modification, Degradation and Stabilisation of Polymers: Concepts and Applications (MoDeSt 2016).
(Cited on page 18)
- [92] Jan Pospíšil. Mechanistic action of phenolic antioxidants in polymers—a review. *Polymer Degradation and Stability*, 20(3):181–202, 1988. Polymer Additives in Stabilisation: Performance and Mechanisms.
(Cited on pages v and 18)
- [93] J. Pospíšil. Transformations of phenolic antioxidants during the inhibited oxidation of polymers. *Pure and Applied Chemistry*, 36(1-2):207–232, 1973.
(Cited on page 18)
- [94] Jan Pospíšil. Chemical and photochemical behaviour of phenolic antioxidants in polymer stabilization—a state of the art report, part i. *Polymer Degradation and Stability*, 40(2):217–232, 1993.
(Cited on page 18)
- [95] YG Hsuan and RM Koerner. Antioxidant depletion lifetime in high density polyethylene geomembranes. *Journal of Geotechnical and Geoenvironmental Engineering*, 124(6):532–541, 1998.
(Cited on pages v and 18)
- [96] Sahar Al-Malaika. Oxidative degradation and stabilisation of polymers. *International Materials Reviews*, 48(3):165–185, 2003.
(Cited on pages 18 and 97)

- [97] Anne Xu, Sébastien Roland, and Xavier Colin. Thermal ageing of a silane-crosslinked polyethylene stabilised with a thiodipropionate antioxidant. *Polymer Degradation and Stability*, 181:109276, 2020.

(Cited on pages 19 and 20)

- [98] M Ferry and Y Ngono. Energy transfer in polymers submitted to ionizing radiation: A review. *Radiation Physics and Chemistry*, 180:109320, 2021.

(Cited on page 20)

- [99] M Ferry, E Bessy, H Harris, PJ Lutz, J-M Ramillon, Y Ngono-Ravache, and E Balanzat. Irradiation of ethylene/styrene copolymers: Evidence of sensitization of the aromatic moiety as counterpart of the radiation protection effect. *The Journal of Physical Chemistry B*, 116(6):1772–1776, 2012.

(Cited on pages v, 20, and 97)

2 - Methodology

2.1 . Introduction

In this chapter, we explain several approaches for optimizing systems and determining equilibrium structures, energy barriers along reaction pathways, and formation energies as the background of our study. Car-Parrinello molecular dynamics (CPMD) is also introduced to investigate the diffusion mechanisms of oxygen or other oxidative reactions. The chapter also describes the computational details used in the study and how PE was modeled using isolated molecules, crystalline solid phase, and the surface between lamellar structures, stressing the importance of the environment in which the reaction takes place. All calculated results were obtained from QUANTUM ESPRESSO (opEn-Source Package for Research in Electronic Structure, Simulation, and Optimization), or QE, which is free software distributed under the GNU General Public License [1]. Based on density functional theory (DFT), plane-wave self-consistent field (PWSCF) calculations can optimize the atomic configuration. Moreover, for more specialized calculations, QE includes other useful packages, for example, i) PWneb: the Nudged Elastic Band (NEB) for energy barriers and reaction pathways, ii) PHonon: Density Functional Perturbation Theory (DFPT) for vibrational properties, and iii) TD-DFPT: spectra from Time Dependent DFPT. Here, we used the packages PWscf, PWneb, and CP. For more information, please refer to Ref.[2].

2.2 . Background of DFT

In contrast to top-down approach, which extracts empirical laws by fitting experimental measurements, bottom-up approach relies on quantum mechanical considerations without requiring empirical parameters. This approach, so-called *ab initio* or DFT (from first principles), requires only a few parameters determined from experiments such as the electron mass, m_e , the electron charge, e , the nuclear masses, M_I , the permittivity of vacuum, ϵ_0 , and the reduced Planck constant, \hbar , and finally, it allows ‘materials modeling’ by making many properties of materials predictable at the atomic scale. In particular, DFT solves an approximate version of the Schrödinger equation that effectively studies various materials or environments, including organic molecules, polymers, metals, surfaces, and interfaces. Historically, Hohenberg and Kohn published the first report on DFT in 1964, entitled ‘Inhomogeneous electron gas’ [3]. It explained the relationship between the total energy of a many electron system in the ground state and a functional of electron density. However, from a practical point of view, this theorem did not suggest specific methods to construct such functional. While such functional is still unknown useful ways to approximate functionals have been developed, starting

from the single particle Schrödinger-like equations proposed by Kohn and Sham[4]:

$$\left[-\frac{1}{2}\nabla^2 + V_n(r) + V_H(r) + V_{xc}(r)\right]\phi_i(r) = \epsilon_i\phi_i(r) \quad (2.1)$$

where appear the external nuclear potential, V_n , the Hartree potential, V_H , the exchange and correlation potential, V_{xc} , and the kinetic energy, $-\nabla^2/2$. Each term is given by:

$$V_n(r) = -\sum_I \frac{Z_I}{|r - R_I|^2} \quad (2.2)$$

$$\nabla^2 V_H(r) = -4\pi n(r) \quad (2.3)$$

$$n(r) = \sum_i |\phi_i(r)|^2 \quad (2.4)$$

$$V_{xc}(r) = \frac{\delta E_{xc}[n]}{\delta n} |_{n(r)} \quad (2.5)$$

Taking a closer look at eqn.2.1, the external nuclear potential, V_n , is the Coulomb potential of the nuclei (clamped) experienced by the electrons, and the Hartree potential, V_H , is the classical electrostatic potential satisfying Poisson's equation with the electronic charge $n(r)$. These two terms describe electrons as single particle wavefunctions based on the independent electrons approximation, and ignore the Pauli's exclusion principle and the quantum contribution to electron-electron interactions. For further improvement, in order to move to the 'quantum' electrons, we consider the exchange and correlation potential, V_{xc} , which takes into account Pauli's exclusion principle and the interaction of electrons, respectively. Finally, eqn.2.1 is called Kohn-Sham (KS) the equation and form the basis of the Kohn-Sham theory [4] (Kohn and Sham, 1965). The goal of the theory is to find the ground state, nuclei are classically treated following the adiabatic approximation that decouples the system of nuclei and electrons (see details in 2.3). This equation proposes a very powerful way of calculating various properties of materials starting from the very basic principles of quantum mechanics. If we knew the exact functional $E_{xc}[n]$, we could calculate the exact ground state energy and density using eqn.2.1 and eqn.2.5. However, we do not know what this functional is. We are left with the problem of devising useful approximations of $E_{xc}[n]$.

2.2.1 . Several functionals

Since the introduction of the Kohn-Sham theory, great effort has been dedicated to constructing $E_{xc}[n]$, in order to solve KS equations. Although we do not know the exact $E_{xc}[n]$ yet, we could set a functional depending on our purpose. The choice of the exchange correlation (xc) functional is guided by a compromise between accuracy and computational cost. Several functionals are available today,

such as the local density approximation (LDA), the generalized gradient approximation (GGA), van der Waals density functional (vdW-DF), and hybrid functionals [5, 6, 7]. The most commonly used approximations are LDA and GGA. The LDA approximates $E_{xc}[n]$ as a local functional of the density, which means

$$E_{xc}^{LDA}[n] = \int n(r)\epsilon_{xc}(n(r))dr \quad (2.6)$$

Where ϵ_{xc} is the exchange-correlation energy per particle of a homogeneous electron gas of charge density $n(r)$. This approximation is simple and, in many cases, a good one. However, due to the local character and the parametrization of a homogeneous system, it is expected to fail in situations where the density changes rapidly, such as in molecules. For the GGA, it could lead to a significant improvement over the LDA by considering the gradient of the electron density; in this case, the exchange-correlation energy can be written as

$$E_{xc}^{GGA}[n] = E_{xc}[n(r), \nabla n(r)] \quad (2.7)$$

This exchange-correlation energy can still be calculated as the integral of a local function, as for the LDA, but it is called a semi-local approximation. In order to improve the calculation of many molecular properties, such as dissociation energies and bond lengths, the exchange-correlation could incorporate a portion of exact Hartree-Fock exchange energy, a so-called hybrid functional. In this thesis, most calculations were obtained with a GGA functional (optB86b+vdW or vdw-df-ob86) containing a long-range nonlocal correlation term, which is known to describe quite well weak interactions [8]. These are important, especially in describing solid PE, where chain-chain interactions are of van der Waals (vdW) type. We also operate the hybrid functional (vdw-df-cx0)[9] including vdW long range correlation part, which is missing in other popular hybrid functionals such as PBE0, HSE, and B3LYP, but only for a few calculations due to a huge computing time.

2.2.2 . Self-consistent calculations

Based on Kohn-Sham equations, we can calculate the total energy of a given structure. The total potential, $V_{tot} = V_n(r) + V_H(r) + V_{xc}(r)$, determines the unknown eigenfunctions, ϕ_i , and eigenvalues, ϵ_i . The electron density calculated from the eigenfunctions, ϕ_i , is linked with the potentials, which implies self-consistency. The algorithm is well explained in Fig.2.1. By specifying the initial nuclear coordinates and assuming the nuclei are fixed, we firstly obtain the nuclear potential, V_n . And then, we guess a possible electron density from the potential in order to have the Hartree and exchange and correlation potentials with a functional that we chose for the total potential. From the total potential, we can obtain the eigenfunctions and the charge density. This process is 'self-consistently operated until the new and old density reach the convergence threshold.

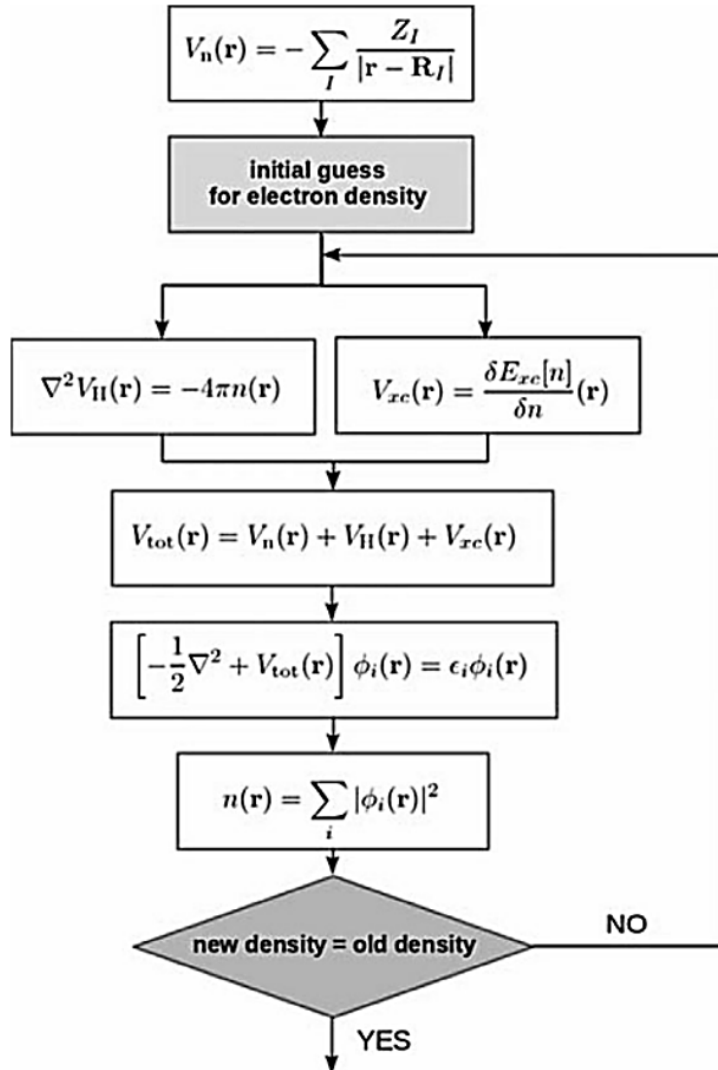


Figure 2.1 - DFT self-consistency algorithm [10]

2.2.3 . Equilibrium structures

The equilibrium structure of a material is obtained by relaxing the atomic positions in the framework of DFT (at $T = 0$) in order to find the minimum of the potential energy surface. The equilibrium structures are reached when the total force acting on each nucleus totally cancels out so that the configuration of the nuclei does not change.

The forces on each of the M atoms (of coordinates R_1, \dots, R_M) are computed at the end of the self-consistent loop thanks to the Hellmann-Feynman theorem:

$$\frac{dE}{dR_I} = \langle \phi_i | \frac{dH}{dR_I} | \phi_i \rangle \quad (2.8)$$

which tells us that the force on atom I , i.e., the derivative of the total energy to

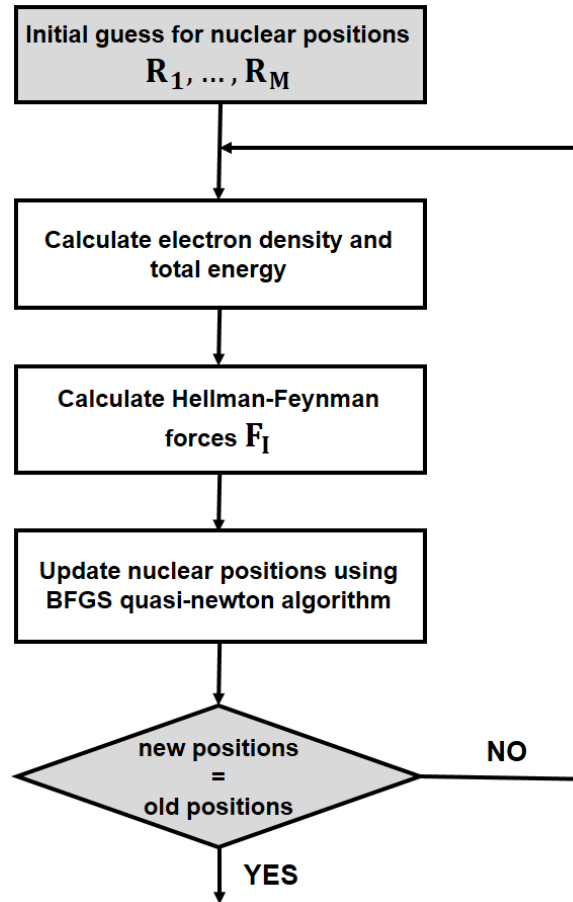


Figure 2.2 – Schematic algorithm for finding the equilibrium structure adapted from Ref.[10]

the coordinate R_I , can be calculated as the expectation value of the derivative of the Hamiltonian, without the need of knowing the derivative of the single particle wave functions ϕ_i . As we know the analytic derivative of the ionic potential (in our case, a pseudopotential), the calculation of forces is straightforward once we know the electron density, $n(r)$, obtained as explained in the section 2.2.2, we could calculate the forces on all the M atoms in our system. Then we adopt the updated atomic positions and compare new positions and old positions. The calculations are terminated when all forces are below a certain fixed threshold. The last atomic positions are the positions of the system's equilibrium configuration. The algorithm is illustrated in Fig.2.2.

2.2.4 . Energy cut-off

To solve KS differential equations, we use a plane-wave (PW) expansion of the one-electron wave-functions. In theory, the plane-wave basis set is composed of an infinite number of elements. However, for the purposes of calculation, the practical solutions in reciprocal space should involve the use of a finite basis set.

It means that we should set a maximum number of basis functions by fixing an energy cut-off [11]. In other words, the kinetic energy of a plane wave of wave vector $k + G$ at each k-point must be lower than a maximum cut-off:

$$\frac{1}{2m_e}|k + G|^2 < E_{cut} \quad (2.9)$$

where G is a vector of the reciprocal lattice. We could set high cut-off energy to increase the number of basis functions to make a more accurate calculation; however, the higher E_{cut} , the higher cost of computing resources is required. Therefore, finding an optimal cut-off energy value for each system is necessary. In practice, because the basis set would require a huge number of elements to describe the core electrons around the nuclei, we can consider only the valence electrons, which are the most sensitive to the chemical environment and we neglect the core electrons, which are tightly bound to the nuclei (the pseudopotential approximation). For PE, 60 Ry cut-off energy ensures a reasonably good convergence with the selected pseudopotentials (Fig. 2.3)

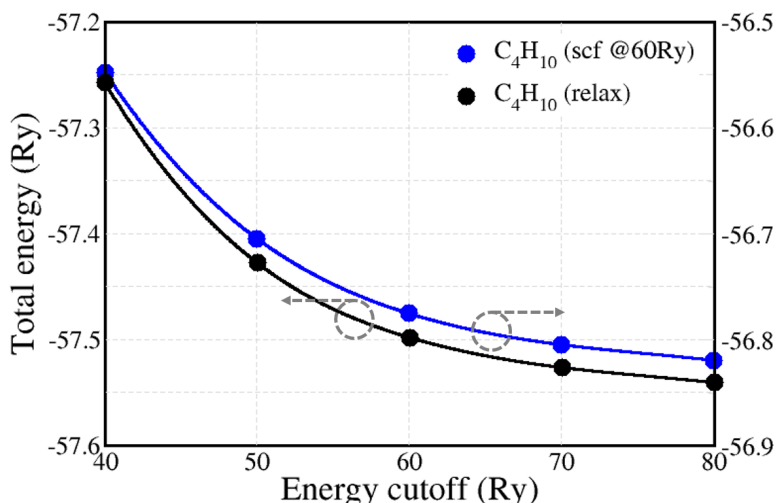


Figure 2.3 – Energy vs. Cut-off energy diagram of C_4H_{10} . The black line connects points representing calculations where atomic positions are relaxed and the blue line represents calculations where atomic positions at fixed structure.

When the atomic positions are relaxed by the algorithm shown in Fig.2.2, 60 Ry appears slightly away from the converged E_{cut} , and the energy difference from 70 Ry is 0.4 eV (Fig. 2.3). Although the larger energy, such as 80 Ry is required for the convergence, it is much more important to approach the calculations in terms of relative energies rather than absolute energies, especially considering that most of the calculations considered in this thesis are NEB and formation energy. Therefore, additional convergence tests are needed to determine the appropriate

energy required for both calculations. It should also be noted that the computation time required increases as the energy increases.

First, to proceed with the convergence test according to E_{cut} , the formation energy of double bond (C_4H_8) was calculated using vdw-df-ob86 and vdw-df-cx0 functionals. The calculated results in Fig.2.4 show that 60 Ry is a reliable value as it does not have a significant difference compared to higher energies. Next, NEB calculations also exhibit reasonable results. The calculation results of the activation energy required for the intramolecular H-transfer reaction in 2-3 alkyl radicals (C_4H_9) are shown in Fig.2.5(a), and the activation energies are well converged from 50 Ry. Fig.2.5(b) shows that, as mentioned earlier, the higher E_{cut} , the more computing time is required. Therefore, based on these convergence test results, we believe that 60 Ry is an appropriate value that can be used in the calculations covered in this thesis.

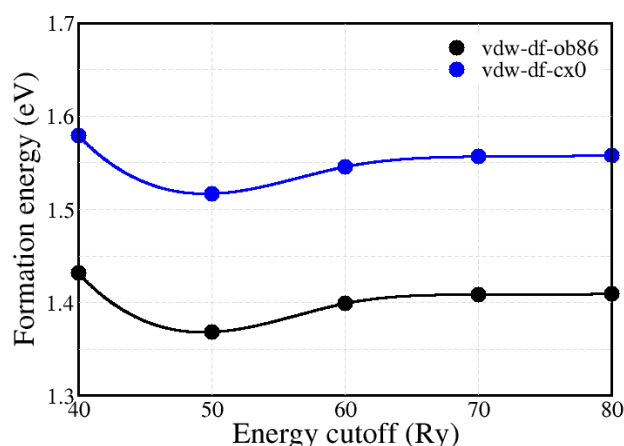


Figure 2.4 – Formation energy of a double bond in an alkane chain with four carbon atoms as a function of the plane-wave energy cut-off, for two xc-functionals. The formation energy is obtained by $E_{form}^{C_4H_8} = E(C_4H_8) - E(C_4H_{10}) + E(H_2)$. See details in Section 2.4

2.2.5 . k-point convergence

In periodic boundary conditions, the problem of convergence in \vec{k} points is directly related to a numerical limitation: computation of integrals. Indeed, to calculate an electronic density, it is necessary to integrate the wave function of the system on the Brillouin zone (BZ). These integrals must be performed on a discrete grid of \vec{k} points in the reciprocal space. The accuracy and computing time of the calculation of integrals depends on the size of the chosen \vec{k} -point grid. Therefore, the optimal size of the grid should result from a trade-off between computing time and required accuracy. We consider grids of dimensions $N \times N \times N$ where the size

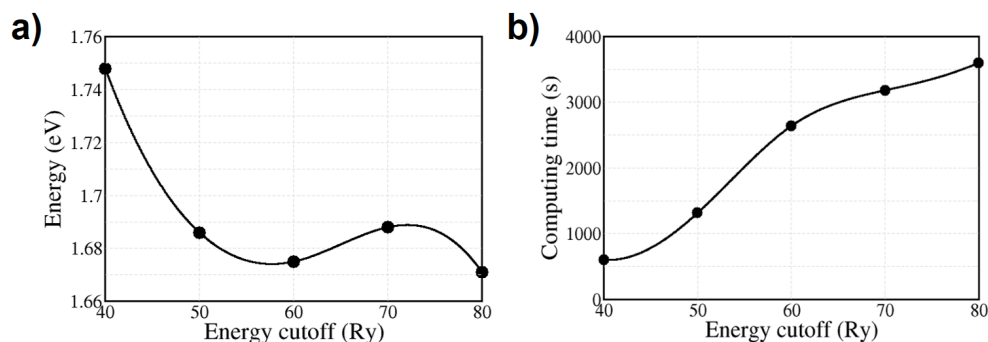


Figure 2.5 – NEB calculation. (a) Calculated activation energies for the reactions of 2-3 intramolecular H-shift in C_4H_9 and (b) computing time corresponding the reactions at each energy cut-off.

N represents the number of \vec{k} points in each of the three Cartesian directions.

For a unit cell of the orthorhombic crystal containing 12 atoms, we sampled the BZ with a $3 \times 3 \times 6$ Γ -centered Monkhorst-Pack mesh [12]. In Fig.2.6, we could see that the convergence of the energy vs. k -point grid size is slower along the z -axis, which is the chain direction of PE. To model isolated defects in the solid, we used a $2 \times 1 \times 4$ supercell containing 96 atoms; for it, we employed a $2 \times 3 \times 2$ Γ -centered Monkhorst-Pack mesh because the volume of the real space varies as the inverse of the volume of the reciprocal space.

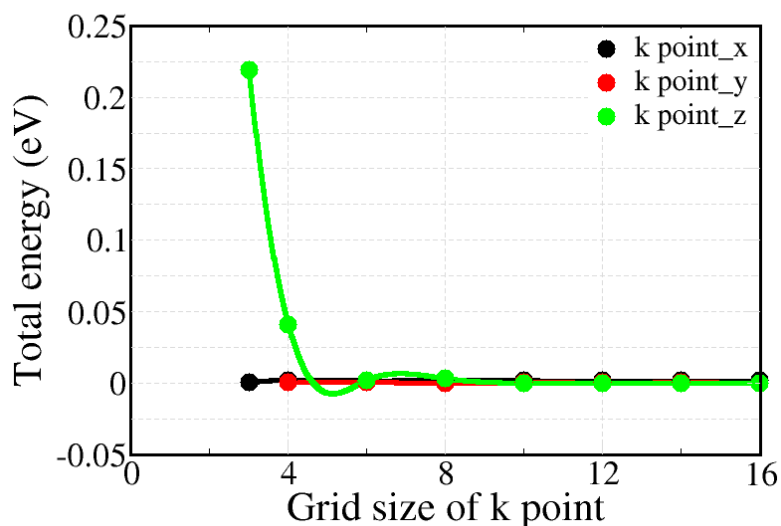


Figure 2.6 – Total energy vs. Grid size of \vec{k} point diagram. When we vary the number of \vec{k} points in one direction, the others are fixed from a $3 \times 3 \times 6$ Γ -centered Monkhorst-Pack mesh

2.3 . Nudged Elastic Band (NEB) Calculation

In order to investigate the reaction pathways of polyethylene degradation, it is important to predict energy barriers and transition states because the reaction rate coefficient (k) is a crucial quantity for kinetic studies and determines the main reactions among the possible competing reactions. In particular, the rate constant is commonly expressed through an Arrhenius equation with activation energy E_a as follows:

$$k = Ae^{-\frac{E_a}{k_B T}} \quad (2.10)$$

where appear also the Boltzmann constant, k_B , and the pre-exponential factor, A . Eqn. 2.10 turns out to well represent in many cases a more general form, known as the Eyring equation, derived from statistical mechanics and Transition State Theory, where instead of the E_a appears the Gibbs activation free energy of activation, expressed by $\Delta G^\ddagger = \Delta H^\ddagger - T\Delta S^\ddagger$, where ΔH^\ddagger is the enthalpy of activation, and the ΔS^\ddagger is the entropy of activation (\ddagger is to specify at the transition state). Therefore, we can develop eqn. 2.10 as follows:

$$k = \frac{\kappa k_B T}{\hbar} e^{\frac{\Delta S^\ddagger}{k_B}} e^{-\frac{\Delta H^\ddagger}{k_B T}} \quad (2.11)$$

where κ is the rate coefficient. Eqn.2.11 can be written in logarithmic form as:

$$\ln \frac{k}{T} = \frac{-\Delta H^\ddagger}{R} \frac{1}{T} + \ln \frac{\kappa k_B}{\hbar} + \frac{\Delta S^\ddagger}{k_B} \quad (2.12)$$

In this thesis, we perform mostly DFT calculation $T = 0K$ (Kelvin), and we do not add a temperature dependent vibrational entropy term, neglecting thus entropic contribution to the activation barriers. This is a reasonable approximation in many cases, using a fixed prefactor as in eqn.2.10.

Calculations of activation energy are performed using the nudged elastic band method [13]. This method aims to find saddle points and minimum energy paths from a complex energy landscape between reactants and products for which we already calculated equilibrium structures. Between these initial and final structures, a number of intermediate configurations, called images, are set by linear interpolation and subsequently optimized. The number of images is a parameter that the user can modify to improve the calculation. As for other parameters, there is a trade-off between accuracy and time. At each NEB iteration, the total energy and the forces are calculated for each image to find the lowest energy while maintaining equal spacing between neighboring images. This is possible by adding spring forces between images by keeping control of the distribution of the images. Therefore, the total force acting on an image is the sum of the spring forces along the local tangent and the true force perpendicular to the local tangent, which follows as:

$$F_i = F_i^s|_{\parallel} - \nabla E(R_i)|_{\perp} \quad (2.13)$$

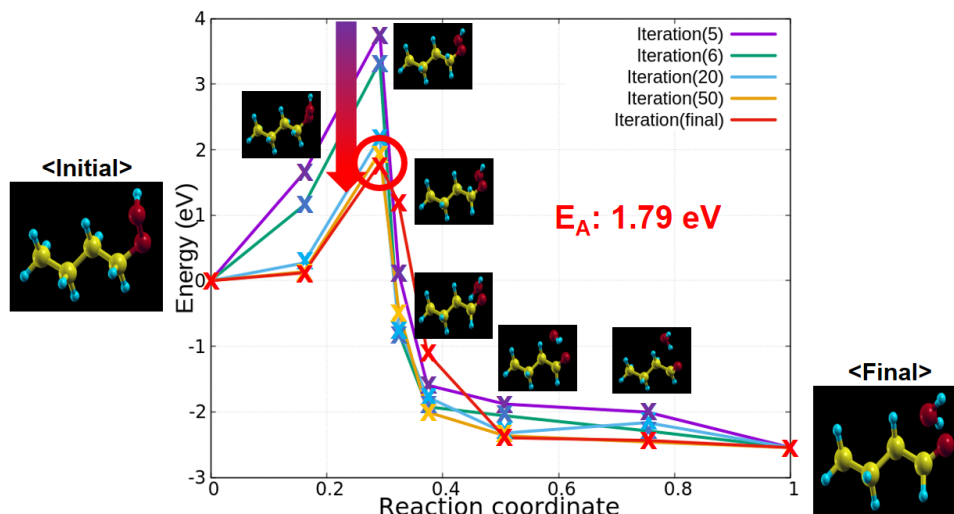


Figure 2.7 – NEB calculation for the reaction of a hydroperoxide leading to a ketone ($C_4H_{10}O_2 \rightarrow C_4H_8O + H_2O$)

Where the spring force is $F_i^s|_{\parallel}$ and the true force is $\nabla E(R_i)|_{\perp}$. For more accurate determination of saddle points, we applied the climbing image algorithm in order to drive the highest energy image to the saddle point. The details of the method can be found in Ref.[13]. Fig.2.7 shows an example of NEB calculation for the reaction of a hydroperoxide leading to a ketone ($C_4H_{10}O_2 \rightarrow C_4H_8O + H_2O$). There are eight images, including local minima of initial and final states. During iteration steps, a transition state is converged to find the minimum energy, and it is not fully relaxed due to spring force. Each image could be visualized by calculation, which is one of the advantages of NEB. The obtained activation energy is 1.79 eV.

2.4 . Formation energy

In order to determine the formation energies in our system, we need to calculate the total energy of its equilibrium structures and its constituent parts. The calculation of the formation energy of a compound with respect to the isolated constituents is then written:

$$E_{form} = E_{tot} - \sum_x E_{tot}(x) \quad (2.14)$$

Where E_{form} is the energy required to dissociate the material into its individual components, x . For hydrocarbon compounds such as C_nH_m , the formation energy could be given by

$$E_{form}^{C_nH_m} = E_{tot} - n\mu_C - m\mu_H \quad (2.15)$$

Where μ_C and μ_H are chemical potentials of reference. In the case of peroxy radical, or other localized modifications of the alkane chain, that we consider as point defects, we take the formation energy with respect to the alkane chain without the defect, using as chemical potentials for extra hydrogen or oxygen atoms their energy in the gas phase (H_2 and O_2).

For example, when we calculate the formation energy of the peroxy radical ($C_nH_{2n+1}O_2$), the equation is as follows:

$$E_{form}^{C_nH_{2n+1}O_2} = E(C_nH_{2n+1}O_2) - E(C_nH_{2n+2}) + \frac{1}{2}E(H_2) - E(O_2) \quad (2.16)$$

The results of calculated formation energies are summarized in Table 2.1. To calculate the formation energy of peroxy radicals, we chose two positions when oxygen reacts in the middle or at the end of the alkyl chain and we vary the length of the chain from $C_4H_9O_2$ to $C_{20}H_{41}O_2$. All energies are negative, which means that the formation of peroxy radicals is exothermic.

Table 2.1 – *Calculated formation energy of peroxy radicals*

	Formation energy (vdW-df-ob86)	
	middle of chain	end of chain
$C_4H_9O_2$	-0.24	-0.06
$C_8H_{17}O_2$	-0.36	-0.17
$C_{12}H_{25}O_2$	-0.45	-0.25
$C_{16}H_{33}O_2$	-0.53	-0.32
$C_{20}H_{41}O_2$	-0.59	-0.38

2.5 . Calculation details

We modeled three PE structures. One is simply made by isolated molecules of varying chain lengths to represent unimolecular reactions occurring in low density regions of the amorphous phase. The second one is crystalline PE (orthorhombic mesh), where uni and bimolecular reactions can occur. The third one, which we call *lamellae surface*, is a slab mimicking the interface between two crystalline regions, with bent polymer chains at the crystal surfaces. We will call them in the following as molecular, crystalline lamellae, and lamellar surface models, respectively. For molecular models, we used body-centered tetragonal unit cells in order to maximize the chain ends distance between periodic images of the molecules; the unit cells were 40×40 bohr wide in the plane perpendicular to the chain, and they exceeded the length of the molecules in the direction parallel to the chain so to have at least a distance of 25 bohr between atoms of two different periodic images. The unit cell of the crystalline lamellae is orthorhombic, containing 12 atoms, and we sampled the BZ with a $3 \times 3 \times 6$ Γ -centered regular k -point mesh. To model isolated

defects in the solid, we used a $2 \times 1 \times 4$ supercell (containing 96 atoms plus defects), and we employed a $2 \times 3 \times 2$ Γ -centered \vec{k} point mesh. The theoretical equilibrium lattice parameters of the orthorhombic unit cell in atomic units were: $a = 9.18$ bohr, $b = 13.14$ bohr, and $c = 19.36$ bohr. The unit cell of the lamellar surface, containing 132 atoms for pure PE, is similar to a model previously used to describe a carboxyl group grafted onto a lamella [14]. The detailed process to construct the models is included in Appendix A. Pseudopotentials, norm-conserving (nc) for C and H and both nc and ultrasoft for oxygen, were generated as described in Ref. [15] and used with the optB86b+vdW exchange-correlation (xc) functional [8]. The functional optB86b+vdW includes a gradient corrected short range xc contribution and a long-range non-local van der Waals correlation term in order to provide a good description of van der Waals interchain interactions in crystalline PE.

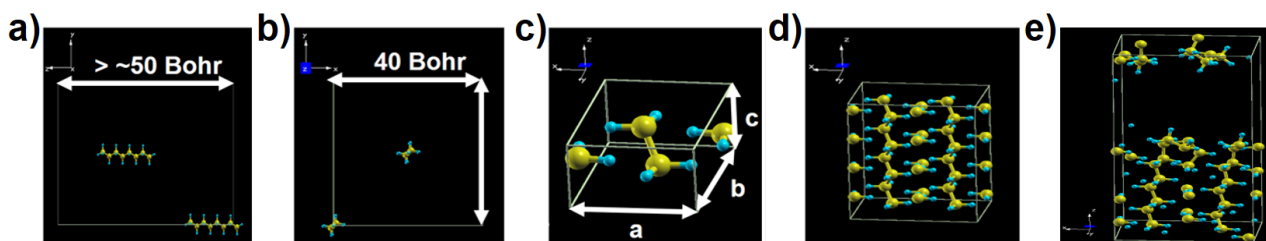


Figure 2.8 – Structure of molecular models seen along (a) the x direction and (b) the z direction. Structure of solid models: (c) unit cell, (d) super cell, and (e) lamellar surface model. Hydrogens are blue and carbons are yellow.

2.6 . Ab initio molecular dynamics (AIMD)

In order to understand the motion of the molecules with the finite temperature, ab initio molecular dynamics is a useful methodology for the free energy calculation because basic potential energy surface analysis by DFT assumes $T = 0K$. The goal of AIMD, as well as classical MD, is to predict atomic trajectories in time by solving Newton's equation of motion from the initial positions and velocities through the calculation of the total energy and forces for the given number of atoms in the structure. By choosing a time interval the small enough Δt for the first order of Taylor expansion, we can get the next position of the atoms, and the calculation can be iterated. In contrast to classical MD, AIMD takes into account, from the point of view of quantum mechanics, the modifications of the electronic states induced by atomic motion and, at the same time, the influence of these evolutions on atomic forces.

There are two main approaches to AIMD (using DFT and a plane wave basis set); one is Born-Oppenheimer molecular dynamics (BOMD), and the other is Car-Parrinello molecular dynamics (CPMD). While BOMD solves the Kohn-Sham

equations at each iteration, CPMD assigns a fictitious mass to the electronic wave functions (in such a way as to decouple the electrons and the nuclei, i.e., adiabatic process) and evolves them in time as for atomic positions. This is a very powerful method because it does not require fully solving DFT equations at each time step.

Bibliography

- [1] Paolo Giannozzi, Stefano Baroni, Nicola Bonini, Matteo Calandra, Roberto Car, Carlo Cavazzoni, Davide Ceresoli, Guido L Chiarotti, Matteo Cococcioni, Ismaila Dabo, Andrea Dal Corso, Stefano de Gironcoli, Stefano Fabris, Guido Fratesi, Ralph Gebauer, Uwe Gerstmann, Christos Gougousis, Anton Kokalj, Michele Lazzeri, Layla Martin-Samos, Nicola Marzari, Francesco Mauri, Riccardo Mazzarello, Stefano Paolini, Alfredo Pasquarello, Lorenzo Paulatto, Carlo Sbraccia, Sandro Scandolo, Gabriele Sclauzero, Ari P Seitsonen, Alexander Smogunov, Paolo Umari, and Renata M Wentzcovitch. QUANTUM ESPRESSO: a modular and open-source software project for quantum simulations of materials. *Journal of Physics: Condensed Matter*, 21(39):395502, sep 2009.
(Cited on page 37)
- [2] S Baroni, de gironcoli s, dal corso a and giannozzi p 2001. *Rev. Mod. Phys*, 73:515.
(Cited on page 37)
- [3] Pierre Hohenberg and Walter Kohn. Inhomogeneous electron gas. *Physical review*, 136(3B):B864, 1964.
(Cited on page 37)
- [4] W. Kohn and L. J. Sham. Self-consistent equations including exchange and correlation effects. *Phys. Rev.*, 140:A1133–A1138, Nov 1965.
(Cited on page 38)
- [5] David M Ceperley and Berni J Alder. Ground state of the electron gas by a stochastic method. *Physical review letters*, 45(7):566, 1980.
(Cited on page 39)
- [6] Kristian Berland, Valentino R Cooper, Kyuho Lee, Elsebeth Schröder, T Thonhauser, Per Hyldgaard, and Bengt I Lundqvist. van der waals forces in density functional theory: a review of the vdw-df method. *Reports on Progress in Physics*, 78(6):066501, 2015.
(Cited on pages 39 and 113)
- [7] J. Heyd, G.E. Scuseria, and M. Ernzerhof. Hybrid functionals based on a screened Coulomb potential. *J. Chem. Phys*, 118(18):8207, 2003.
(Cited on page 39)
- [8] J Klimeš, DR Bowler, and A Michaelides. Van der waals density functionals applied to solids. *Physical Review B*, page 195131.
(Cited on pages 39 and 48)

- [9] Kristian Berland, Yang Jiao, Jung-Hoon Lee, Tonatiuh Rangel, Jeffrey B Neaton, and Per Hyldgaard. Assessment of two hybrid van der waals density functionals for covalent and non-covalent binding of molecules. *The Journal of Chemical Physics*, 146(23):234106, 2017.
(Cited on page 39)
- [10] Feliciano Giustino. *Materials modelling using density functional theory: properties and predictions*. Oxford University Press, 2014.
(Cited on pages 40 and 41)
- [11] Andrea Dal Corso et al. Density-functional theory beyond the pseudopotential local density approach: a few cases studies. 1993.
(Cited on page 42)
- [12] Hendrik J Monkhorst and James D Pack. Special points for brillouin-zone integrations. *Physical review B*, 13(12):5188, 1976.
(Cited on page 44)
- [13] Graeme Henkelman, Blas P Uberuaga, and Hannes Jónsson. A climbing image nudged elastic band method for finding saddle points and minimum energy paths. *The Journal of chemical physics*, 113(22):9901–9904, 2000.
(Cited on pages 45 and 46)
- [14] Davide Ceresoli, Erio Tosatti, Sandro Scandolo, G Santoro, and S Serra. Trapping of excitons at chemical defects in polyethylene. *The Journal of chemical physics*, 121(13):6478–6484, 2004.
(Cited on pages 5, 16, 18, and 48)
- [15] Guido Roma, Fabien Bruneval, and Layla Martin-Samos. Optical properties of saturated and unsaturated carbonyl defects in polyethylene. *The Journal of Physical Chemistry B*, 122(6):2023–2030, 2018.
(Cited on pages 48 and 113)

3 - Oxidation of PE: from the initiation step to ketones

In this chapter, as a part of the overall oxidation process, we approach the reactions from the initiation step to the formation of ketones. Because ketones are the dominant products of thermo- and photo-oxidation, it is important to investigate the reaction pathway for the formation of ketones. Moreover, the conventional reaction scheme generated from a hydroperoxide is not plausible due to the high activation energy, so other reaction pathways should be considered.

On the other hand, the formation of hydroperoxides, which are regarded as important intermediate products, is also discussed with various aspects (intra-, intermolecular reactions, w/ and w/o defects). In general, the formation of hydroperoxides is described as an H-abstraction reaction. However, the alkyl radical formed as the final product is very unstable, as it has an energy value similar to the transition state, implying that the reaction cannot occur efficiently because the backward reaction is much more probable than the forward one. As alternative paths, one possibility would be that defects stabilize the alkyl radical produced together with hydroperoxides [1], or that other radical species such as a hydroxyl radical ($^{\circ}\text{OH}$) and hydroperoxyl radical ($^{\circ}\text{OOH}$) could engage in the reaction to form hydroperoxides.

3.1 . Initiation step

In general, the initiation step describes the formation of the first radicals (i.e., alkyl radicals), which subsequently react with oxygen or other radical species, causing oxidative degradation of PE. The reported C-H bond dissociation energies from methane to propane are in the range of 407.6 – 439.7 kJ/mol (4.25 – 4.58 eV) from experiments, and 397.5 – 437.6 kJ/mol (4.14 – 4.56 eV) from calculations [2, 3]. In the case of C-C bond, the energy is in the range of 250 - 375 kJ/mol (2.59 - 3.89 eV) from experiments [4, 5, 6] and 345.6 - 376.3 (3.58 - 3.9 eV) from calculation at zero strain [5, 7]. While we consider that alkyl radicals are formed through the C-H bond dissociation by γ -irradiation (Reaction 3.1), we also include other reactions which possibly take place as follows:





where PH, P° , and ${}^\circ OOH$ represent secondary alkyl chain, alkyl, and hydroperoxyl radicals, respectively. The calculated energy profiles are shown in Fig.3.1. The activation energy of reaction 3.2 is of the same order of magnitude of reaction 3.1 because the reaction is also caused by C-H bond dissociation. However, a further reaction is possible following the latter, which is the formation of an oxygen molecule and a double bond ($P^\circ + H^\circ \rightarrow P=P + H_2$); this reaction was not investigated in this thesis, but should be checked in the future, to better understand the formation of transvinilenes and hydrogen release. The activation energy of reaction 3.3 also exhibits the similar value with the references [5, 7]. Reaction 3.4 has a lower activation energy, but the backward path along the reaction coordinate does not have a barrier, which means that a hydroperoxyl radical easily loses a hydrogen atom to an alkyl radical unless the product diffuses after the reaction. Previously reported energies for this reaction are in the range of 1.3 - 1.95 eV [8, 9]

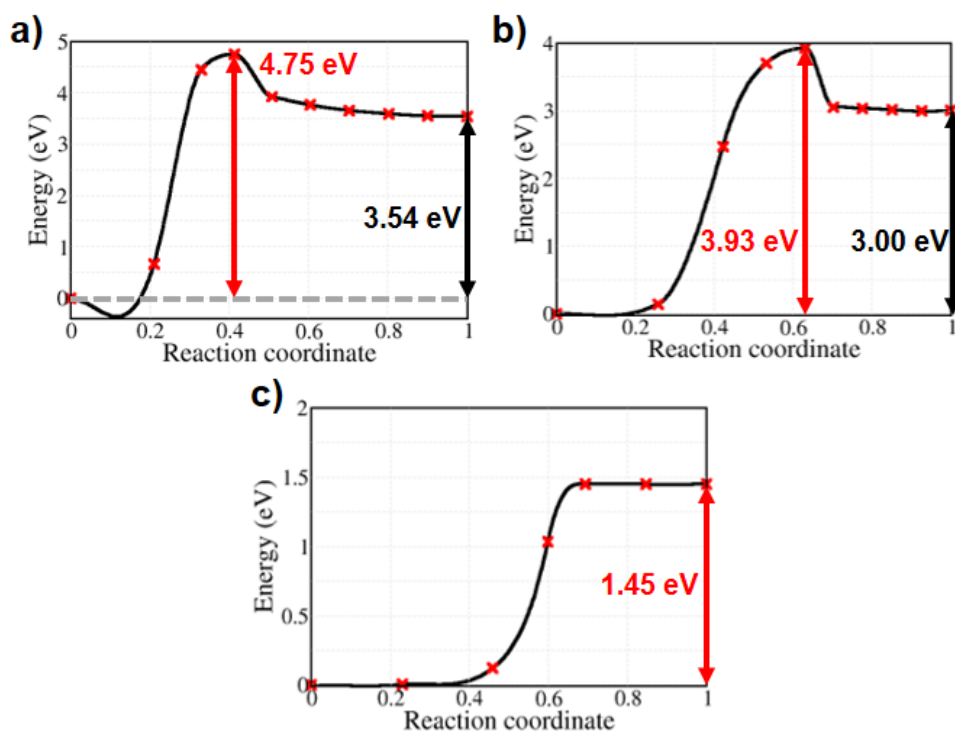


Figure 3.1 – NEB calculations for surface model: (a) Reaction 3.2: $PH \rightarrow 2P^\circ + H_2$, (b) Reaction 3.3: $PH \rightarrow 2P^\circ$, and (c) Reaction 3.4: $PH + O_2 \rightarrow P^\circ + {}^\circ OOH$

3.2 . Formation of hydroperoxides

3.2.1 . Peroxy radical

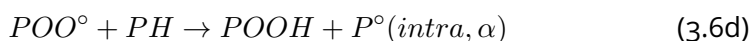
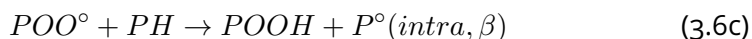
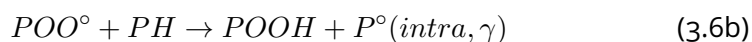
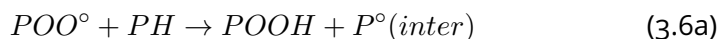
After alkyl radicals are produced in the initiation step, oxygen can be captured without any energy barrier at a $-\dot{\text{C}}\text{H}-$ site by forming a peroxy radical in the propagation step (reaction 3.5).



where POO° represents a peroxy radical. For the molecular model, we calculated the energy profile by varying chain lengths and the position of alkyl radicals where oxygen is captured (approximately in the middle of the molecule or at the chain end) (Fig. 3.2(a) and 3.2(b)). The formation of peroxy radicals is a spontaneous reaction without an energy barrier for all environments (alkyl chains, crystalline PE, and lamellæ surface) and has a high exothermic enthalpy (Fig. 3.2). The values are 1.78 eV (chain centre, average), 1.75 eV (chain end, average), 2.36 eV (PE crystal), and 1.46 eV (lamellæ surface). These high values of enthalpy mean that the products are stable and do not spontaneously dissociate after the reaction.

3.2.2 . Conventional pathways

After the formation of peroxy radicals in the propagation step, it is generally described that the peroxy radicals lead to the formation of hydroperoxides by abstracting a hydrogen atom and forming radical centers as final products. Two reaction pathways, inter (3.6a) and intramolecular (3.6b - 3.6d) H-abstraction, could be considered. The formed radical center influences the possible following steps of oxidative degradation. For example, it can react with oxygen or other neighboring radical species. Several possible positions of a hydrogen atom abstracted are as follows:



Where POOH represents hydroperoxides. For the intermolecular H-abstraction, a peroxy radical grabs an H atom in adjacent polymer chains to form a hydroperoxide. We selected the closest H atom to the peroxy radical in crystalline PE in order to calculate this intermolecular H-abstraction (reaction 3.6a, Fig.3.3). The molecular model is not involved in intermolecular reactions because the model only reflects isolated molecules.

For the formation of a hydroperoxide by H-abstraction from the same alkyl chain (i.e., intramolecular reaction); it is labeled γ , β , and α depending on its

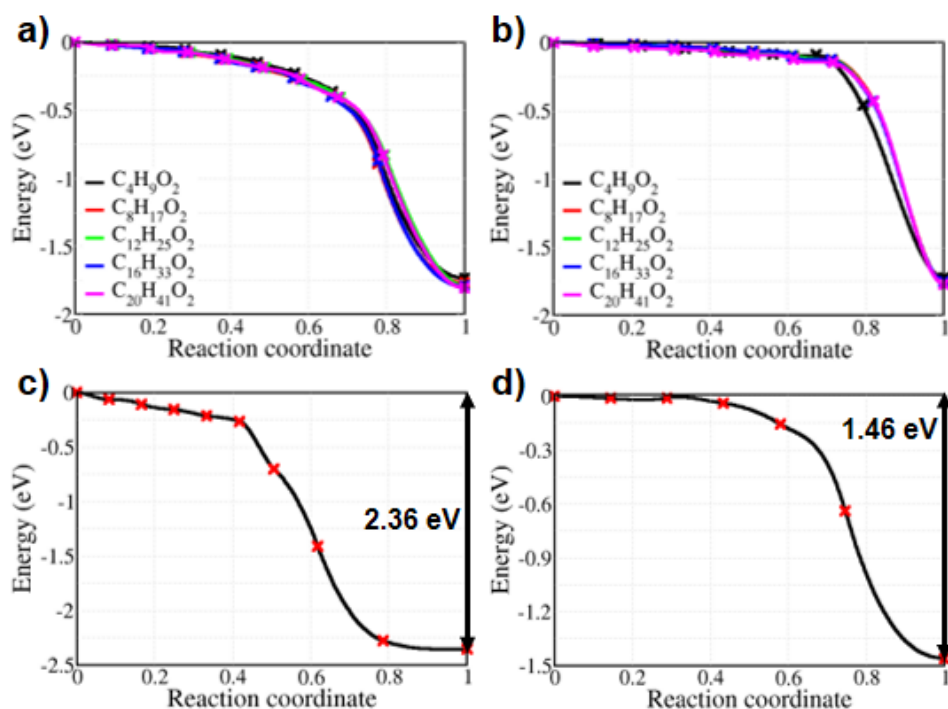


Figure 3.2 – The capture of an oxygen molecule by an alkyl radical occurs spontaneously, as shown by the energy profiles shown here: (a) capture by an alkyl radical situated on an internal carbon (chain center) on alkane molecules of varying length (b) capture by an alkyl radical situated on an end-chain carbon of alkane molecules of varying length (c) capture by an alkyl radical in a crystalline region of PE (d) capture by an alkyl radical on the lamellæ surface.

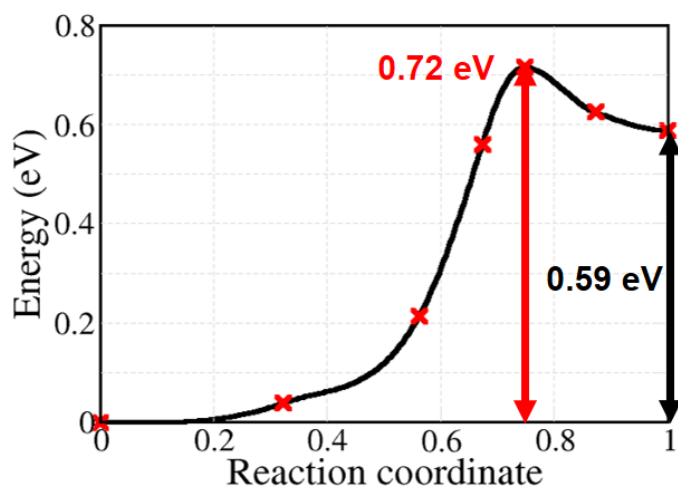


Figure 3.3 – The energy profile calculated for the intermolecular reaction 3.6a in crystalline PE

position as shown in Fig.3.4. Distances longer than γ -position (e.g., from δ -position) were not taken into account as the reaction does not occur because the alkyl chains hardly bend in the crystalline PE or at the lamellæ surface, which would be unfavorable pathways.

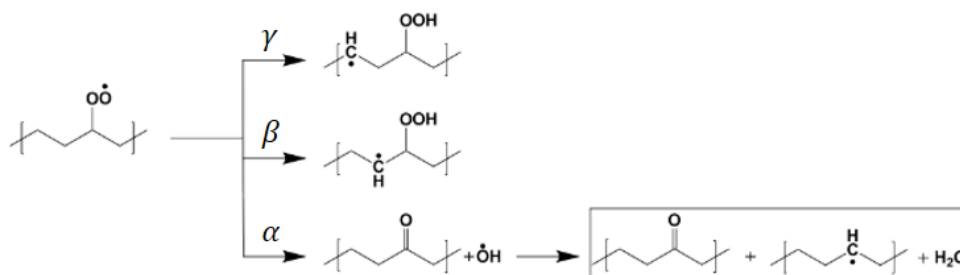


Figure 3.4 – Intramolecular reaction for the formation of hydroperoxides. Hydrogen atoms are abstracted from γ , β , and α positions, respectively.

Fig.3.5 shows calculated activation energies for both molecular and solid models. The activation energy of H-abstraction from the γ position has the lowest values among the intramolecular H-abstractions: it amounts to 0.84 eV and 0.82 eV for the molecular and the solid model, respectively, (Fig.3.5a and b). H-abstraction from β position shows higher energy barriers of 1.37 eV and 1.41 eV for the molecular and the solid model, respectively (Fig.3.5c and d). γ and β H-abstraction both are endothermic, which means that a reverse reaction is more likely than the forward one (0.13 eV and 0.14 eV for γ position and 0.61 eV and 0.59 eV for β position), reducing the effective rate constant of hydroperoxide production. In contrast, α hydrogen abstraction is exothermic, with the final equilibrium structure being much more stable than the other reactions. However, reaction 3.6d forms a ketone and a water, not hydroperoxides, because the O-O bond of the intermediate state, α -alkyl-hydroperoxy radical, is very unstable and spontaneously dissociates. Although the reaction directly leads to the initially targeted ketone product, the high activation energy of the reaction (1.71 eV for the molecular model and 1.54 eV for the solid) indicates that it is unlikely to occur. Nevertheless, this reaction presents interesting steps that may suggest the reactivity of hydroxyl radicals in crystalline PE. In contrast to reaction 3.6b and 3.6c, which show the same product between molecular and solid models, reaction 3.6d produces final products in crystalline PE that differ from the molecular model: ketone, alkyl radical, and water. During the reaction, a hydroxyl radical is generated from the dissociation of $P^{\circ}O-OH$ (ketone formation) and reacts with a hydrogen atom from other adjacent polymer chains to form an alkyl radical and a water molecule in crystalline PE. This additional process occurs spontaneously, as seen in structural relaxation in Fig.3.6. Although the instability of α -alkyl-hydroperoxy radical and the reactivity of hydroxyl radical have already been investigated in simple molecular systems, not much has been done concerning these reactions in crystalline polymers nor their

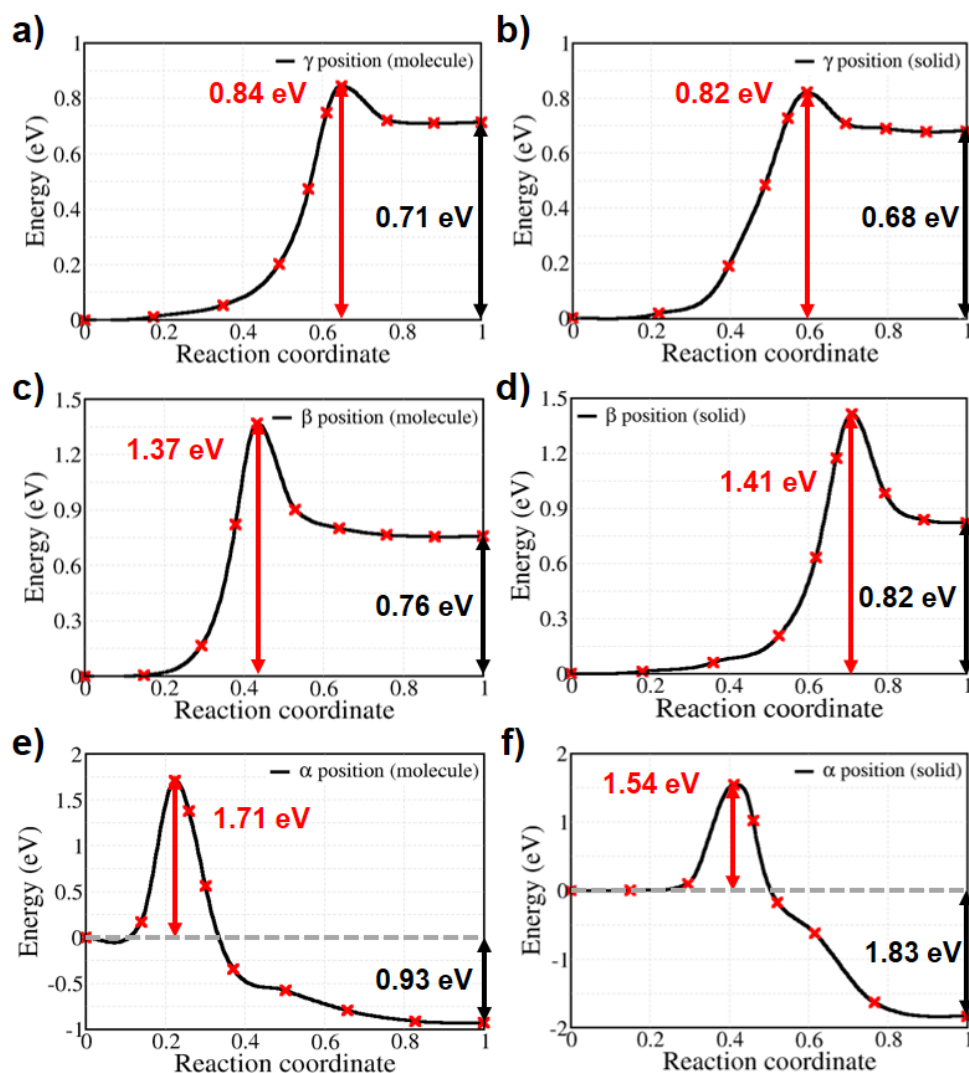


Figure 3.5 – Energy profiles for reactions labeled 3.6b - 3.6d. Panels (a-b): H-abstractions from γ -position for molecular and solid models. As the same order, panels (c-d) from β -position, and panels (e-f) α -position respectively.

role in a global kinetic pathway. Regarding the hydroxyl radical, its role in catalyzing hydroperoxide decomposition will be discussed in detail. Reactions involving additional steps are marked by rectangles in Fig.3.4.

Since the lowest activation energy among the intramolecular reactions is found for the H-abstraction from γ position, the energy profiles are compared with the intermolecular reaction on the lamellæ surface (Fig. 3.7). In the intermolecular reaction, despite a slight decrease in the activation energy from 0.72 eV to 0.65 eV, the difference between activation energy and enthalpy was rather reduced from 0.13 eV to 0.1 eV. This means that the H-abstraction reaction hardly occurs in any en-

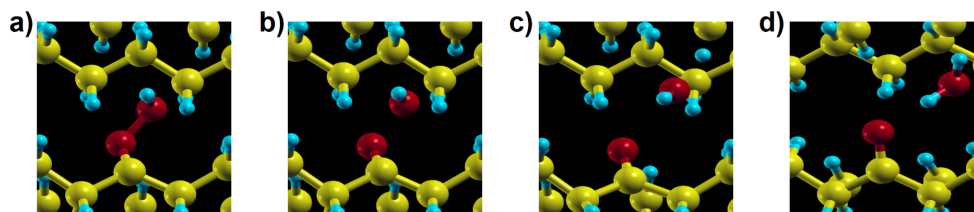


Figure 3.6 – The four snapshots (a-d) are representative steps of the relaxation from an (unstable) α -alkyl-hydroperoxy radical to the endpoint of reaction 3.6d in crystalline PE.

vironment (i.e., molecular, solid, and surface model) in the saturated polyethylene structure.

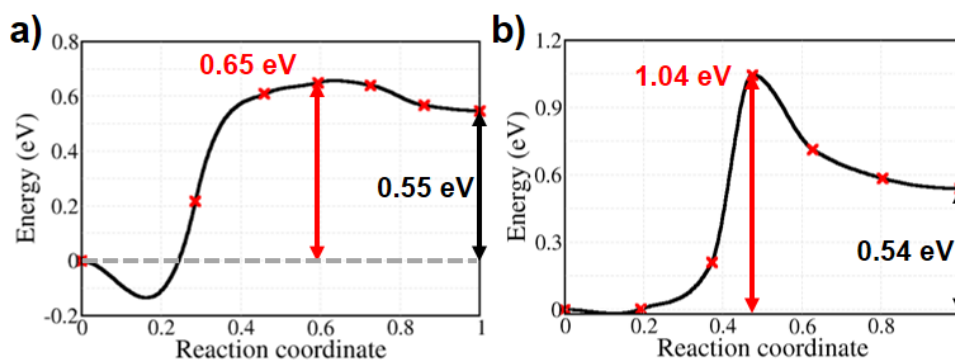


Figure 3.7 – Energy profiles for the H-abstraction reactions on the lamellæ surface (a) reaction 3.6a (inter) and reaction 3.6b (intra)

3.2.3 . Alternative pathways

In the previous section, we discussed the conventional reaction pathways of the formation of hydroperoxides. There were two pathways from intermolecular and intramolecular reactions. However, the calculated activation energies were relatively high; the lowest barrier was 0.65 eV from the intermolecular reaction on the lamellæ surface, to take place in normal condition. In addition, all energy profiles showed high endothermic reactions because reverse path barriers are lower than forward path ones and decrease the reaction rates. Therefore, the reactions for the formation of hydroperoxides are not well explained from both kinetic and thermodynamic points of view. From the thermodynamic points of view, Gryn'ova *et al.* studied the stabilization of an alkyl radical center to decrease the energy of the final products and make exothermic reactions, which are thermodynamically favorable [1]. An adjacent double bond, which features a π bond, can stabilize a single unpaired electron by forming a resonance structure. Therefore, by considering possible oxidative products in PE, we take into account six types of defects, which contain double bonds, lone pair electrons (esters), the combination of them (enone), and methyl group (Fig.3.8).

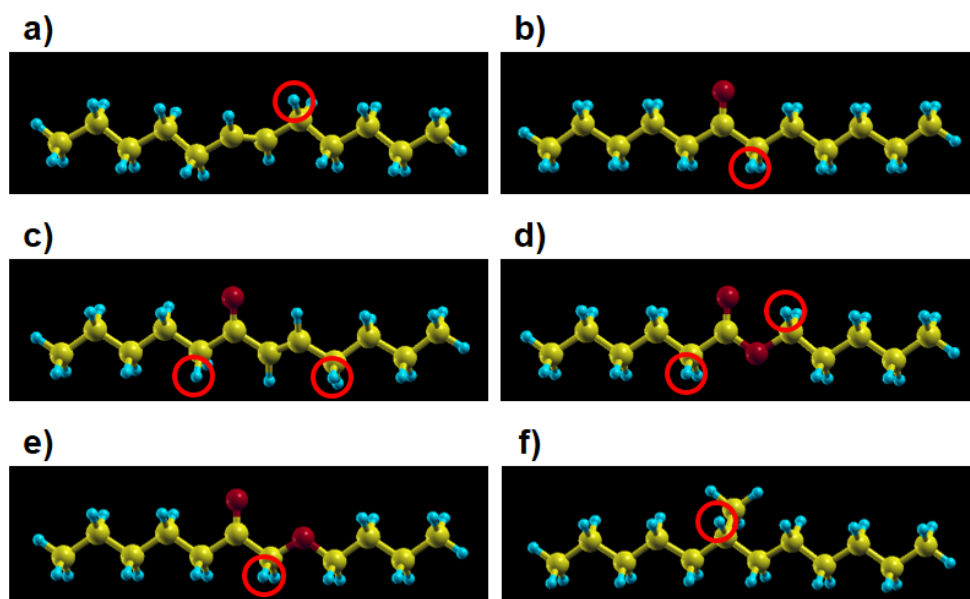
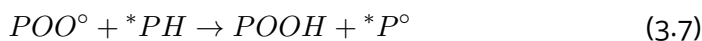


Figure 3.8 – Six types of defects for the stabilization of an alkyl radical centre. (a) double bond, (b) ketone, (c) enone, (d) ester, (e) ketone + ether, and (f) methyl substituent (forming a tertiary radical). Position of alkyl radicals are marked by red circles

Therefore, reaction 3.6a can be modified by the formation of hydroperoxides in presence of defects as follows:



where the * indicates the presence of a defect.

Energy profiles for reaction 3.7 in crystalline PE with various defects are shown in Fig. 3.9. Compared to the alkyl radical center formed by the saturated carbon (0.72 eV), double bond, enone, and ketone+ether decrease the barriers. In addition, these energy profiles show exothermic reactions. Based on the calculated results in crystalline PE, we picked the defects (double bond and enone), which have low activation energies, and the calculated activation energy of the same structure on the lamellæ surface (Fig.3.10). The calculated activation energy is further decreased from 0.65 eV (saturated chain) to 0.48 eV (double bond) and 0.53 eV (enone), although it is a slightly endothermic reaction; a rough estimation of the rate constant in the case of the double bond gives $9 \times 10^4 \text{ s}^{-1}$ at 300K, i.e., at least three orders of magnitudes higher than without a double bond. Therefore, the energy profiles show that the defects effectively stabilize the alkyl radical center in the final state and decrease activation energies.

On the other hand, Chen *et al.* proposed another alternative pathway for the formation of hydroperoxide from a hydroperoxyl radical based on atmospheric chemistry [10, 11, 12].

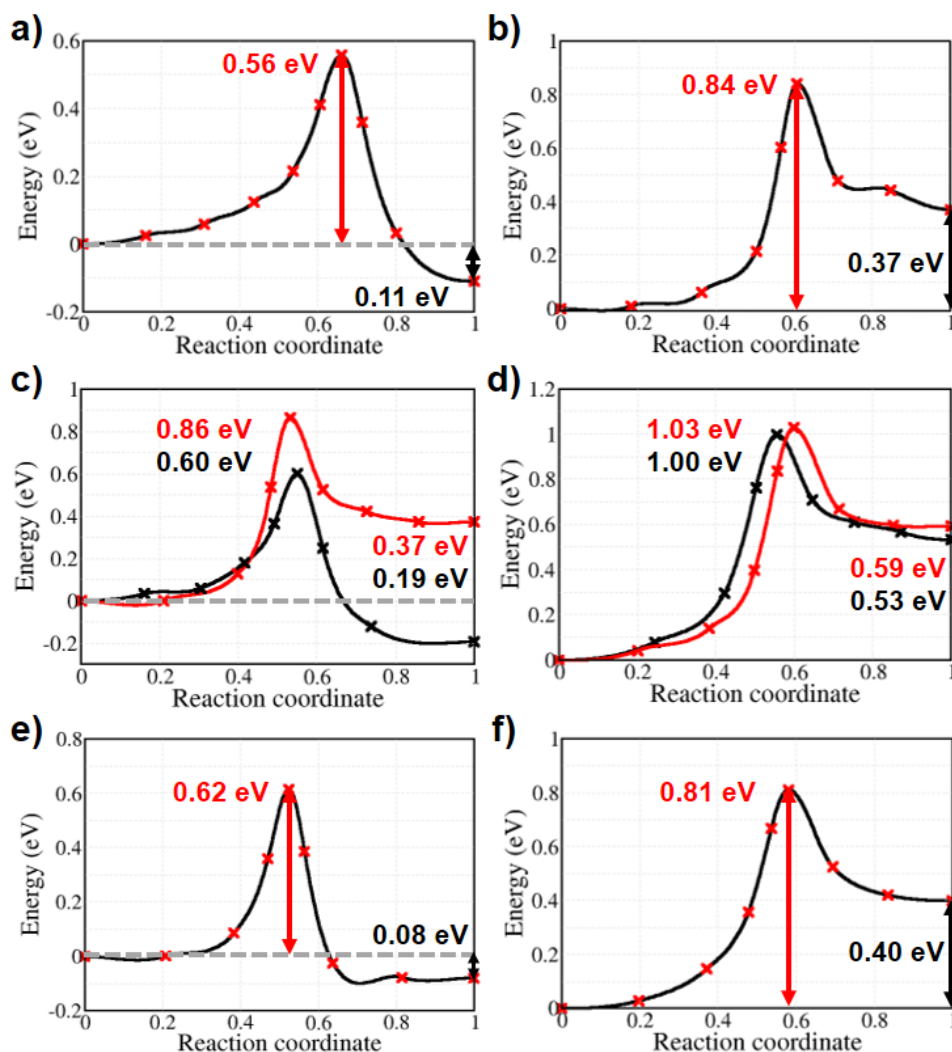
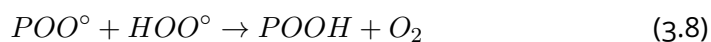


Figure 3.9 – Calculated energy profiles of H-abstraction reactions with six types of defects for the stabilization of an alkyl radical centre (crystalline PE). (a) double bond, (b) ketone, (c) enone (black line: alkyl on double bond side, red line: alkyl on carbonyl side), (d) ester (black line: alkyl next to the carbon atom, red line: alkyl next to the oxygen atom), (e) ketone + ether, and (f) methyl substituent (forming a tertiary radical).



The reactions show barrierless energy profiles (Fig.3.11). In particular, oxygen molecules are recreated after the reaction so that they can trigger other reactions, such as the formation of peroxy radicals, and the latter can abstract a hydrogen atom again and form hydroperoxides. However, abstracting a hydrogen atom from

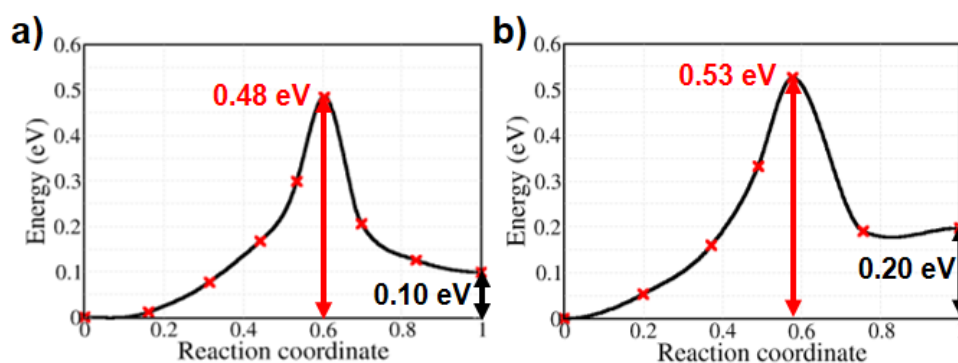


Figure 3.10 – Calculated energy profile of H-abstraction reaction on the lamellæ surface with (a) double bond and (b) enone (double bond side)

alkyl chains needs 1.45 eV, and a hydroperoxyl radical can easily give back a hydrogen atom to an alkyl radical (Fig. 3.1b), which would be a competitive reaction with reaction 3.8. Although we can assume that oxygen molecules can react with a hydrogen atom dissociated from C-H bonds under irradiation condition, the formation of hydroperoxyl radicals should be studied in detail.

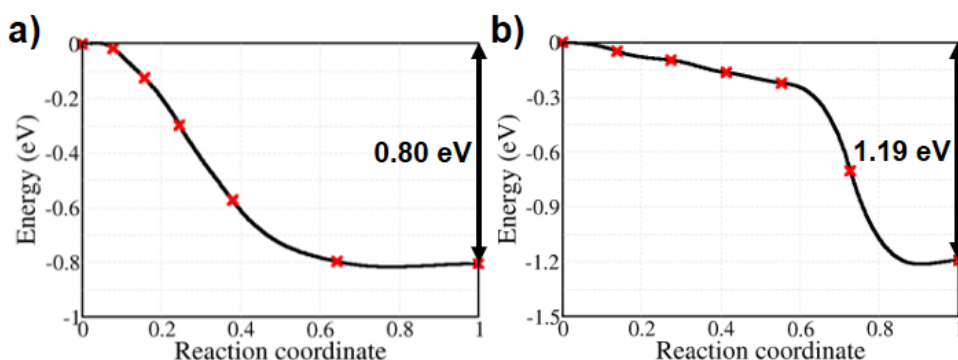
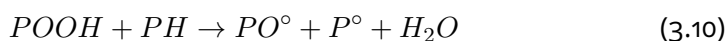
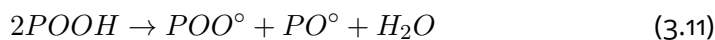


Figure 3.11 – Calculated energy profile of the formation of hydroperoxides from hydroperoxyl radicals according to reaction 3.8 (a) molecular model and (b) surface model

3.3 . Formation of ketones

After their formation, hydroperoxides can be broken down in the chain branching step by three main decomposition reactions.(reaction 3.9 - 3.11) [13, 14, 15, 4].





Where PO° and $^\circ OH$ represent alkoxy and hydroxyl radicals.

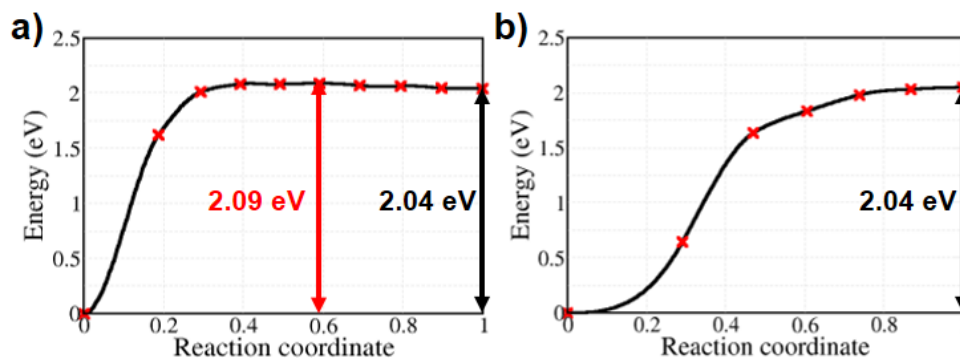


Figure 3.12 – Calculated energy profile of the unimolecular decomposition of hydroperoxides (reaction 3.9). (a) molecular model, and (b) lamellar surface model

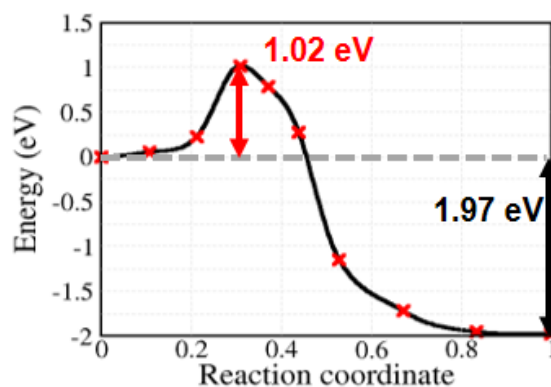


Figure 3.13 – Calculated energy profile of the pseudo unimolecular decomposition of hydroperoxides in crystalline PE (reaction 3.10).

The first reaction is a unimolecular PO-OH bond cleavage, in which a single hydroperoxide O-O bond is broken. (reaction 3.9). The activation energy would be similar to the O-O bond strength because other species such as alkyl chain, oxidative products, and radicals are not involved in the reaction, and various activation energy estimations for this reaction have been proposed in both experimental [16, 17, 18, 19] and theoretical calculations [20, 21, 22, 23].

Experimentally the energies are between 0.7 eV and 1.6 eV, and theoretical calculations show slightly higher values from 1.8 to 2.1 eV with different levels of theory. As shown in Fig. 3.12, the reaction that we calculated also shows the high activation energy (2.09 eV for the solid model and 2.04 eV for the surface

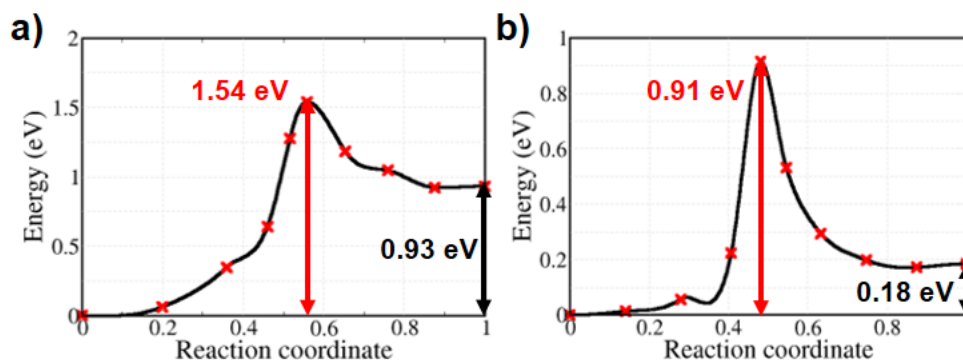
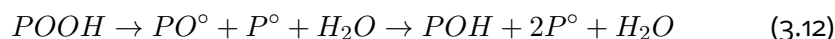


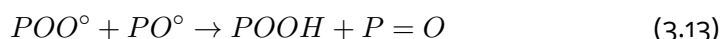
Figure 3.14 – Calculated energy profile of the bimolecular decomposition of hydroperoxides (reaction 3.11). (a) solid model, and (b) lamellar surface model

model). The contribution of this reaction in the experimental kinetics of hydroperoxide decomposition is only up to 2% below 200 °C [24] due to its high activation energy, which means that other reactions having lower activation energies or a pseudo-unimolecular POOH decomposition that includes other alkyl chains (reaction 3.10) would prevail. The reaction 3.10 would be more significant when the concentration of hydroperoxide is much lower than that of alkyl chains in the matrix ($[PH] \gg [POOH]$). This is because when the concentration of POOH is low enough, bimolecular reactions that require relatively high hydroperoxide concentrations rarely occur. For reaction 3.10, additional products are formed in crystalline PE. The alkoxy radical formed by the cleavage of the O-O bond of the hydroperoxide spontaneously abstracts an H atom from another alkyl chain by forming an alcohol (reaction 3.12).



Where POH represents an alcohol. That is, when a hydroperoxide is decomposed by Reaction 3.12, it forms an additional alkyl radical chain that can participate in oxidation reactions. These alkyl radicals can diffuse along or across the chain. Otherwise, the alkyl radicals will react with oxygen to form a peroxy radical (3.5). As the concentration of hydroperoxides increases, bimolecular reactions (3.11) also begin to take place. However, the calculated activation energy is relatively high to account for the decomposition of hydroperoxides (1.54 eV for the solid model, and 0.91 eV for the surface model) and endothermic reaction, similar to PO-OH bond cleavage reactions (reaction 3.9). Nevertheless, the peroxy radicals and alkoxy radicals produced after the reaction can proceed toward a reaction that produces ketones and hydroperoxides. To calculate this reaction, we assumed that the generated water molecule has diffused far away, and then we optimized the structure again only with a peroxy and alkoxy radical. The peroxy radical then abstracts a hydrogen atom attached to the alkoxy radical to form a ketone

(reaction 3.13). Although the activation energy is low (0.20 eV, solid model) and the reaction has high exothermic enthalpy, note that the previous reaction (reaction 3.11) is unlikely to occur due to the high activation energy. In the case of the lamellar surface, the reaction is structurally difficult to take place because an alkoxy radical affects an H atom while a peroxy radical abstracts it, which makes high activation energy (Fig. 3.15).



Where P=O represents ketones.

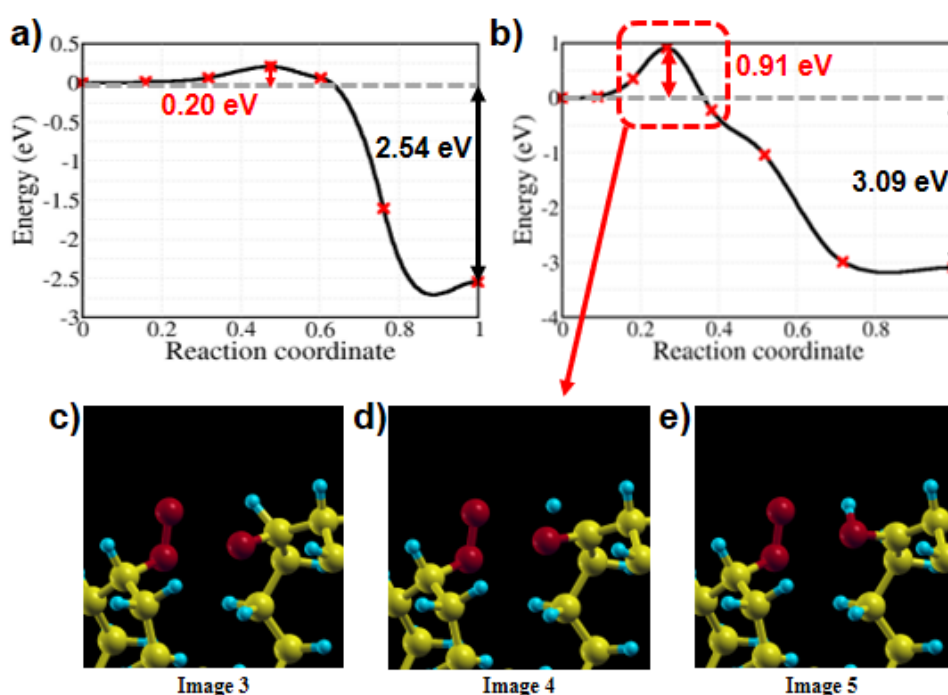


Figure 3.15 – Calculated energy profile of the formation of hydroperoxides and ketones by peroxy and alkoxy radicals (reaction 3.13). (a) solid model, (b) surface model, and panels (c-e) image numbers corresponding to panel (b)

Another reaction pathway consists of the decomposition of a hydroperoxide giving a ketone and water.



Reaction 3.14 starts from a hydroperoxide and gives a ketone and water in the final state. For the molecular model, we calculated the activation energy by varying the number of carbon from 4 to 12 (Fig. 3.16a). The barriers are large, regardless of the size of the molecules, showing an average value of 1.73 eV. The activation energies of the solid and surface model also have higher values of 2.06

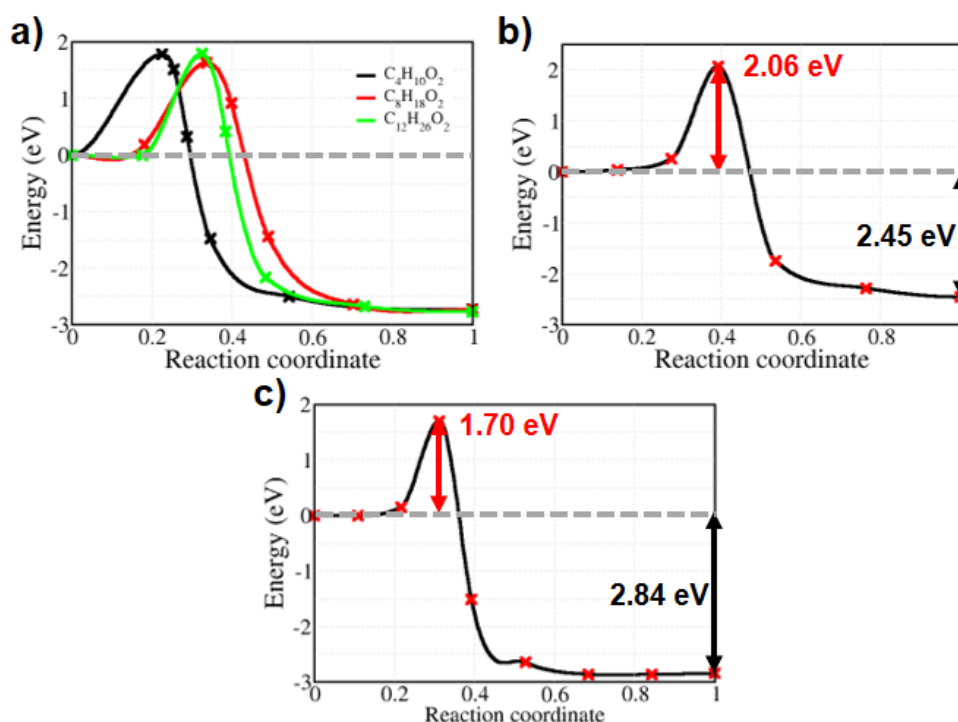
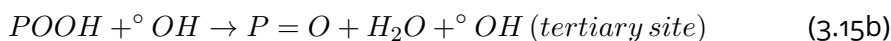
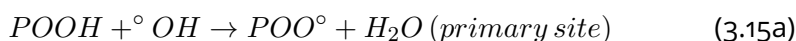


Figure 3.16 – Calculated energy profile of the formation of ketones by hydroperoxides (reaction 3.14). (a) molecular model, (b) solid model, and (c) surface model

eV and 1.70 eV, respectively (Fig. 3.16b and c). The activation energy is not far from that of reaction 3.9, describing the dissociation of a PO–OH bond, whereas the reaction 3.14 is strongly exothermic.

As a result of examining the three main decomposition reactions of hydroperoxides (i.e., unimolecular PO–OH bond cleavage, pseudo-unimolecular POOH decomposition, and bimolecular POOH decomposition) (reaction 3.9 - 3.11) and unimolecular POOH decomposition (3.14), it was found that most reactions showed the high activation energy (0.91 - 2.06 eV) despite having exothermic enthalpy. It means that the decomposition of hydroperoxide itself hardly occurs regardless of uni or bimolecular reactions, so other reaction pathways should be considered. Other possible reactions can take place when a tertiary hydrogen atom is attacked by other species and abstracted by forming an α -alkyl-hydroperoxy radical; such reactions are suggested by the previously observed instability of the $P^\circ O-OH$ radical in the H-abstraction reaction (reaction 3.6d), where the $P^\circ O-OH$ bond is spontaneously decomposed, and ketones are formed. Therefore, we considered hydroxyl, peroxy and alkyl radical species that can attack a tertiary H atom. The hydroxyl radical has high reactivity and easily abstracts an H atom from the alkyl chain. The reported rate constants for hydroxyl radicals abstracting H atoms are in the range of $10^{12-13} \text{ cm}^3 \text{ mol}^{-1} \text{ s}^{-1}$ [23]. This is because the highly reactive hydroxyl

radical easily removes an H atom from alkyl chains; similar rate constants are reported by experimental estimations for °OH radical H-abstraction reactions with alkyl hydroperoxides [25, 26, 27]. Furthermore, the amount of hydroperoxides decomposed by hydroxyl radicals under thermal conditions can reach 54% of the total hydroperoxide decomposition channels [23]. Moreover, since the size of °OH radical is smaller than O₂, the permeability of hydroxyl radicals in PE is expected to be relatively higher than that of oxygen [28]. H-abstraction of a tertiary site hydrogen atom in crystalline PE would form additional products as shown in Reaction 3.6d. Therefore, we calculated the reaction by placing a hydroxyl radical next to a hydroperoxide at the primary and tertiary sites for reactions 3.15a and 3.15b here below, respectively, by taking into account that different reaction sites may give rise to different products:



Reaction 3.15a leads to a peroxide radical and a water molecule as the hydroxyl radical abstracts the primary H atom. For reaction 3.15b, an intermediate α -alkyl-hydroperoxy radical and a water molecule are formed as the hydroxyl radical abstracts the tertiary H atom of the hydroperoxide. Because the P°O-OH bond is very unstable, the O-O bond breaks down immediately to form ketones and hydroxyl radicals. Both of these reactions take place spontaneously.

Since the positions of the hydroperoxide and the hydroxyl radical are randomly determined in the initial state, in order to check the reactivity according to the initial position, we performed the relaxation of the structures at various distances between the tertiary H atom of the secondary hydroperoxide and the oxygen atom of the hydroxyl radical. Regarding the capture of the H atom by the oxygen atom, the reactions take place during the relaxation, which means that there are no barriers to be overcome to trigger the reaction. The detailed description regarding the reactivity is discussed in Appendix D.2 with ab initio molecular dynamics. We also verified the spontaneous H-abstraction by °OH radicals by confirming the energy profile calculated by the structural relaxation with hybrid functional calculations.

Fig. 3.17 shows the intermediate process during structural relaxation (reactions 3.15a and 3.15b) where the hydroxyl radical abstracts the H atom and the P°O-OH bond breaks down, meaning that the reaction occurs spontaneously. In particular, it can be seen in reaction 3.15b that a hydroxyl radical is obtained again as a product, which means that this hydroxyl radical can successively react with other alkyl chains or defects in crystalline PE as shown in reaction 3.6d. This is important because the reaction is consecutive and spontaneously produces alkyl radicals and ketones.

The reaction process taking place during the structural relaxation of reactions 3.15a and 3.15b in crystalline PE is shown in Fig. 3.18. Fig.3.18a-c shows the

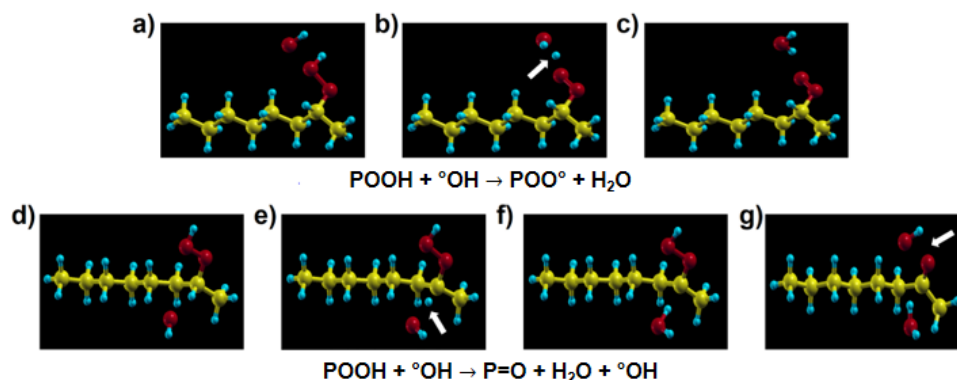
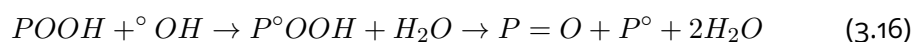
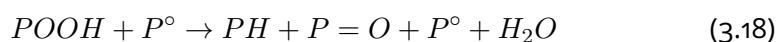
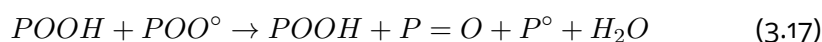


Figure 3.17 – Intermediate steps of reactions 3.15a (panels (a–c)) and 3.15b (panels (d–g)), showing two possible channels of hydroperoxide decomposition due to the action of a hydroxyl radical in a molecular model. The different outcome of the two reactions stems from the initial position of the hydroxyl relative to the hydroperoxide group.

same product as its molecular model, but reaction 3.15b shows, as mentioned earlier, that the hydroxyl radical decomposed from the $P^\circ O-OH$ bond abstracts an H atom from another alkyl chain by forming an alkyl radical and a water molecule (Fig.3.18d–i). The overall reaction process of reaction 3.15b in crystalline PE proceeds as follows:



One could suspect that a tertiary H-abstraction reaction of a hydroxyl radical might occur with other radical types. Among them, we considered peroxy and alkyl radicals abstracting a tertiary H atom in the same way as a hydroxyl radical. The reactions were calculated in crystalline PE (Fig.3.19).



Reaction 3.17 is not spontaneous and has a relatively high activation energy, but it is noteworthy that hydroperoxide is regenerated during the reaction. This is important because a constant rate of formation is observed in the early stages of oxidation [29, 30]. Reaction 3.18 shows an even higher activation energy of 1.54 eV. This means that an H abstraction at the tertiary site is not significantly affected by alkyl radicals located in neighboring polymer chains. Therefore, considering the calculated activation energies, the reactivity is concluded in the order of hydroxyl, peroxy, and alkyl radicals, and all reactions show high exothermic enthalpy.

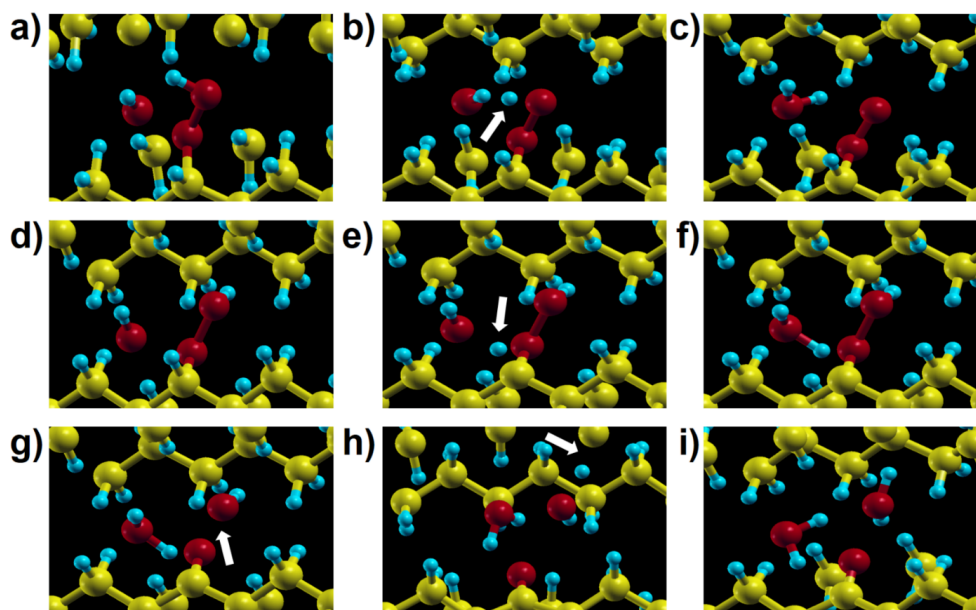


Figure 3.18 – Intermediate steps of reactions 3.15a (panels (a–c)) and reaction 3.15b (panels (d–i)) in crystalline PE. The outcome of reaction 3.15b in the solid is different from the analogous one in the molecular model (Fig.3.17d–g), because here the remaining °OH radical reacts with a neighbouring chain (see the arrow in panel (h)) giving one more water molecule (panel (i)).

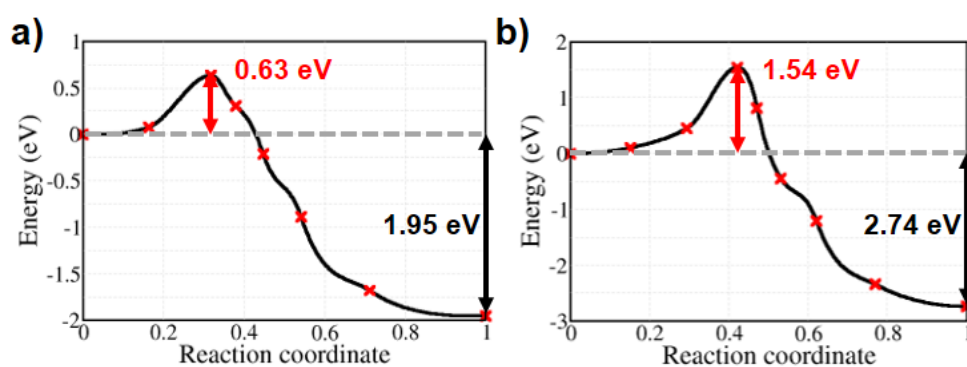


Figure 3.19 – Energy profiles for hydroperoxide decomposition reactions induced by (a) a peroxy radical (b) an alkyl radical, sitting on a nearby polymer chain.

3.4 . Summary and Conclusions

All calculated activation energies are summarized in Table 3.1. Degradation mechanisms leading to PE oxidation were investigated by calculating activation energies in small molecules, crystalline polyethylene, and on the surface between lamellæ structures. We studied three main parts of the oxidation process: (i) the

Table 3.1 – Summarized NEB calculations for oxidative reactions

Label	Chemical reaction equations	Activation energy [eV]			Reaction enthalpy [eV]		
		Molecule	Solid	Surface	Molecule	Solid	Surface
3.1	$\text{PH} \rightarrow \text{P}^\bullet + \text{H}^\bullet$	-	-	-	-	-	-
3.2	$\text{PH} \rightarrow 2\text{P}^\bullet + \text{H}_2$	-	*	4.75	-	*	3.54
3.3	$\text{PH} \rightarrow 2\text{P}^\bullet$	-	*	3.93	-	*	3.00
3.4	$\text{PH} + \text{O}_2 \rightarrow \text{P}^\bullet + {}^\bullet\text{OOH}$	-	Not observed	1.45	-	Not observed	1.45
3.5	$\text{P}^\bullet + \text{O}_2 \rightarrow \text{POO}^\bullet$	0.0	0.0	0.0	-1.78 (avg, center) -1.75 (avg, end)	-2.36	-1.46
3.6a	$\text{POO}^\bullet + \text{PH} \rightarrow \text{POOH} + \text{P}^\bullet$	-	0.72 (inter)	0.65 (inter)	-	0.59 (inter)	0.55 (inter)
3.6b		0.84 (γ , intra)	0.82 (γ , intra)	1.04 (γ , intra)	0.71 (γ , intra)	0.68 (γ , intra)	0.54 (γ , intra)
3.6c		1.37 (β , intra)	1.41 (β , intra)	-	0.76 (β , intra)	0.82 (β , intra)	-
3.6d		1.71 (α , intra)	1.54 (α , intra)	-	-0.93 (α , intra)	-1.83 (α , intra)	-
3.7	$\text{POO}^\bullet + {}^\bullet\text{PH} \rightarrow \text{POOH} + {}^\bullet\text{P}^\bullet$ (double bond)	-	0.56	0.48	-	-0.11	0.10
3.8	$\text{POO}^\bullet + \text{HOO}^\bullet \rightarrow \text{POOH} + \text{O}_2$	0.0	*	0.0	-0.80	*	-1.19
3.9	$\text{POOH} \rightarrow \text{PO}^\bullet + {}^\bullet\text{OH}$	2.09	Not observed	2.04	2.04	Not observed	2.04
3.10	$\text{POOH} \rightarrow \text{PO}^\bullet + \text{P}^\bullet + \text{H}_2\text{O}$ (3.12)	-	1.02	*	-	-1.97	*
3.11	$2\text{POOH} \rightarrow \text{POO}^\bullet + \text{PO}^\bullet + \text{H}_2\text{O}$	-	1.54	0.91	-	0.93	0.18
3.12	$\text{POOH} \rightarrow \text{POH} + 2\text{P}^\bullet + \text{H}_2\text{O}$	-	-	-	-	-	-
3.13	$\text{POO}^\bullet + \text{PO}^\bullet \rightarrow \text{POOH} + \text{P}=\text{O}$	-	0.20	0.91	-	-2.54	-3.09
3.14	$\text{POOH} \rightarrow \text{P}=\text{O} + \text{H}_2\text{O}$	1.73 (avg)	2.06	1.70	-2.74	-2.45	-2.84
3.15a	$\text{POOH} + {}^\bullet\text{OH} \rightarrow \text{POO}^\bullet + \text{H}_2\text{O}$ (primary)	No barrier	No barrier	-	-	-	-
3.15b	$\text{POOH} + {}^\bullet\text{OH} \rightarrow \text{P}=\text{O} + \text{H}_2\text{O} + {}^\bullet\text{OH}$ (tertiary)						
3.16	$\text{POOH} + {}^\bullet\text{OH} \rightarrow \text{P}=\text{O} + \text{P}^\bullet + 2\text{H}_2\text{O}$ (tertiary) (3.15b)	-	-	-	-	-	-
3.17	$\text{POOH} + \text{POO}^\bullet \rightarrow \text{POOH} + \text{P}=\text{O} + \text{P}^\bullet + \text{H}_2\text{O}$ (tertiary)	-	0.63	*	-	-1.95	*
3.18	$\text{POOH} + \text{P}^\bullet \rightarrow \text{PH} + \text{P}=\text{O} + \text{P}^\bullet + \text{H}_2\text{O}$ (tertiary)	-	1.54	*	-	-2.74	*

*: Not calculated

initiation step, (ii) the formation of hydroperoxides from peroxy radicals, and (iii) the formation of ketones. While we assumed that alkyl radicals are produced under the possible irradiation conditions (e.g., γ -rays, electrons, swift heavy ions) in nuclear power plants, we also considered other initiation reactions such as chain scission or formation of alkyl radicals by oxygen. After alkyl radical production, oxygen reacts spontaneously with the radicals, although diffusion of the alkyl radicals in PE matrix could be limited due to the high activation energy.

Reaction pathways of hydroperoxide formation were considered in various aspects. Since it has been reported that the previously suggested reaction pathways (basic auto-oxidation scheme) involve a key reaction which has high activation energy and positive enthalpy, we checked whether the local environment (crystalline, surface) could reduce energy barriers; we also checked the possible influence of nearby defects. In the basic auto-oxidation scheme, from peroxy radicals, hydroperoxides are formed by intramolecular or intermolecular H-abstractions on saturated alkyl chains. We considered the H-abstraction from α , β , and γ positions. Among the intramolecular reactions, abstraction from the γ position has the lowest acti-

vation energies, which are 0.84 eV, 0.82 eV, and 1.04 eV for molecular, solid, and surface model, respectively. The energy barriers of intermolecular H-abstraction are 0.72 eV and 0.65 eV for the solid and the surface model, respectively, exhibiting slightly lower activation energies. Still, the activation energies are relatively high and reactions are endothermic; thus, to account for the experimentally measured concentration of hydroperoxides we considered alternative pathways. One of the proposed strategies is to stabilize the product, the alkyl radical center, through nearby defects, to trigger an exothermic reaction that is thermodynamically favorable. Six types of defects were considered, and among them, double bonds exhibited a large amount decrease of the activation energies from 0.65 eV to 0.48 eV as well as the enthalpy from 0.55 eV to 0.10 eV on the lamellæ surface, although the reaction is slightly endothermic. Another possible strategy is to consider the role of hydroperoxyl radicals. They can spontaneously give a hydrogen atom to a peroxy radical to form a hydroperoxide and oxygen. The reaction creates an oxygen, which can lead to further oxidation in PE matrix. However, as the activation energy for the formation of hydroperoxyl radicals amounts to 1.45 eV, the question about the concentration or the origin of hydroperoxyl radicals remains. One possibility, that could be investigated, is that $^{\circ}\text{OH}$ species come from hydrolysis of water initially present in PE.

On the other hand, some calculations showed further reaction paths, which are not shown in the molecular model, such as reaction 3.6d (H-abstraction from α position), 3.9 (PO–OH bond cleavage), and 3.15b (POOH decomposition through $^{\circ}\text{OH}$ radical), have different outcomes between crystalline PE or an isolated alkane molecule. In particular, in the presence of hydroxyl radical, the activation energy of the decomposition of hydroperoxide varies largely. Without the hydroxyl radical, the reaction of pseudo unimolecular decomposition of hydroperoxides in crystalline PE showed the minimum activation energy of 1.02 eV. For isolated molecules, the activation energy of the unimolecular dissociation of PO–OH is much higher, 2.09 eV. This implies that hydroperoxides are not easily decomposed themselves. In contrast, H-abstraction by hydroxyl radical is spontaneous regardless of its position in the crystal and on an alkane molecule. Especially, H-abstraction from a hydroperoxide at the tertiary site leads to successive reactions with other alkyl chains and finally leaves an alkyl radical chain. Comparing the energy of C–H bond dissociation in pure crystalline PE, which is up to 439.7 kJ/mol, this mechanism forming alkyl radical chains is much more favorable. Therefore, we conclude that even in the presence of low concentrations of hydroxyl radicals, their role is important, and the reactions that they induce can lead to severe degradation of PE matrix.

Bibliography

- [1] Ganna Gryn'ova, Jennifer L Hodgson, and Michelle L Coote. Revising the mechanism of polymer autooxidation. *Organic & biomolecular chemistry*, 9(2):480–490, 2011.
(Cited on pages 9, 10, 16, 53, and 59)
- [2] Ondrej Kysel', Šimon Budzák, Miroslav Medved', and Pavel Mach. A dft study of h-isomerisation in alkoxy-, alkylperoxy-and alkyl radicals: Some implications for radical chain reactions in polymer systems. *Polymer degradation and stability*, 96(4):660–669, 2011.
(Cited on pages 9, 16, 17, 53, and 78)
- [3] Yu-Ran Luo. *Handbook of bond dissociation energies in organic compounds*. CRC press, 2002.
(Cited on pages 9 and 53)
- [4] F Gugumus. Physico-chemical aspects of polyethylene processing in an open mixer. discussion of hydroperoxide formation and decomposition. *Polymer degradation and stability*, 68(3):337–352, 2000.
(Cited on pages 53 and 62)
- [5] Gary S Kedziora, James Moller, Rajiv Berry, and Dhriti Nepal. Ab initio molecular dynamics modeling of single polyethylene chains: Scission kinetics and influence of radical under mechanical strain. *The Journal of Chemical Physics*, 155(2):024102, 2021.
(Cited on pages 53 and 54)
- [6] Yu-Ran Luo. *Comprehensive handbook of chemical bond energies*. CRC press, 2007.
(Cited on page 53)
- [7] JCL Hageman, GA De Wijs, RA De Groot, and Robert J Meier. Bond scission in a perfect polyethylene chain and the consequences for the ultimate strength. *Macromolecules*, 33(24):9098–9108, 2000.
(Cited on pages 16, 53, 54, and 87)
- [8] KU Ingold. Inhibition of the autoxidation of organic substances in the liquid phase. *Chemical Reviews*, 61(6):563–589, 1961.
(Cited on pages 9 and 54)
- [9] KU Ingold. Kinetics of oil oxidation inhibitors. *Journal of the Institute of Petroleum*, 45:244–251, 1959.
(Cited on page 54)

- [10] Liang Chen, Shogo Yamane, Tomohiro Sago, Hideaki Hagihara, Shuzo Kutsuna, Tadafumi Uchimaru, Hiroyuki Suda, Hiroaki Sato, and Junji Mizukado. Experimental and modeling approaches for the formation of hydroperoxide during the auto-oxidation of polymers: Thermal-oxidative degradation of polyethylene oxide. *Chemical Physics Letters*, 657:83–89, 2016.
(Cited on pages 11 and 60)
- [11] Roger Atkinson. Kinetics and mechanisms of the gas-phase reactions of the hydroxyl radical with organic compounds under atmospheric conditions. *Chemical Reviews*, 86(1):69–201, 1986.
(Cited on pages 11 and 60)
- [12] Phillip D Lightfoot, RA Cox, JN Crowley, M Destriau, GD Hayman, ME Jenkin, GK Moortgat, and F Zabel. Organic peroxy radicals: kinetics, spectroscopy and tropospheric chemistry. *Atmospheric Environment. Part A. General Topics*, 26(10):1805–1961, 1992.
(Cited on pages 11 and 60)
- [13] JL Bolland. Kinetic studies in the chemistry of rubber and related materials. i. the thermal oxidation of ethyl linoleate. *Proceedings of the Royal Society of London. Series A. Mathematical and Physical Sciences*, 186(1005):218–236, 1946.
(Cited on pages 7, 9, and 62)
- [14] Arthur V Tobolsky, Donald J Metz, and Robert B Mesrobian. Low temperature autoxidation of hydrocarbons: the phenomenon of maximum rates¹, 2. *Journal of the American Chemical Society*, 72(5):1942–1952, 1950.
(Cited on page 62)
- [15] X Colin, B Fayolle, L Audouin, and J Verdu. The classical kinetic model for radical chain oxidation of hydrocarbon substrates initiated by bimolecular hydroperoxide decomposition. *International journal of chemical kinetics*, 38(11):666–676, 2006.
(Cited on page 62)
- [16] Liang Chen, Shuzo Kutsuna, Shogo Yamane, and Junji Mizukado. ESR spin trapping determination of the hydroperoxide concentration in polyethylene oxide (PEO) in aqueous solution. *Polymer Degradation and Stability*, 139:89–96, 2017.
(Cited on pages 63 and 77)
- [17] Jacqueline L Henry, Ascencion L Ruaya, and Andrew Garton. The kinetics of polyolefin oxidation in aqueous media. *Journal of Polymer Science Part A: Polymer Chemistry*, 30(8):1693–1703, 1992.
(Cited on pages 11, 63, and 77)

- [18] Pieter Gijssman, Jan Hennekens, and Jef Vincent. The mechanism of the low-temperature oxidation of polypropylene. *Polymer Degradation and Stability*, 42(1):95–105, 1993.
(Cited on pages 11, 63, and 77)
- [19] B Fayolle, J Verdu, M Bastard, and D Piccoz. Thermooxidative ageing of polyoxymethylene, part 1: chemical aspects. *Journal of applied polymer science*, 107(3):1783–1792, 2008.
(Cited on pages 11, 63, and 77)
- [20] Ibukun Oluwoye, Mohammednoor Altarawneh, Jeff Gore, and Bogdan Z Dlugogorski. Oxidation of crystalline polyethylene. *Combustion and Flame*, 162(10):3681–3690, 2015.
(Cited on pages 11, 16, 17, 19, 63, 77, and 78)
- [21] Yunho Ahn, Xavier Colin, and Guido Roma. Atomic scale mechanisms controlling the oxidation of polyethylene: A first principles study. *Polymers*, 13(13):2143, 2021.
(Cited on pages 63, 77, 78, and 117)
- [22] John M Simmie, Gráinne Black, Henry J Curran, and John P Hinde. Enthalpies of formation and bond dissociation energies of lower alkyl hydroperoxides and related hydroperoxy and alkoxy radicals. *The Journal of Physical Chemistry A*, 112(22):5010–5016, 2008.
(Cited on pages 11, 63, and 77)
- [23] Pascal de Sainte Claire. Degradation of peo in the solid state: A theoretical kinetic model. *Macromolecules*, 42(10):3469–3482, 2009.
(Cited on pages 11, 16, 17, 63, 66, 67, 77, 78, and 87)
- [24] F Gugumus. Thermolysis of polyethylene hydroperoxides in the melt: 1. experimental kinetics of hydroperoxide decomposition. *Polymer degradation and stability*, 69(1):23–34, 2000.
(Cited on pages 17 and 64)
- [25] James R Dunlop and Frank P Tully. Catalytic dehydration of alcohols by hydroxyl: 2-propanol; an intermediate case. *The Journal of Physical Chemistry*, 97(24):6457–6464, 1993.
(Cited on page 67)
- [26] Mark A Blitz, Dwayne E Heard, and Michael J Pilling. Wavelength dependent photodissociation of ch₃ooh: Quantum yields for ch₃o and oh, and measurement of the oh + ch₃ooh rate coefficient. *Journal of Photochemistry and Photobiology A: Chemistry*, 176(1-3):107–113, 2005.
(Cited on page 67)

- [27] Ghanshyam L Vaghjiani and AR Ravishankara. Kinetics and mechanism of oh reaction with ch_3ooH . *J. phys. Chem*, 93(5):1948–1959, 1989.

(Cited on pages 17 and 67)

- [28] CE Rogers. Polymer permeability. *Elsevier, New York*, pages 11–73, 1985.

(Cited on page 67)

- [29] Jaroslav Petrøuj and Jean Marchal. Mechanism of ketone formation in the thermooxidation and radiolytic oxidation of low density polyethylene. *Radiation Physics and Chemistry (1977)*, 16(1):27–36, 1980.

(Cited on page 68)

- [30] F Gugumus. Physico-chemical aspects of polyethylene processing in an open mixer. part 16: Mechanisms and kinetics of ketone formation at low temperature. *Polymer degradation and stability*, 90(1):53–66, 2005.

(Cited on page 68)

4 - The role of alkoxy radicals

In the previous chapter, we studied the overall oxidative reaction pathways from the initiation step to the formation of ketones. Although we focused on the pathways for ketones, which are the majority oxidative products, many other reactions could branch into other termination products. In this chapter, we consider that the reactions until the formation of peroxy radicals and hydroperoxides occur following the same reaction pathway as in the previous chapter, and we study other reactions that can occur from them. In particular, since the activation energy of the formation of hydroperoxides was estimated (both experimentally [1] and theoretically to be around 0.7 eV [2]), other reactions, which bypass the formation of hydroperoxides, could also be considered.

Nevertheless, once it is assumed that hydroperoxides are formed during oxidation, or initially included during polymerization [3], according to the BAS, hydroperoxides are decomposed by three main reaction pathways -as chain branching steps- by forming radical species: i) an alkoxy radical and a hydroxyl radical ($\text{POOH} \rightarrow \text{PO}^\circ + \text{}^\circ\text{OH}$, unimolecular decomposition, reaction 3.9), ii) an alkoxy, an alkyl radical, and a water molecule ($\text{POOH} \rightarrow \text{PO}^\circ + \text{P}^\circ + \text{H}_2\text{O}$, pseudo-unimolecular decomposition, reaction 3.10) and iii) a peroxy radical, an alkoxy radical, and a water molecule ($2\text{POOH} \rightarrow \text{POO}^\circ + \text{PO}^\circ + \text{H}_2\text{O}$, bimolecular decomposition, reaction 3.11). The comparison of the activation energies of these reactions is important in order to elucidate the mechanism controlling the OIT where the concentration of hydroperoxides reaches a maximum and finally decreases [1].

The activation energies for the first reaction, unimolecular decomposition, have been variously estimated by experiments [3, 4, 5, 6] and by theoretical calculations [2, 7, 8, 9]. Experimental results show values between 0.7 eV and 1.6 eV, while the theoretical values are higher than the experimental values with smaller intervals between 1.8 and 2.1 eV, obtained with various levels of theory, including hybrid functionals.

These high activation energies, as well as other decomposition energies of hydroperoxides, question the role of the proposed mechanism by BAS, suggesting that the overall scheme should be thoroughly compared with other possible decomposition reactions leading to the formation of radical species. The reactions also depend on the concentration of hydroperoxides (e.g., unimolecular decomposition vs bimolecular decomposition) and/or diffusion of other species, which react with hydroperoxides. The radical species such as peroxy, alkoxy, and hydroxyl radicals produced by the decomposition of hydroperoxides lead to other oxidative reactions contributing to auto-oxidation. In particular, among radical species, alkoxy radicals play an important role because they are involved in various reactions such as crosslinking (e.g., $2\text{PO}^\circ \rightarrow \text{POOP}$), chain scission (e.g., $\text{PO}^\circ \rightarrow \text{P-CHO} + \text{}^\circ\text{CH}_2\text{-P}$), and the formation of carbonyl defects ($2\text{PO}^\circ \rightarrow \text{P=O} +$

POH). Recently, De Keer et al. [10] studied some of these mechanisms based on reaction rates from ab initio calculations and built kinetic models of PE as well as other types of polymers, which support our global conclusions. However, the model is limited to small molecules, which cannot represent complex microstructures of PE (crystalline, amorphous, or at the interface between the two). In the previous chapter, the role of alkoxy radicals is not stressed because we focused on the BAS mechanisms where alkoxy radicals cannot be produced unless overcoming a high activation energy. Therefore, in this chapter, from the formation of alkoxy radicals, we investigate subsequent reactions such as crosslinking, chain scission, and carbonyl defects, which could be in competition with each other and with other possible pathways.

Another point is the microstructure of PE, neglected in most studies where calculations are performed on small molecules and the reactions are assumed to occur in the gas phase [11, 8, 12, 13, 10]. The fact that should be emphasized is that PE is a semicrystalline polymer including crystalline, amorphous, and interface regions, and such local environments potentially affect the various reaction rates. Environments, such as crystalline or surface, have been recently considered [9, 2] and this issue relates to understanding the actual reaction pathways in more realistic PE structures, allowing more detailed analysis.

Typical thickness of crystalline lamellæ is around 10 nm, [14, 15] and amorphous regions separate them. As the degradation of PE (or embrittlement) is mainly caused between crystalline PE and amorphous regions [16, 17], each local environment (i.e., amorphous phase, inside crystalline lamellæ, or at their surface) should be taken into account to investigate which reaction is dominant depending on the environment. This factor can thoroughly be inspected by atomic scale calculations, while it is more difficult to address through experiments.

Keeping in mind these two aspects (reactions related to alkoxy radicals and local environments), this chapter will analyze the overall reaction scheme shown in Fig. 4.1. The first line from PE to hydroperoxide follows the reaction pathways discussed in the previous chapter. Based on the three intermediate products (alkyl and peroxy radicals, and hydroperoxides), first, possible reactions for the formation of alkoxy radicals are considered with each local environment. After assuming the alkoxy radicals are produced, we investigate the following reactions that occur between the intermediate products. For example, crosslinking reactions take place by the combination of radical species among alkyl, peroxy, and alkoxy radicals. Ketones and alcohols are produced from hydroperoxides, as studied in the previous chapter, but other possible reactions are also considered involving alkoxy radicals. A representative reaction of chain scission reactions is the β -scission from an alkoxy radical, thus we studied it with various lengths of alkyl chains and varying positions on the surface of crystalline lamellæ. The results show that the local environment significantly affects the activation energy of oxidation reactions, and even in a similar environment (the surface), the relative position of the radicals in some

cases influences the energy barrier associated with the reaction.

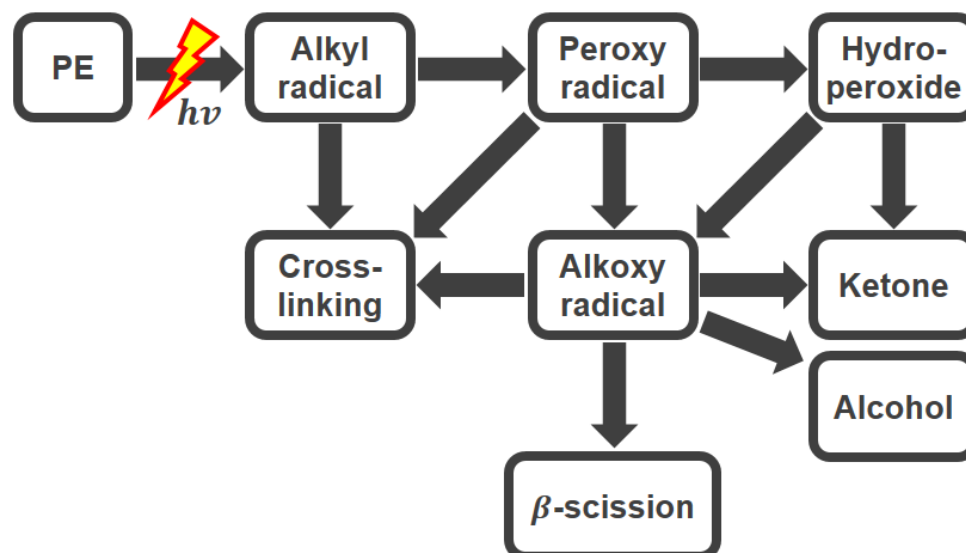


Figure 4.1 – Summary of reaction pathways for the overall oxidation process of polyethylene.

4.1 . Formation of alkoxy radicals

4.1.1 . From hydroperoxides

In general, the formation of alkoxy radicals or other radical species is described by the decomposition of hydroperoxides (reaction 3.9 - 3.11). However, because of the high activation energies calculated in the previous chapter, other reactions, such as the combination with alkyl radicals or alcohols, could also be considered in order to form alkoxy radicals. In this respect, Fig. 4.2 and 4.3 show the reactions for the decomposition of hydroperoxides and the calculated energy profiles, respectively.

In Fig.4.3, the reactions without radical species in the initial states show higher activation energies than the other reactions with alkyl radicals (4.1a and 4.2a, intra-, and intermolecular reactions) as shown in the previous chapter (reaction 3.9 - 3.11). However, the energy barriers are still relatively high for the reactions to occur at room temperature, except reaction 4.2a in crystalline PE (0.11 eV). This means that the formation of alkoxy radicals from hydroperoxides does not easily take place in many cases, implying that alternative reactions should be considered: not only through hydroperoxides but also starting from other radicals, such as peroxy ones, should be considered. On the other hand, the results show that the local environment can significantly affect the activation energies of the reactions (e.g., reaction 4.2a between solid and surface models), suggesting that the place where the reaction takes place cannot be ignored and the role of local environments should be stressed when discussing kinetic pathways.

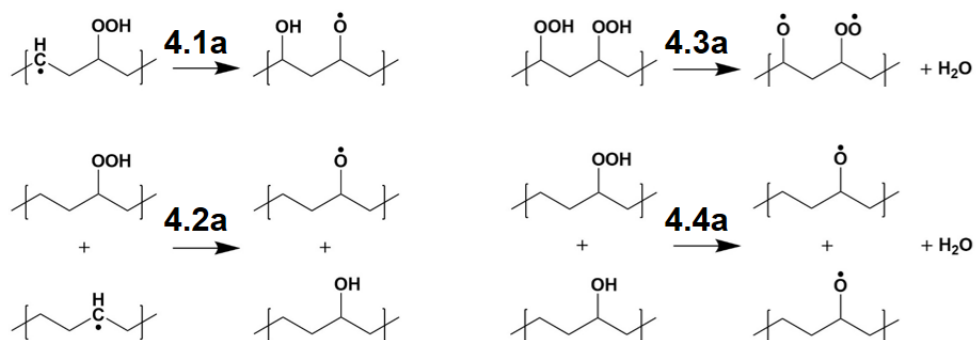


Figure 4.2 – Reaction pathways leading to the production of alkoxy radicals from decomposition of hydroperoxides either through alkyl radicals (reaction 4.1a and 4.2a), or by bimolecular conversion (reaction 4.3a) or reusing an alcohol (reaction 4.4a).

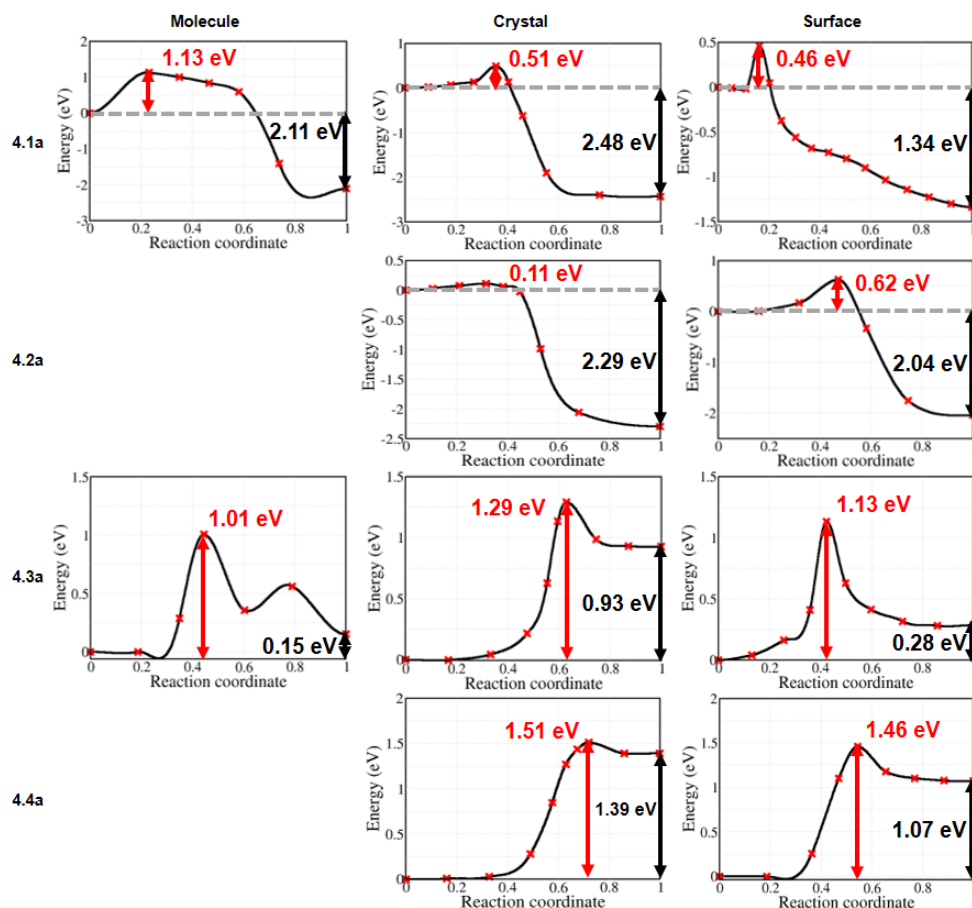


Figure 4.3 – Summary of energy profiles of reactions in Fig. 4.2 leading to alkoxy radical outcomes from hydroperoxide decomposition.

Although the activation energy of reaction 2a in crystalline PE is low, the reaction depends on the presence of alkyl radicals and hydroperoxides inside crystalline lamellæ which, for the latter, is affected by diffusion of oxygen. Oxygen diffusion is normally considered in the amorphous phase [18], but even in the amorphous phase understanding gas diffusion is quite complex [19, 20]. Therefore, the study of elementary migration mechanisms in various local environments through molecular modeling is necessary in order to understand the energies associated with permeation, solution, and migration of oxygen in the semicrystalline polymer matrix. For example, the calculated solution energy in crystalline PE is in the range of 0.8-1.0 eV, which is high, while the migration barrier is only 0.07 eV. Further details on the calculations we performed on oxygen diffusion are in Appendix (B.1).

4.1.2 . From peroxy radicals

As reported in the previous section, the formation of alkoxy radicals from hydroperoxides is not favorable regardless of the presence of alkyl radicals, at least at room temperature, and implies that other reactions are necessary. Therefore, in this section, we elucidate another reaction ($2\text{POO}^\bullet \rightarrow [\text{PO}^\bullet + \text{}^\bullet\text{OP}]_{\text{cage}} + \text{O}_2$) as shown in Fig. 4.4, which does not stem from hydroperoxides but from peroxy radicals. As peroxy radicals are spontaneously formed during radio-oxidation, the formation of alkoxy radicals can directly lead to the termination steps without stopping by hydroperoxides.

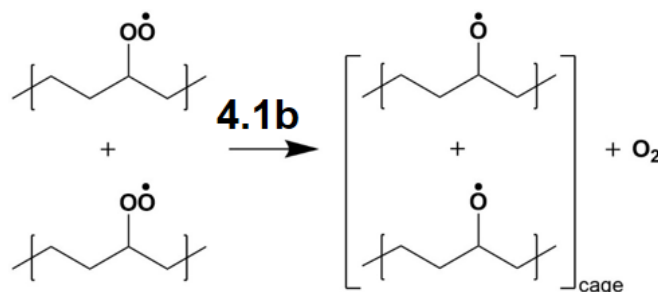


Figure 4.4 – Graphical representation of a bimolecular reaction leading to the formation of alkoxy radicals from two adjacent peroxy ones.

Since the formation of hydroperoxides by H-abstraction reaction has recently been questioned because of its high activation energy, other reactions bypassing hydroperoxides, such as reaction 4.1b, have been considered to be relevant for a kinetic study [10]. The need to consider this reaction had previously been stressed in the framework of kinetic studies of radio-chemical degradation of PE [21, 22] in order to correctly describe the variation of OIT with various parameters (temperature, dose, concentration of antioxidants) and the reach of a steady oxidation state. Including relevant peroxy radical reactions should also help to correctly describe the competition between terminating and non-terminating reactions (35-40 % at

45 °C). Because of the importance of this reaction, we set four different starting configurations on the surface of lamellæ in order to consider the potential factors, such as the steric hindrance or the cage effect, which could affect the activation energy. As shown in Fig.4.5a, we fixed one of the two peroxy radicals of the bimolecular reaction and varied the position of the other peroxy radical from H1 to H4. Fig.4.5b shows the calculated energy profiles and the results are summarized in Table 4.1, including the activation energy calculated in crystalline PE. The difference in activation energies is quite remarkable because it obviously depends on the local environments. While the activation energy in crystalline PE is 1.30 eV, which is high and might be related to solution energy of oxygen, the reaction easily occurs on the surface of lamellæ with no barriers. It means that once two peroxy radicals end up close to each other, alkoxy radicals are easily formed. Compared to the decomposition of hydroperoxides, which requires high activation energies, this reaction is much more favorable, and it can bypass the formation of hydroperoxides according to the calculated activation energies. This is also confirmed by ab initio molecular dynamics in Appendix D.3 that the reaction from two peroxy radicals takes place within a few picoseconds. However, the reaction is bimolecular, which means that it needs high concentration of peroxy radicals or a favorable pair correlation between them. Diffusion of peroxy radicals could also be considered, but in general, it is excluded [23].

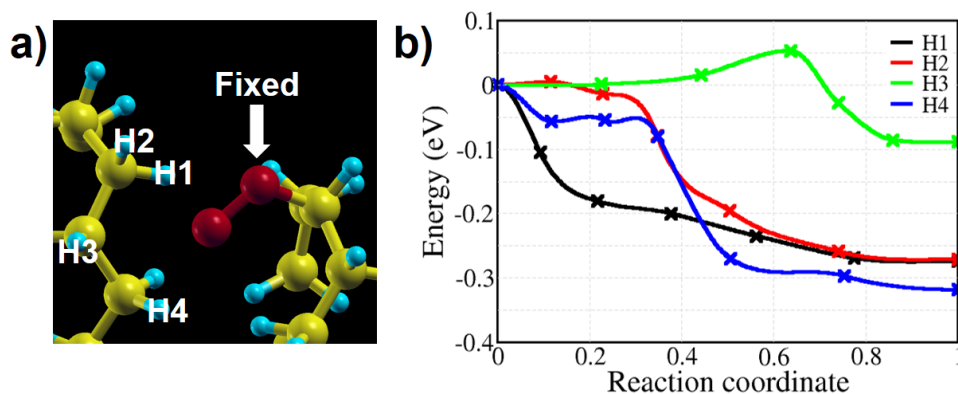


Figure 4.5 - a) The starting configurations of reaction 4.1b ($2\text{POO}^\circ \rightarrow [\text{PO}^\circ + {}^\circ\text{OP}]_{\text{cage}} + \text{O}_2$) on the lamellæ surface. While one peroxy radical is fixed, the positions from H1 to H4 indicate the other peroxy radical of the pair (not shown) for the bimolecular reaction. b) Calculated energy profiles for reactions (H1-H4).

Although entropic contribution is not considered because of its complexity, low activation energies from various configurations leading to the formation of alkoxy radicals suggest that low entropic barriers would be expected (no rotational contribution). Possible products of the reactions in which alkoxy radicals can participate are crosslinking, chain scission, and carbonyl defects. In the following

Table 4.1 – Summary of activation energies and enthalpies of the bimolecular reaction depicted in Fig.4.4, describing the formation of alkoxy radicals directly from peroxy radicals. The role of the environment is highlighted through four different starting configurations (H1-H4) on the lamellæ surface, and the reaction starting from two neighboring peroxy radicals in crystalline environment.

Reaction	Activation energy (E_a)		Enthalpy	
	Crystal	Surface	Crystal	Surface
4.1b	1.30	0.00 (H1)	0.90	-0.27
		0.00 (H2)		-0.27
		0.05 (H3)		-0.09
		0.00 (H4)		-0.32

[eV]

sections, we will elucidate these reactions by calculating their energy profiles and assessing the role of the local environment.

4.2 . Crosslinking reactions

Crosslinking reactions take place from the combination of radical species: alkyl, alkoxy, and peroxy radicals. In oxidative environment, the competition with chain scission will affect the chemicrystallisation, which causes cracks of PE and finally embrittlement. From the reaction between two alkyl radicals at low O_2 pressure, several combinations of radical species can be considered for crosslinking as shown in Fig.4.6. Since all reactions need two chains (bimolecular reactions), the reactions are focused on crystalline PE or the surface of lamellæ; the molecular model, which can represent amorphous regions with fairly low density, is not considered.

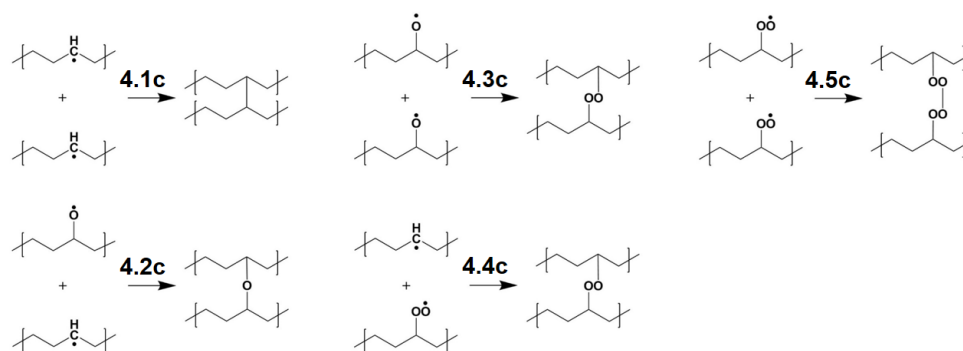


Figure 4.6 – Graphical representation of reactions where two radicals lead to crosslinking.

The results are summarized in Fig. 4.7. All reactions remove radicals because crosslinking reactions constitute a termination step. Reaction 4.1c shows a high activation energy, which might be coming from the steric hindrance of the structure and produces saturated chains. Due to instability, a final state of reaction 4.5c on the surface of a lamella was not found. Except for reaction 4.1c, the other reactions take place without barrier, which means that when the concentration of radicals is sufficient and they are located close enough, crosslinking reactions would be dominant over chain scission. Besides, because the reactions are highly exothermic, once the reactions occur, the bonds of crosslinking are hardly broken. On the other hand, the concentration of oxygen also affects the reactions because a secondary alkyl radical is stable around 15 hours after irradiation [24] and spontaneously reacts with oxygen by forming peroxy radicals. The position of radical species is also important because the migration energy of alkyl radicals is high (over 1.67 eV: along the alkyl chain, and around 1 eV: across alkyl chains; see Appendix B.2) and peroxy radicals are also expected to have high migration energy because of their stability.

Because two close alkoxy radicals formed by reaction 4.1b can lead to crosslinking, β -scission, and carbonyl defects, the positional effect induced by varying the starting configuration of alkoxy radicals is tested in a similar way as shown for reaction 4.1b in Fig.4.5. Fig.4.8 shows the starting configurations and calculated energy profiles. In contrast with reaction 4.1b, depending on the positions, the calculated activation energy varies from null to almost 0.4 eV, implying that even in the same local environment, the reactions are affected by the starting configurations. The fact that some of the calculated barriers are not negligible (up to almost 0.4 eV) can lead to competition with the other reactions (β -scission and carbonyl defects), which will be discussed in the following sections. Due to these different activation energies depending on the starting configurations, each configuration described in Fig.4.8 is also performed by ab initio molecular dynamics at room temperature to observe the final products in Appendix D.4.

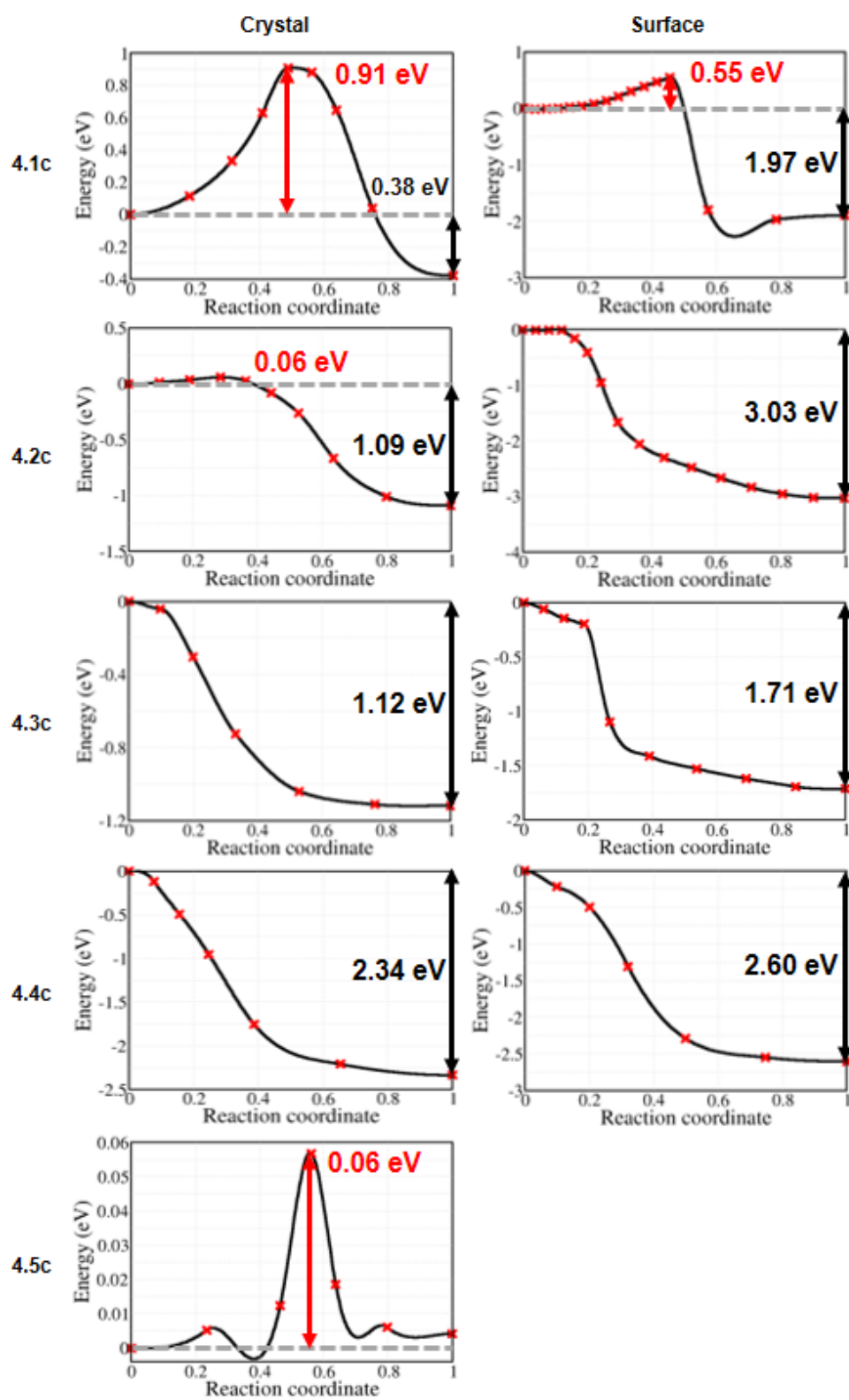


Figure 4.7 – Calculated energy profiles for crosslinking, corresponding to reactions shown in Fig. 4.6

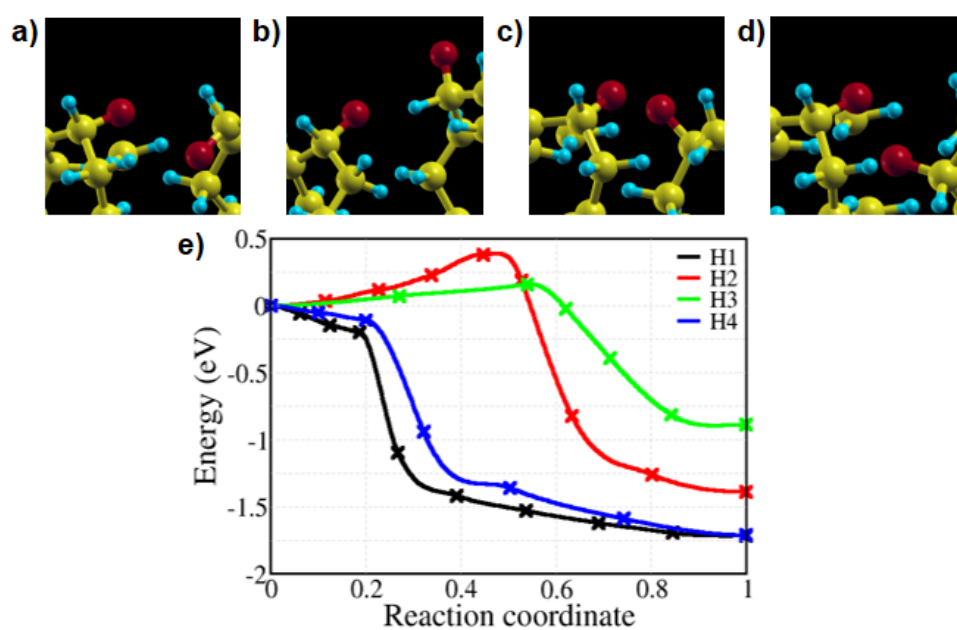


Figure 4.8 – Illustration of four initial alternative configurations for reaction 4.3c (see Fig.4.5 and 4.6) on the surface of lamellæ (panels a-d), and the corresponding energy profiles (panel e). H1 to H4 label the four starting configurations, which are analogous to those shown in Fig. 4.5.

4.3 . Chain scission reactions

While carbon-carbon bond scission shows high activation energy (3.9 eV [25]), the presence of radical species can decrease the activation of chain scission reactions [8]. This is firstly checked before studying β -scission of alkoxy radicals, which is generally proposed as chain scission reactions. An alkyl radical on the surface of lamellæ induces chain scission as follows:

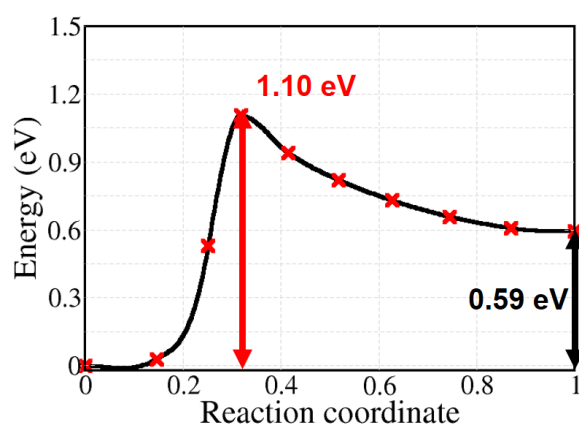


Figure 4.9 - Energy profiles of chain scission in the presence of an alkyl radical.

Compared to the energy profile of carbon-carbon chain scission on saturated alkyl chains (Fig. 3.1b), the activation energy is much reduced from 3.93 eV to 1.10 eV, which confirms the role of radical species.

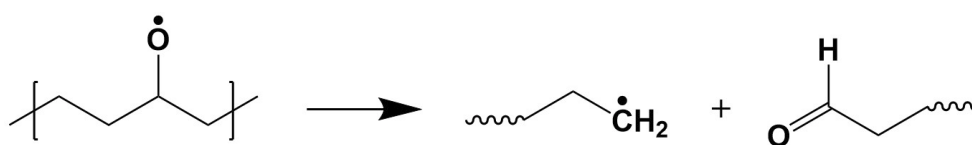


Figure 4.10 - Graphical illustration of a β -scission reaction starting from an alkoxy radical leading to an aldehyde and a primary alkyl radical.

The reaction scheme of β -scission induced by an alkoxy radical is shown in Fig. 4.10. In the scheme, an aldehyde and a primary alkyl radical are produced by the decomposition of an alkoxy radical. Each local environment is considered to calculate the energy profiles of the reaction. While obtaining an optimized final state, it turned out that the reaction in crystalline PE was not favorable. During the calculation, the distance between carbon and carbon at the broken chain ends was firstly constrained, and then the system was relaxed. However, after removing

the constraint on the distance, a broken chain was spontaneously restored by its surrounding chains, and finally, the chain returned to the starting configuration. Nevertheless, Fig.4.11 shows the energy difference depending on the constrained carbon-carbon distance in crystalline PE.

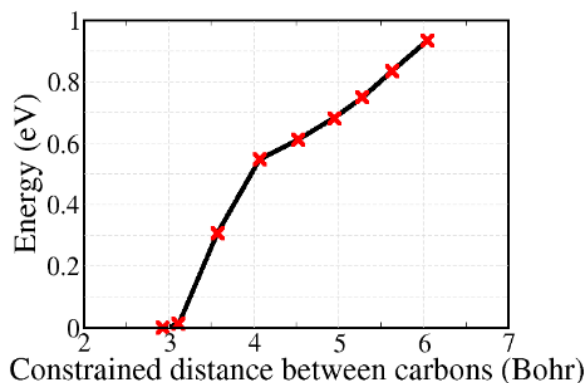


Figure 4.11 – Energy as a function of the constrained carbon-carbon distance at the broken chain ends in crystalline PE.

For the molecular model, we varied chain lengths from C_4H_9O to $C_{12}H_{25}O$ to consider how the chain length affects the activation energy. The calculated activation energy is around 0.4 eV, which is similar to the value of crosslinking reaction from the H2 position. In the case of the surface model, we also studied it by changing the position of an alkoxy radical (see position information in Fig. 4.5). The calculated activation energies on the surface of lamellæ are slightly lower than the values of the molecular model and show exothermic reactions. The calculated energy profiles and values are summarized in Fig.4.12 and Table 4.2, respectively.

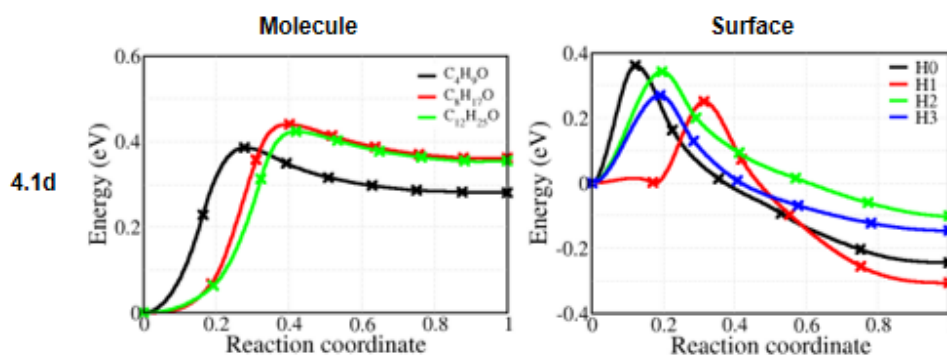


Figure 4.12 – Energy profiles for β -scission reactions with a) molecular and b) surface model. Information on positions can be found in Appendix C.

Table 4.2 – Summary of activation energies and reaction enthalpies for the β -scission reaction shown in Fig.4.12. This reaction can take place at the surface of a PE crystalline lamella, but not inside it (the final state is unstable).

Reaction	Activation energy (E_a)		Enthalpy	
	Molecule	Surface	Molecule	Surface
4.1d	0.39 (C ₄ H ₉ O)	0.36 (H0)	0.28	-0.24
	0.44 (C ₈ H ₁₇ O)	0.25 (H1)	0.36	-0.31
	0.42 (C ₁₂ H ₂₅ O)	0.34 (H2)	0.35	-0.10
		0.27 (H3)		-0.15

[eV]

4.4 . Termination through alcohol and ketone groups

Not only crosslinking reactions but the formation of alcohols and ketones is also involved in the termination step because alkoxy radicals can abstract hydrogen atoms. In this section, possible reaction pathways leading to ketones and/or alcohols from alkoxy radicals are considered. These reactions can be examined in comparison with other termination reactions (e.g., crosslinking) or β -scission reactions because they share alkoxy radicals as an initial state and could be in competition with one another. For example, an alkoxy radical can lead to an alcohol, β -scission, or crosslinking reaction with an alkyl radical. Fig.4.13 shows the considered reaction pathways starting from alkoxy radicals such as unimolecular reactions, bimolecular ones, or reactions with alkyl radicals. The calculated energy profiles for three different local environments are summarized in Fig.4.14

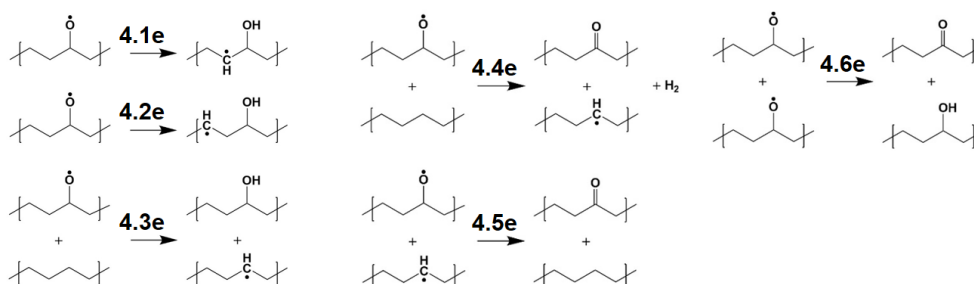


Figure 4.13 – Graphical illustration of the formation of ketones or alcohols starting from one or two alkoxy radicals.

Reaction 4.1e and 4.2e are H-abstraction reactions along the chain (intramolecular reactions) from β - and γ positions and reaction 4.3e is the same reaction occurring between two neighboring chains (intermolecular reactions). Similarly to H-abstraction by peroxy radicals, for the intramolecular reactions, the activation energy for γ position is lower than for β position, and they tend to have higher barriers than intermolecular reactions (reaction 4.3e). All these H-abstraction reactions from an alkoxy radical have negative reaction enthalpies, independently of the environment, at variance with H-abstraction by a peroxy radical (see Fig. 3.5). For reaction 4.4e, a hydrogen atom at α position is abstracted by forming a ketone. This can be compared to reaction 4.5e and 4.6e, which are basically the same reaction but in the presence of an alkyl and an alkoxy radical at neighboring chains, respectively. The activation energies are much reduced for the last two mentioned reactions, implying the importance of the role of radical species. Therefore, for the termination step with alkoxy radicals, reaction 4.5e and 4.6e on the surface of lamellæ are the most favorable reaction pathways leading to ketones and alcohols.

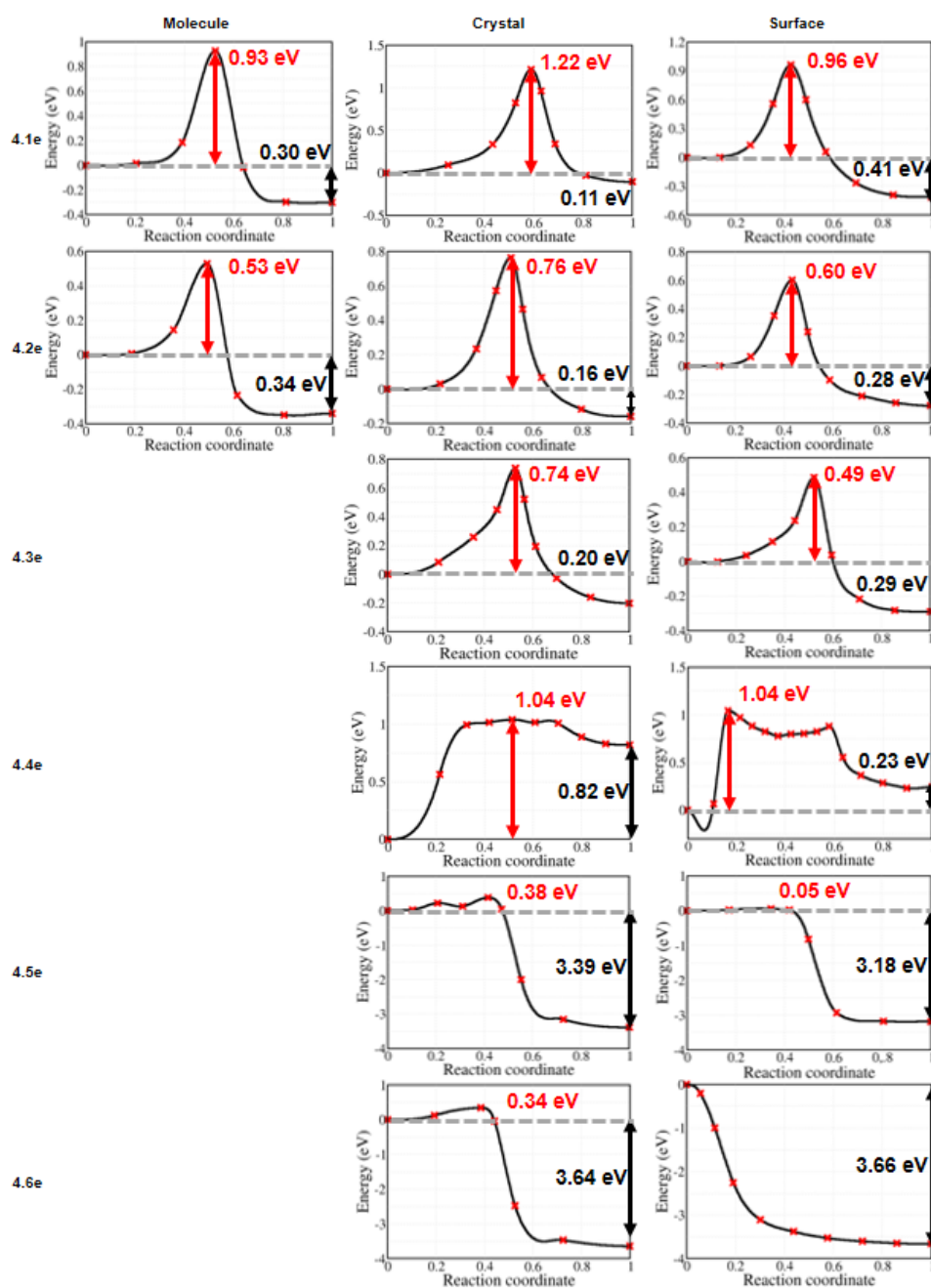


Figure 4.14 – Energy profiles for reactions leading to the formation of ketones or alcohols starting from alkoxy radicals.

4.5 . Summary and Conclusions

The previous sections presented energy profiles for reactions related to alkoxy radicals, from their formation to reactions where they participate and eventually disappear. For the formation of alkoxy radicals, the decomposition of hydroperoxides and bimolecular reactions involving two peroxy radicals are considered. Despite including the conventional pathways and radical species (except hydroperoxyl radicals), decomposition of hydroperoxides is not easy on the surface of lamellæ at room temperature, and the lowest energy found is 0.46 eV for reaction 4.1a (decomposition by intramolecular reaction with an alkyl radical), if we exclude the reactions occurring in crystalline PE, probably hindered by the high permeation energy of oxygen. On the other hand, the formation of alkoxy radicals by two peroxy radicals is spontaneous on the surface of lamellæ. The situation is different in crystalline PE, where the activation energy is up to 1.30 eV, implying the importance of the local environment. As the reaction is bimolecular, the concentration of peroxy radicals affects the reaction rate.

The presence of alkoxy radicals can induce crosslinking, β -scissions, and the formation of ketones and alcohols. Crosslinking reactions take place with the combination of radical species. Alkyl, alkoxy, and peroxy radicals are considered. Except for the reaction of alkyl-alkyl radicals, most of the considered reactions are spontaneous and strongly exothermic. However, similarly to the formation of alkoxy radicals, they are bimolecular reactions and require high concentration of the involved species. Some of them have activation energies up to 0.4 eV, depending on their starting configurations. This means that if the starting configurations are sterically hindered, the reactions can be competitive with β -scission reactions, which have similar barriers. The calculated activation energies of β -scission reactions are from 0.28 eV to 0.36 eV on the surface of lamellæ. In contrast with crosslinking reactions, β -scission reactions are unimolecular reactions, so they do not need high concentration of alkoxy radicals. For the formation of ketones and alcohols, reaction 4.5e and 4.6e are almost spontaneous. Let us note that alcohols are produced only from reaction 4.6e, which produces ketones at the same rate. As ketones are also produced by reaction 4.5e then, the ratio of alcohols to ketones should be lower than one.

On the other hand, radical species globally decrease activation energies of the oxidative reactions compared to the reactions without them. In other words, radical species accelerate the oxidation of PE, and deactivating radicals could play a key role in preventing the oxidative degradation of PE. The general strategy is the incorporation of antioxidants. For example, phenolic antioxidants could deactivate peroxy radicals through the formation of hydroperoxides by H-transfer reactions. However, because energy profiles of such reactions at the atomic scale have been hardly studied, in the following chapter, we will discuss H-transfer reactions by phenolic antioxidants with three radical species: alkyl, alkoxy, and peroxy radicals.

Bibliography

- [1] Manuela Da Cruz, Laetitia Van Schoors, Karim Benzarti, and Xavier Colin. Thermo-oxidative degradation of additive free polyethylene. part i. analysis of chemical modifications at molecular and macromolecular scales. *Journal of Applied Polymer Science*, 133(18), 2016.
(Cited on pages 5, 6, 7, 10, 14, and 77)
- [2] Yunho Ahn, Xavier Colin, and Guido Roma. Atomic scale mechanisms controlling the oxidation of polyethylene: A first principles study. *Polymers*, 13(13):2143, 2021.
(Cited on pages 63, 77, 78, and 117)
- [3] Liang Chen, Shuzo Kutsuna, Shogo Yamane, and Junji Mizukado. ESR spin trapping determination of the hydroperoxide concentration in polyethylene oxide (PEO) in aqueous solution. *Polymer Degradation and Stability*, 139:89–96, 2017.
(Cited on pages 63 and 77)
- [4] Jacqueline L Henry, Ascencion L Ruaya, and Andrew Garton. The kinetics of polyolefin oxidation in aqueous media. *Journal of Polymer Science Part A: Polymer Chemistry*, 30(8):1693–1703, 1992.
(Cited on pages 11, 63, and 77)
- [5] Pieter Gijsman, Jan Hennekens, and Jef Vincent. The mechanism of the low-temperature oxidation of polypropylene. *Polymer Degradation and Stability*, 42(1):95–105, 1993.
(Cited on pages 11, 63, and 77)
- [6] B Fayolle, J Verdu, M Bastard, and D Piccoz. Thermooxidative ageing of polyoxymethylene, part 1: chemical aspects. *Journal of applied polymer science*, 107(3):1783–1792, 2008.
(Cited on pages 11, 63, and 77)
- [7] John M Simmie, Gráinne Black, Henry J Curran, and John P Hinde. Enthalpies of formation and bond dissociation energies of lower alkyl hydroperoxides and related hydroperoxy and alkoxy radicals. *The Journal of Physical Chemistry A*, 112(22):5010–5016, 2008.
(Cited on pages 11, 63, and 77)
- [8] Pascal de Sainte Claire. Degradation of PEO in the solid state: A theoretical kinetic model. *Macromolecules*, 42(10):3469–3482, 2009.
(Cited on pages 11, 16, 17, 63, 66, 67, 77, 78, and 87)

- [9] Ibukun Oluwoye, Mohammednoor Altarawneh, Jeff Gore, and Bogdan Z Dlugogorski. Oxidation of crystalline polyethylene. *Combustion and Flame*, 162(10):3681–3690, 2015.
(Cited on pages 11, 16, 17, 19, 63, 77, and 78)
- [10] Lies De Keer, Paul Van Steenberge, Marie-Françoise Reyniers, Ganna Gryn’Ova, Heather M Aitken, and Michelle L Coote. New mechanism for autoxidation of polyolefins: kinetic monte carlo modelling of the role of short-chain branches, molecular oxygen and unsaturated moieties. *Polymer Chemistry*, 13(22):3304–3314, 2022.
(Cited on pages 11, 78, 81, and 135)
- [11] Jim Pfaendtner, Xinrui Yu, and Linda J Broadbelt. Quantum chemical investigation of low-temperature intramolecular hydrogen transfer reactions of hydrocarbons. *The Journal of Physical Chemistry A*, 110(37):10863–10871, 2006.
(Cited on page 78)
- [12] Carrigan J Hayes and Donald R Burgess Jr. Kinetic barriers of h-atom transfer reactions in alkyl, allylic, and oxoallylic radicals as calculated by composite ab initio methods. *The Journal of Physical Chemistry A*, 113(11):2473–2482, 2009.
(Cited on pages 16 and 78)
- [13] Ondrej Kysel’, Šimon Budzák, Miroslav Medved’, and Pavel Mach. A dft study of h-isomerisation in alkoxy-, alkylperoxy- and alkyl radicals: Some implications for radical chain reactions in polymer systems. *Polymer degradation and stability*, 96(4):660–669, 2011.
(Cited on pages 9, 16, 17, 53, and 78)
- [14] Hongyi Zhou and GL Wilkes. Comparison of lamellar thickness and its distribution determined from dsc, saxs, tem and afm for high-density polyethylene films having a stacked lamellar morphology. *Polymer*, 38(23):5735–5747, 1997.
(Cited on pages 78 and 114)
- [15] RC Savage, N Mullin, and JK Hobbs. Molecular conformation at the crystal–amorphous interface in polyethylene. *Macromolecules*, 48(17):6160–6165, 2015.
(Cited on pages 78, 114, and 117)
- [16] Bruno Fayolle, Emmanuel Richaud, Xavier Colin, and Jacques Verdu. Degradation-induced embrittlement in semi-crystalline polymers having their amorphous phase in rubbery state. *Journal of materials science*, 43(22):6999–7012, 2008.

(Cited on pages 13, 14, and 78)

- [17] AK Rodriguez, B Mansoor, G Ayoub, Xavier Colin, and AA Benzerga. Effect of uv-aging on the mechanical and fracture behavior of low density polyethylene. *Polymer Degradation and Stability*, 180:109185, 2020.

(Cited on pages 13 and 78)

- [18] Alan S Michaels and Harris J Bixler. Flow of gases through polyethylene. *Journal of Polymer Science*, 50(154):413–439, 1961.

(Cited on pages 81 and 117)

- [19] Anders Börjesson, Edvin Erdtman, Peter Ahlström, Mikael Berlin, Thorbjörn Andersson, and Kim Bolton. Molecular modelling of oxygen and water permeation in polyethylene. *Polymer*, 54(12):2988–2998, 2013.

(Cited on page 81)

- [20] Peyman Memari, Véronique Lachet, and Bernard Rousseau. Molecular simulations of the solubility of gases in polyethylene below its melting temperature. *Polymer*, 51(21):4978–4984, 2010.

(Cited on page 81)

- [21] N Khelidj, X Colin, L Audouin, J Verdu, C Monchy-Leroy, and V Prunier. Oxidation of polyethylene under irradiation at low temperature and low dose rate. part ii. low temperature thermal oxidation. *Polymer degradation and stability*, 91(7):1598–1605, 2006.

(Cited on pages 10 and 81)

- [22] N Khelidj, X Colin, L Audouin, J Verdu, C Monchy-Leroy, and V Prunier. Oxidation of polyethylene under irradiation at low temperature and low dose rate. part i. the case of “pure” radiochemical initiation. *Polymer degradation and stability*, 91(7):1593–1597, 2006.

(Cited on page 81)

- [23] Pierangiola Bracco, Luigi Costa, Maria Paola Luda, and Norman Billingham. A review of experimental studies of the role of free-radicals in polyethylene oxidation. *Polymer Degradation and Stability*, 155:67–83, 2018.

(Cited on page 82)

- [24] Shun-Ichi Ohnishi, Shun-Ichi Sugimoto, and Isamu Nitta. Electron spin resonance study of radiation oxidation of polymers. iii. results for polyethylene and some general remarks. *Journal of Polymer Science Part A: General Papers*, 1(2):605–623, 1963.

(Cited on page 84)

- [25] JCL Hageman, GA De Wijs, RA De Groot, and Robert J Meier. Bond scission in a perfect polyethylene chain and the consequences for the ultimate strength. *Macromolecules*, 33(24):9098–9108, 2000.

(Cited on pages 16, 53, 54, and 87)

5 - Antioxidants

In this chapter, we study a possible mechanism explaining the action of phenolic antioxidants. In the previous chapters, we showed that radical species decrease the activation energies by accelerating the oxidation process (e.g., 4.4e and 4.5e). Therefore, deactivating such radicals can play a key role in preventing the oxidation of PE. We can consider two mechanisms by which antioxidants protect the polymer matrix from oxidation. Firstly, aromatic rings (i.e., benzene) in antioxidants can preferentially absorb the energy of incident photons, acting as an energy sink and thus preventing the formation of alkyl radicals [1, 2]. In other words, energy transfer between aliphatic and aromatic parts takes place, and the energy from electronic excitation of BHT is more likely to be transferred evenly among several phonons instead of causing C-H bond dissociation (i.e., formation of alkyl radicals). Secondly, H-transfer reaction by hindered phenol function can deactivate radical species (e.g., scavenging peroxy radicals) by blocking the propagation and/or chain branching steps [3, 4, 5, 6, 7, 8]. Here, we focus on the second mechanism, which is more related to kinetic studies, but the first one will also be discussed.

Butylated hydroxytoluene (BHT) and octadecyl-3-(3,5-di-*tert*-butyl-4-hydroxyphenyl)propionate (Irganox 1076) shown in Fig.5.1 are well known primary antioxidants that effectively deactivate radical species. For the sake of calculation, BHT is easier to deal with than Irganox 1076 because it contains fewer atoms (40 instead of 100), whereas a similar chemical stabilization mechanism is expected between hindered phenols and radical species [9].

Although the most commonly considered scavenging reaction involves the antioxidant and a peroxy radical [8, 10], other radical species such as alkyl and alkoxy radicals could react with the phenol function as follows:



where AO and AO° represent antioxidants and phenoxy radicals in antioxidants after H-transfer reactions. For the calculation, in the case of the molecular model, a peroxy radical was randomly put close to a phenol function, and then the system was relaxed. After obtaining the equilibrium structure, alkoxy and alkyl radicals were subsequently relaxed by removing, each time, an oxygen atom. In the case of the surface model, BHT was put flat on the surface of a lamella where only saturated alkyl chains are present, and then the relaxation of the structure was performed. During the relaxation, the phenol function moves towards the surface,

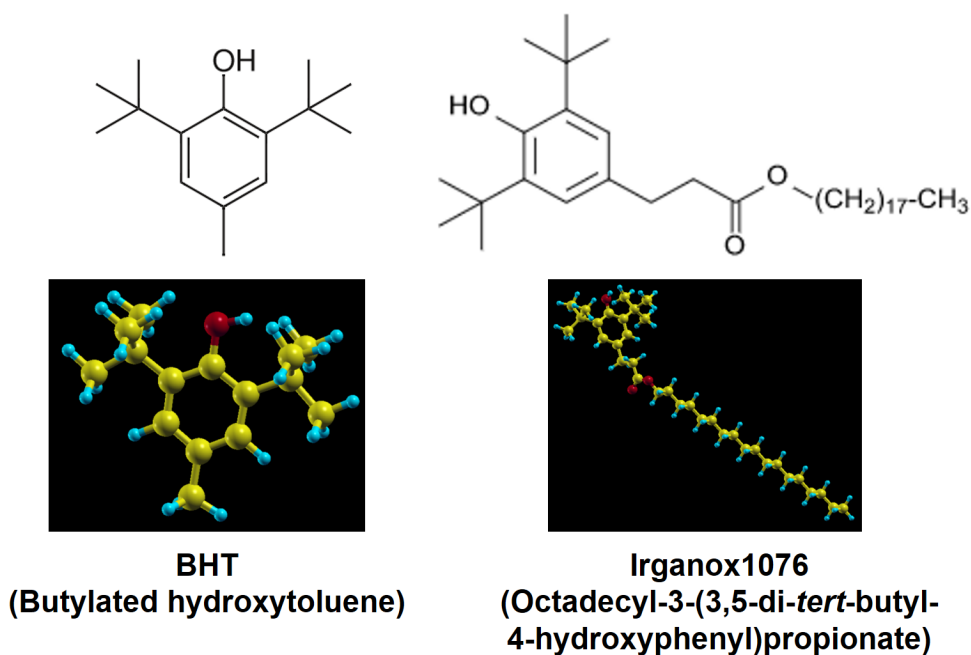


Figure 5.1 – Molecule structures of antioxidants: BHT and Irganox 1076.

while the *para*- substituent group heads to the amorphous region (Fig. 5.2). After obtaining the equilibrium structure, a peroxy radical was put close to the phenol group, and then the structure was relaxed again. The structures for alkoxy and alkyl radicals were obtained from the peroxy radical structure as for the molecular model. The calculated formation energy of BHT on the lamellæ surface (Fig. 5.2) is -1.34 eV, meaning that BHT molecules are stable on the surface of lamellæ. Besides, we have calculated the formation energy of the orthorhombic BHT crystal [11], which is -6.78 eV, showing that this phase is much more stable than the absorbed BHT molecule on the surface of a PE lamella. The crystallization of phenolic antioxidants (in this case, Irganox 1076) is indeed observed as the blooming structures onto the polymer film surface when the phase separation occurs due to the high concentration of the antioxidants [7].

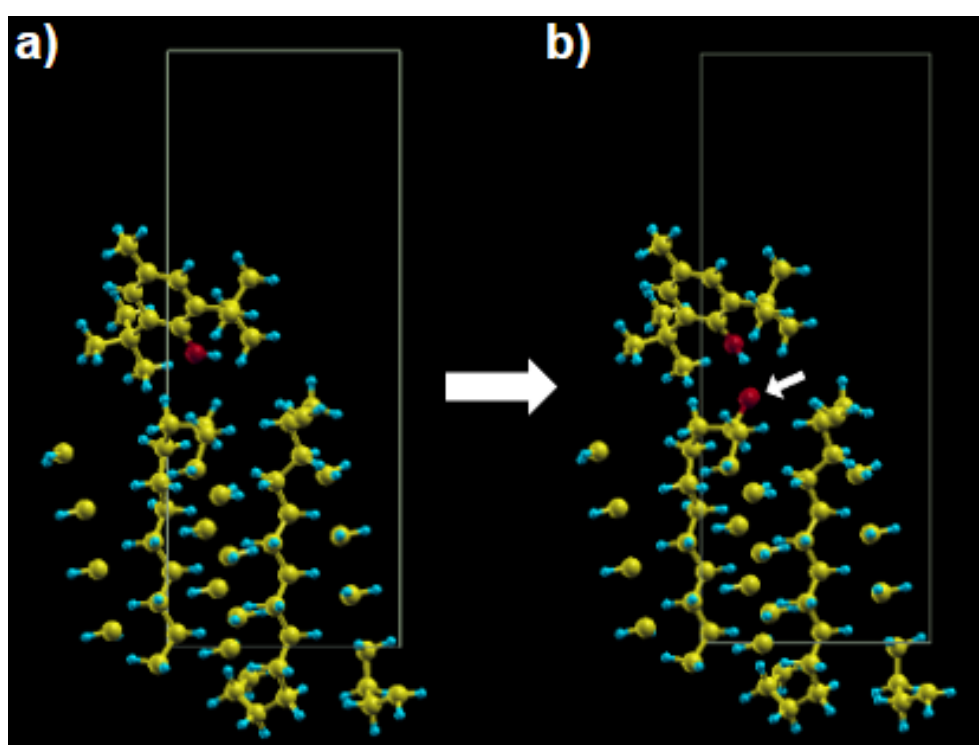


Figure 5.2 – The structure of BHT (a) on the pure lamellæ surface and (b) on the lamellæ surface with a peroxy radical.

From the relaxed structures, NEB calculations were then performed for reaction 5.1 - 5.3.

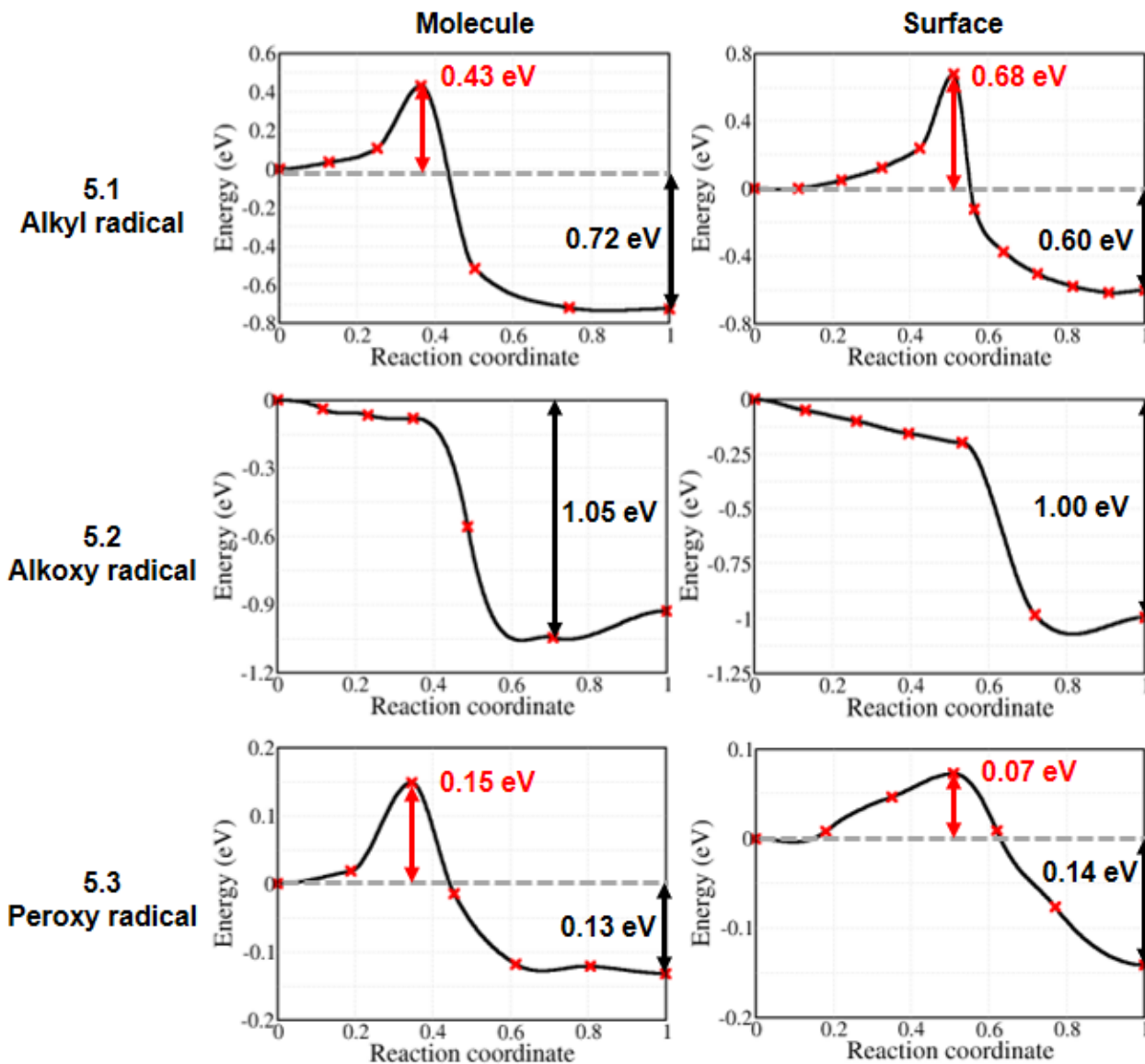


Figure 5.3 – Calculated energy profiles of H-transfer reactions between antioxidants and radical species.

Fig.5.3 shows the calculated energy profiles of H-transfer reactions between BHT and radical species. Calculated activation energies are 0.43 eV, 0.0 eV, and 0.15 eV for the molecular model, and 0.68 eV, 0.0 eV, and 0.07 eV for the surface model for alkyl, alkoxy, and peroxy radicals, respectively. All reactions are exothermic. The activation energy for scavenging peroxy radicals is much lower than that obtained by experiments (around 0.62 - 0.83 eV determined by Arrhenius plot [9]).

The discrepancy could come from the fact that the experimental study relies on the carbonyl absorbance from FTIR spectroscopy and their kinetic modeling based on BAS. Although the concentration of phenoxy radicals could be tracked, such as by electron paramagnetic resonance (EPR) [12], some radicals could be hardly detected when they are highly reactive and thus very short lived. If some of those reactive radicals are neglected or if their concentration is underestimated in the BAS, the determination of the scavenging rate constant on the basis of the stable carbonyl species might be biased.

Besides, other mechanisms could hinder the measurement of the activation energy. Firstly, as energy transfer between aliphatic and aromatic parts is observed [2], we can suppose that alkyl and peroxy radicals are less likely to be produced in the vicinity of the antioxidant molecule because the energy from electronic excitation of BHT is more likely to be transferred to phonons. Moreover, due to this effect, when such radicals do not exist in the vicinity of BHT, the antioxidant molecule has to diffuse to reach other radicals which are far away. Thus, the measured activation energy might include the migration energy of BHT on the surface. On the other hand, other theoretical calculations span a broad range of activation energies (0.10 to 1.04 eV) [13, 14, 15]. However, the calculations are performed with small molecules, and the specific local environment is not considered.

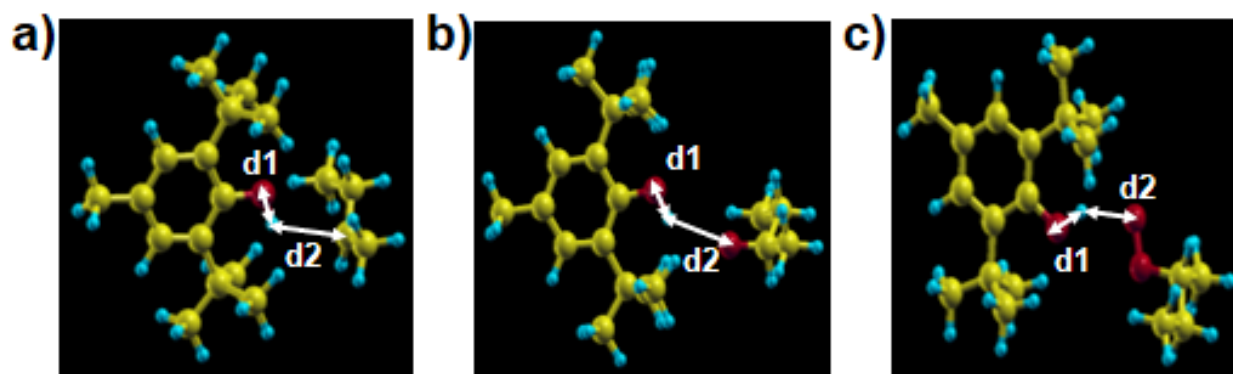


Figure 5.4 – Distances d_1 and d_2 . d_1 is the length of the O-H bond of the hindered phenol function, and d_2 is the distance between the hydrogen atom of the hindered phenol function and the radical species: a) alkyl radical, b) alkoxy radical, and c) peroxy radical.

Further analysis is performed by comparing the length of the O-H bond of the hindered phenol function (d_1) and the distance between the hydrogen atom of the hindered phenol function and the radical species (d_2) as shown in Fig. 5.4 and 5.1. The trend of the calculated values of d_1 is peroxy > alkoxy > alkyl radicals, and for d_2 is alkyl > alkoxy > peroxy radicals for both models at the initial states. Let us note that the activation energy decreases in the order of

Table 5.1 – Summary of the calculated distances d_1 and d_2 . Initial and final states are corresponding to reaction 5.1 - 5.3

Alkyl radical	Molecular		Surface	
	Initial	Final	Initial	Final
d1	0.977	2.523	0.976	3.020
d2	2.672	1.106	3.628	1.109
Alkoxy radical				
d1	0.980	3.058	0.980	2.309
d2	2.427	0.976	2.716	0.982
Peroxy radical				
d1	0.987	1.871	1.003	1.651
d2	1.958	0.994	1.696	1.008

[Unit:Å]

alkyl, peroxy, and alkoxy radicals. If the activation energy were only affected by the distance, the larger d_1 and the smaller d_2 would be expected to reduce the barrier. However, when comparing alkoxy and peroxy radicals, such assumption is not correct because alkoxy radicals react spontaneously, which means that alkoxy radicals are more reactive than peroxy radicals to abstract a hydrogen atom despite the larger distance d_2 . On the other hand, in the case of alkyl radicals, d_1 is smaller and d_2 is larger than for the other radicals at the initial states, so that the high barrier could be expected due to the distance. Although a shorter d_2 can be imposed as a starting configuration for a calculation within the molecular model to obtain a lower activation energy, the equilibrium distance after the relaxation of d_2 at the initial state would not much deviate from the distance in the equilibrium structure on the surface of a lamella. In this respect, the influence of distance can also be studied carefully by molecular dynamics.

In any case, based on our calculations, H-transfer reactions effectively take place for alkoxy and peroxy radicals by forming alcohols and hydroperoxides, but alkyl radicals are not easily removed. This is also observed when peroxy and alkyl radicals attack a hydrogen atom at the tertiary site of hydroperoxides in crystalline PE (Fig. 3.19 in Chapter 3). The calculated activation energies are 0.63 eV and 1.54 eV for peroxy and alkyl radicals, respectively (reaction 3.17 and 3.18, and Fig.3.19). Given that the lowest activation energy of decomposition of hydroperoxides is 0.46 eV on the surface of lamellæ, hydroperoxides and alcohols are stable in comparison to radical species such as alkoxy and peroxy radicals, which cause an acceleration of auto-oxidation. In other words, by removing such radicals effectively, BHT can block the crosslinking, chain scission, and the formation of carbonyl groups (i.e., ketones), which otherwise could be generated without barrier as discussed in Chapter 4. Besides, once they are formed, hydroperoxides and alcohols are less likely to participate in oxidative reactions, and the OIT is prolonged.

On the other hand, H-transfer reactions from antioxidants are not efficient for deactivating alkyl radicals directly. However, with the observation of the stable phenoxy radicals [16, 17, 18], the role of antioxidants in reducing alkyl radicals and crosslinking reactions [19, 20, 12] has been observed by experiments. This implies that antioxidants also contribute to lowering the concentration of alkyl radicals. Although a low reaction rate is expected between antioxidants and alkyl radicals based on the calculation, other factors can explain how antioxidants affect the concentration of alkyl radicals:

- i) hydroperoxides and alcohols, which can be formed from antioxidants, are stable in PE matrix: the associated phenoxy radicals can further react with alkyl radicals.
- ii) Although the reaction between antioxidants and alkyl radical is less likely than with alkoxy or peroxy radicals, it is nevertheless globally more favorable than the cross-linking between two alkyl radicals, which has an activation energy of 0.91 eV in crystalline PE and 0.55 eV on the surface of lamellæ;
- iii) Alkyl radicals spontaneously react with oxygen by forming peroxy radicals; if peroxy radicals produced are scavenged by antioxidants or react with other alkyl radicals, an indirect estimation of alkyl radical concentration based on the concentration of peroxy radicals would be biased.

In this chapter, H-transfer reactions with radical species are elucidated as the main role of antioxidants. However, there are further chemical reactions that could contribute to stabilization from *para*- substituent groups [21, 3, 4]. For example, cyclohexadienonyl radicals rearranged from phenoxy radicals can lead to quinone methide or deactivate peroxy radicals (alkylperoxycyclohexadienone) [8]. However, as the *para*- substituent group heads to the amorphous region on the surface during the structural relaxation, the reactions in the amorphous region should deserve further attention. In the meanwhile, as quinone methides are detected by discoloration along with the consumption of antioxidants and the intensity of photoluminescence increases due to the contribution of unsaturated carbonyls [22], the optical properties of the quinoid species and oxidation products (especially for carbonyl defects) should also be studied to track the consumption of stabilizers. Moreover, as introduced at the beginning of this section, aromatic rings (e.g., benzene) also contribute to the stabilization of the polymer matrix by energy transfer of the excitation energy, so the optical properties between aliphatic and aromatic parts are interesting studies as an outlook of future work.

Bibliography

- [1] M Ferry, E Bessy, H Harris, PJ Lutz, J-M Ramillon, Y Ngonon-Ravache, and E Balanzat. Irradiation of ethylene/styrene copolymers: Evidence of sensitization of the aromatic moiety as counterpart of the radiation protection effect. *The Journal of Physical Chemistry B*, 116(6):1772–1776, 2012.
(Cited on pages v, 20, and 97)
- [2] M. Ferry, E. Bessy, H. Harris, P. J. Lutz, J.-M. Ramillon, Y. Ngonon-Ravache, and E. Balanzat. Aliphatic/aromatic systems under irradiation: Influence of the irradiation temperature and of the molecular organization. *The Journal of Physical Chemistry B*, 117(46):14497–14508, 2013. PMID: 24168676.
(Cited on pages 97 and 101)
- [3] Jan Pospíšil. Chemical and photochemical behaviour of phenolic antioxidants in polymer stabilization—a state of the art report, part i. *Polymer Degradation and Stability*, 40(2):217–232, 1993.
(Cited on pages 97 and 103)
- [4] Jan Pospíšil. Chemical and photochemical behaviour of phenolic antioxidants in polymer stabilization: a state of the art report, part ii. *Polymer degradation and stability*, 39(1):103–115, 1993.
(Cited on pages 97 and 103)
- [5] Jan Pospíšil. Mechanistic action of phenolic antioxidants in polymers—a review. *Polymer degradation and stability*, 20(3-4):181–202, 1988.
(Cited on page 97)
- [6] Sahar Al-Malaika. Oxidative degradation and stabilisation of polymers. *International Materials Reviews*, 48(3):165–185, 2003.
(Cited on pages 18 and 97)
- [7] Anne Xu, Sebastien Roland, and Xavier Colin. Physico-chemical characterization of the blooming of irganox 1076® antioxidant onto the surface of a silane-crosslinked polyethylene. *Polymer Degradation and Stability*, 171:109046, 2020.
(Cited on pages 97 and 98)
- [8] Anne Xu, Sébastien Roland, and Xavier Colin. Thermal ageing of a silane-crosslinked polyethylene stabilised with an excess of irganox 1076©. *Polymer Degradation and Stability*, 189:109597, 2021.
(Cited on pages v, 5, 18, 20, 97, and 103)
- [9] Emmanuel Richaud, Bruno Fayolle, and Jacques Verdu. Polypropylene stabilization by hindered phenols—kinetic aspects. *Polymer degradation and stability*, 96(1):1–11, 2011.

(Cited on pages 97 and 100)

- [10] J Pospíšil. Transformations of phenolic antioxidants during the inhibited oxidation of polymers. *Pure and Applied Chemistry*, 36(1-2):207–232, 1973.

(Cited on page 97)

- [11] R Raja, S Seshadri, T Gnanasambandan, and RR Saravanan. Crystal growth and properties of nlo optical crystal–butylated hydroxy toluene (bht). *Spectrochimica Acta Part A: Molecular and Biomolecular Spectroscopy*, 138:13–20, 2015.

(Cited on page 98)

- [12] Grażyna Przybytniak, Jarosław Sadło, Marta Walo, Norbert Wróbel, and Pavel Žák. Comparison of radical processes in non-aged and radiation-aged polyethylene unprotected or protected by antioxidants. *Materials Today Communications*, 25:101521, 2020.

(Cited on pages 101 and 103)

- [13] Oksana Tishchenko and Donald G Truhlar. Benchmark ab initio calculations of the barrier height and transition-state geometry for hydrogen abstraction from a phenolic antioxidant by a peroxy radical and its use to assess the performance of den sity functionals. *The Journal of Physical Chemistry Letters*, 3(19):2834–2839, 2012.

(Cited on page 101)

- [14] Shogo Tomiyama, Shogo Sakai, Tomihiro Nishiyama, and Fukiko Yamada. Factors influencing the antioxidant activities of phenols by an ab initio study. *Bulletin of the Chemical Society of Japan*, 66(1):299–304, 1993.

(Cited on page 101)

- [15] Kazunori Tanaka, Shogo Sakai, Shogo Tomiyama, Tomihiro Nishiyama, and Fukiko Yamada. Molecular orbital approach to antioxidant mechanisms of phenols by an ab initio study. *Bulletin of the Chemical Society of Japan*, 64(9):2677–2680, 1991.

(Cited on page 101)

- [16] E Jaworska, I Kałuska, G Strzelczak-Burlińska, and J Michalik. Irradiation of polyethylene in the presence of antioxidants. *International Journal of Radiation Applications and Instrumentation. Part C. Radiation Physics and Chemistry*, 37(2):285–290, 1991.

(Cited on page 103)

- [17] K Naskar, D Kokot, and JWM Noordermeer. Influence of various stabilizers on ageing of dicumyl peroxide-cured polypropylene/ethylene-propylene-diene

thermoplastic vulcanizates. *Polymer degradation and stability*, 85(2):831–839, 2004.

(Cited on page 103)

- [18] HE Bair. Exudation of an antioxidant additive from thin polyethylene films. *Polymer Engineering & Science*, 13(6):435–439, 1973.

(Cited on page 103)

- [19] OS Gal, VM Marković, Lj R Novaković, and VT Stannett. The effects of the nature of the antioxidant on the radiation crosslinking of polyethylene. *Radiation Physics and Chemistry (1977)*, 26(3):325–330, 1985.

(Cited on page 103)

- [20] Takanori Yamazaki and Tadao Seguchi. Esr study on chemical crosslinking reaction mechanisms of polyethylene using a chemical agent—ii. the effect of phenolic antioxidants. *Journal of Polymer Science Part A: Polymer Chemistry*, 35(12):2431–2439, 1997.

(Cited on page 103)

- [21] Ivan Vulic, Giacomo Vitarelli, and John M Zenner. Structure-property relationships: phenolic antioxidants with high efficacy and low color contribution. In *Macromolecular symposia*, volume 176, pages 1–16. Wiley Online Library, 2001.

(Cited on page 103)

- [22] Klemens Grabmayer, Gernot M Wallner, Susanne Beißmann, Ulrike Braun, Ronald Steffen, David Nitsche, Beate Röder, Wolfgang Buchberger, and Reinhold W Lang. Accelerated aging of polyethylene materials at high oxygen pressure characterized by photoluminescence spectroscopy and established aging characterization methods. *Polymer degradation and stability*, 109:40–49, 2014.

(Cited on page 103)

6 - Conclusion & Perspectives

In this manuscript, we have investigated radio-oxidation degradation mechanisms of polyethylene and the role of antioxidants through density functional theory. The overall reaction pathways are dealt with, especially concerning activation energy and reaction enthalpy. We followed the conventional reaction pathways generally explaining the degradation mechanisms of polyethylene, and we revisited several reactions by a careful atomic scale study in order to determine whether they are unfavorable or if, on the contrary, they compete with other reactions with similar activation energies. In order to explore the effect of the local environment on the reaction rates, we considered three models, which can represent amorphous regions, crystalline PE, and the surface of lamellæ. Based on these strategies, we found several results which, in our view, lead to a more detailed understanding of the kinetic pathway leading to PE radio-oxidation.

From the initiation steps, we can assume that alkyl radicals are produced by the dissociation of C-H bonds under irradiation. Oxygen does not react easily with saturated alkyl chains because of the high activation energy (1.45 eV) to abstract a hydrogen atom, but it spontaneously reacts with alkyl radicals by forming peroxy radicals. Concerning the formation of ketones, one of the major oxidation products, there are several bottlenecks to reach them by following the conventional reaction pathways because, for example, the reaction of hydrogen abstraction leading to hydroperoxides presents an activation energy (0.6-0.7 eV) that makes it unlikely at room temperature. Incorporating other defects, which can stabilize an alkyl radical center as a final product, only slightly decreases the activation energy down to 0.48 eV on the surface of lamellæ. Nevertheless, even if we assume that hydroperoxides are produced in one way or another, the reactions leading to their decomposition are also not plausible. In the meanwhile, the presence of radical species affects the activation energy. For example, without neighboring radical species, the minimum barrier of the decomposition of hydroperoxides is 0.91 eV, but in the presence of alkyl radicals, the barrier decreases to 0.46 eV on the surface of lamellæ, which is still relatively high. Therefore, regarding the bottlenecks of the formation and decomposition of hydroperoxides, alternative reaction pathways could be proposed; for example, other radical species participate in oxidative reactions. Otherwise, oxidative reactions bypassing the formation of hydroperoxides could also be considered.

As for other radical species, hydroxyl and hydroperoxyl radicals are considered. They both are reactive and can participate in oxidative reactions. In the case of hydroxyl radicals, they spontaneously abstract a hydrogen atom at the primary or tertiary site of hydroperoxides. In particular, when a hydrogen atom is removed at the tertiary site, O-O bond in α -alkyl-hydroperoxy radical is spontaneously decomposed by forming a ketone and a hydroxyl radical, which leads to further reactions.

Therefore, hydroxyl radicals effectively decompose hydroperoxides without barriers, and this explains how humidity is involved in the degradation of PE. In the meanwhile, hydroperoxyl radicals transfer a hydrogen atom to peroxy radicals leading to the formation of hydroperoxides. Therefore, each of the mentioned radicals plays a key role, respectively, in decomposing and forming hydroperoxides. However, mechanisms explaining the formation of such radicals need to be further investigated in the future.

Once established that the decomposition of hydroperoxides is not easy, other reactions, which bypass hydroperoxides, could also be considered. A possible reaction is the bimolecular decomposition of two peroxy radicals, which leads to two alkoxy radicals and one oxygen molecule. Since the reaction shows a barrierless and exothermic energy profile, this is much more favorable than the H-abstraction by peroxy radicals. However, the overall reaction pathway triggered by (or in competition with) this reaction is complex because alkoxy radicals can also branch out into many reactions, such as crosslinking, chain scission, and the production of alcohols and carbonyl defects. These reactions can be more or less probable according to the specific positions of the radical on the surface of lamellæ, which controls the steric hindrance. Besides, the concentration of radical species would also affect the relative weight of these reactions because while chain scission can be triggered by a single alkoxy radical, the others require two radical species.

To delay oxidation induction time and protect polyethylene, the role of antioxidants is important. In this thesis, we mainly coped with primary antioxidants as concerns the H-transfer reaction between hindered phenol function and radical species. The reaction is effective in stopping the auto-oxidation scheme of the propagation and/or chain branching steps by removing radical species. I studied three radicals, which are alkyl, alkoxy, and peroxy radicals, within the molecular and surface models. While the activation energy of the H-transfer reaction to deactivate alkyl radicals is high, the deactivation of the two other radicals is spontaneous. In other words, primary antioxidants, at least in the case of BHT considered in this study, stabilize the polymer matrix by forming hydroperoxides and alcohols. In particular, removing alkoxy radicals is the most effective from both the kinetic and thermodynamic points of view (the reaction is barrierless and strongly exothermic). Therefore, a crucial role of antioxidants is to deactivate alkoxy radicals that cause severe degradation of polyethylene.

I believe that this thesis work helps to understand the oxidative reaction scheme and contributes to the studies unveiling the degradation mechanism of polyethylene by providing a useful database of the energetics of relevant reactions taking place. Our approach can also be applied to other types of polymers, such as poly(ethylene oxide) or polypropylene. The study can be further developed by considering photochemical degradation such as Norrish (type I & II) reactions in which excited states are involved, which were out of the scope of this thesis. In this respect, investigating optical properties is important because the formation of carbonyls is

also known to be responsible for photoluminescence. In other words, electronic excitation of ketones can lead to chain scission and/or photoluminescence. Although the formation of ketones means that the polymer matrix already underwent oxidation, the mechanisms of radiative and non-radiative decay of ketones can help to further advance in the understanding of the kinetics pathways under irradiation. Besides, the enhancement of photoluminescence in the polymer matrix after oxidative degradation has been reported; this might come from the decay of electronic excitations of antioxidants, which are responsible for energy transfer between aromatic (e.g., benzene rings) and aliphatic parts. It would be then important to elucidate the behavior of excitons, which could possibly participate in the degradation of PE. Moreover, since quinone methides, which are formed after the consumption of antioxidants, cause discoloration and act as quenchers, their optical properties contributing to photoluminescence could also be studied. Therefore, elucidating optical properties from pure antioxidants (aromatic rings)/polyethylene (saturated chains) to degraded antioxidants (quinone methides)/polyethylene (ketones) would be interesting studies as an outlook of future work.

Appendices

A - Modelling polyethylene structure

Before studying the oxidative degradation mechanisms of PE, it is necessary to find the theoretical equilibrium structure.

The structural parameters of crystalline PE used here basically follow the results presented in [1]. It consists of a simple orthorhombic crystal structure established by x-ray and neutron scattering experiments [2, 3, 4, 5, 6]. The theoretical equilibrium structure of crystalline PE is found by plotting the curve of total energy versus interchain distance and selecting the lowest energy as shown in Fig. A.1 [1].

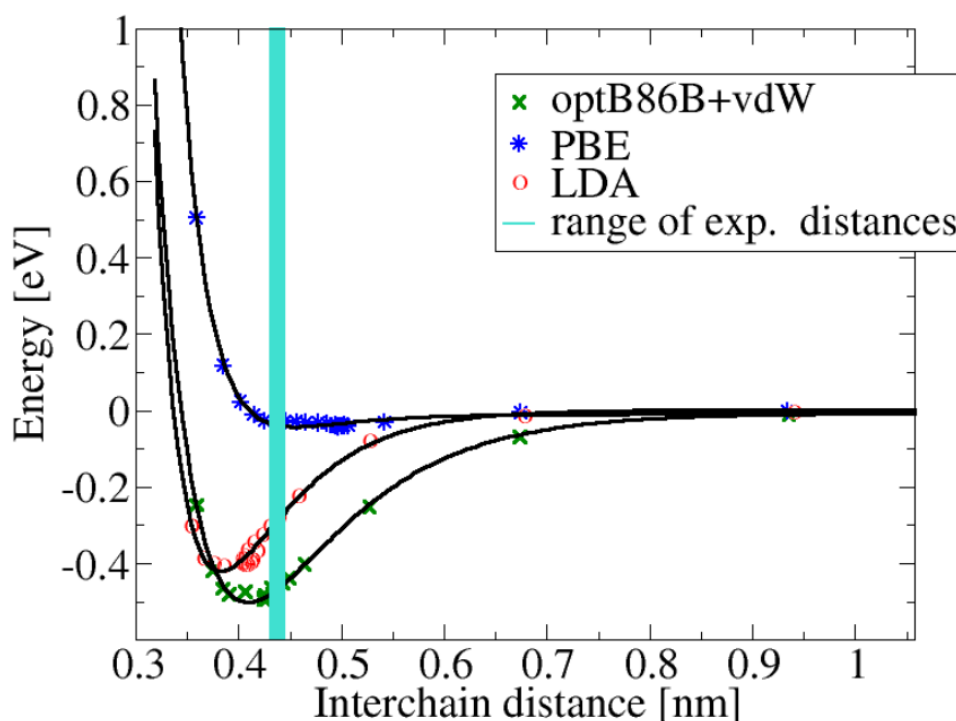


Figure A.1 – Energy vs. interchain distance for LDA, GGA-PBE and optB86b+vdW exchange correlation functionals. The light blue stripe represent the range of experimental results [1].

Various exchange-correlation functionals were tested in Ref. [1] and the functional optB86b+vdW shows a reasonable energy curve to find the theoretical equilibrium structure of PE. The functional considers chain-chain interaction with van der Waals term, which is important in crystalline PE. In addition to the results of Ref. [1] I calculated the same curve with hybrid functional (vdw-df-cx0) [7] and they both show the same optimized interchain distance, which is 0.424 nm (Fig. A.2).

Based on the optimized crystalline PE, we can build on this structure to con-

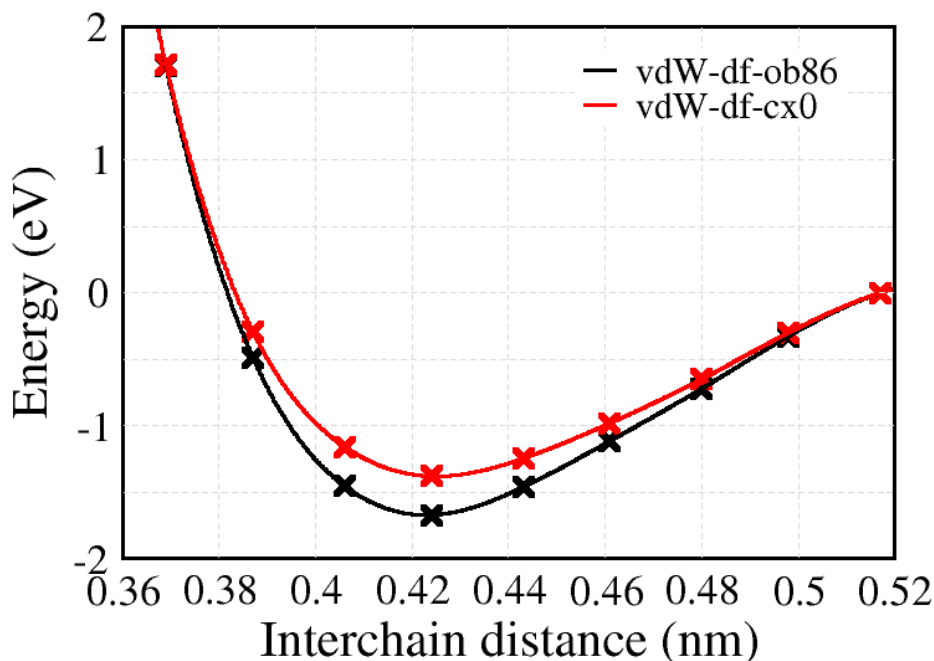


Figure A.2 – Energy vs. interchain distance for vdW-df-ob86 and vdW-df-cx0 exchange correlation functionals.

struct a lamellar surface mimicking the interface between two crystalline regions, with bent polymer chains at the crystal surfaces. The detailed process is shown in Fig.A.3. Firstly, I enlarged the lattice parameter along the chain direction, z in our case, cutting a slab from optimized crystalline PE.

The broken chains at the surface were passivated with twelve CH_2 units (six on each slab surface) and then the system was relaxed. The lattice parameters are fixed during the relaxation in order to keep the optimized crystalline PE interchain distance. The distance between the two facing surfaces is approximately 7 \AA along the z direction. The distance is much smaller than what can be found in real PE microstructures [8, 9], but the interaction between the facing surfaces is already small and should not influence the activation energies of reactions occurring on the surface.

The calculated surface to volume ratio (0.7 nm^{-1}) has the same order of magnitude with Ref. [9] ($\sim 0.4 \text{ nm}^{-1}$) estimated from the given experimental data.

For molecular models, in order to maximize the distance between the chains, we used body-centered tetragonal unit cells. The size of the unit cells was 40×40 bohr in the xy plane and sufficiently large in the z direction so that chain ends did not interact with each other. Detailed information is shown in Fig.A.4-A.6.

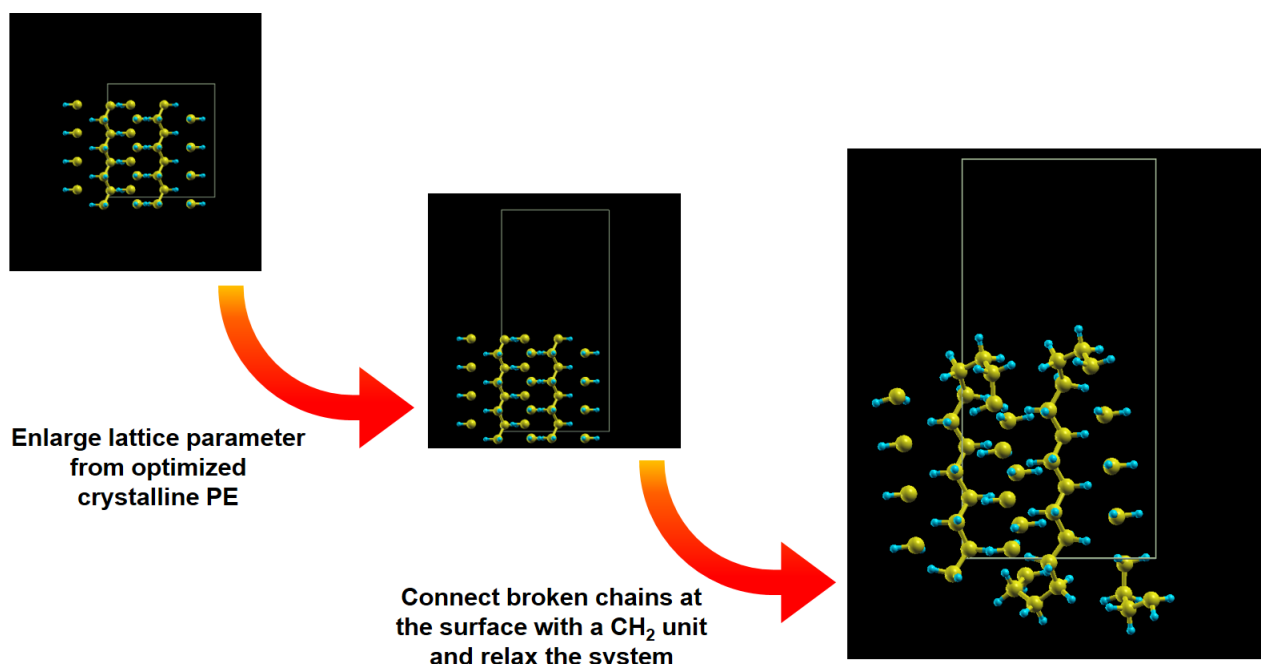
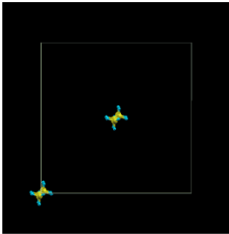
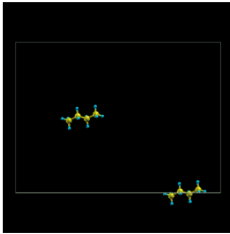
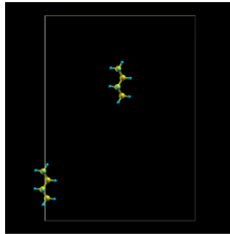


Figure A.3 – A graphical sketch of the procedure used to produce the slab model used for calculation on a lamella surface.

xy plane


yz plane


xz plane


	a	b	c
C ₄ H ₁₀	40		54.25
C ₈ H ₁₈			63.72
C ₁₂ H ₂₆			73.16
C ₁₆ H ₃₄			82.60
C ₂₀ H ₄₂			92.04

[Bohr]

Figure A.4 – Views of the unit cell for the molecular model, here with *n*-Butane. The table gives the lattice parameters in Bohr.

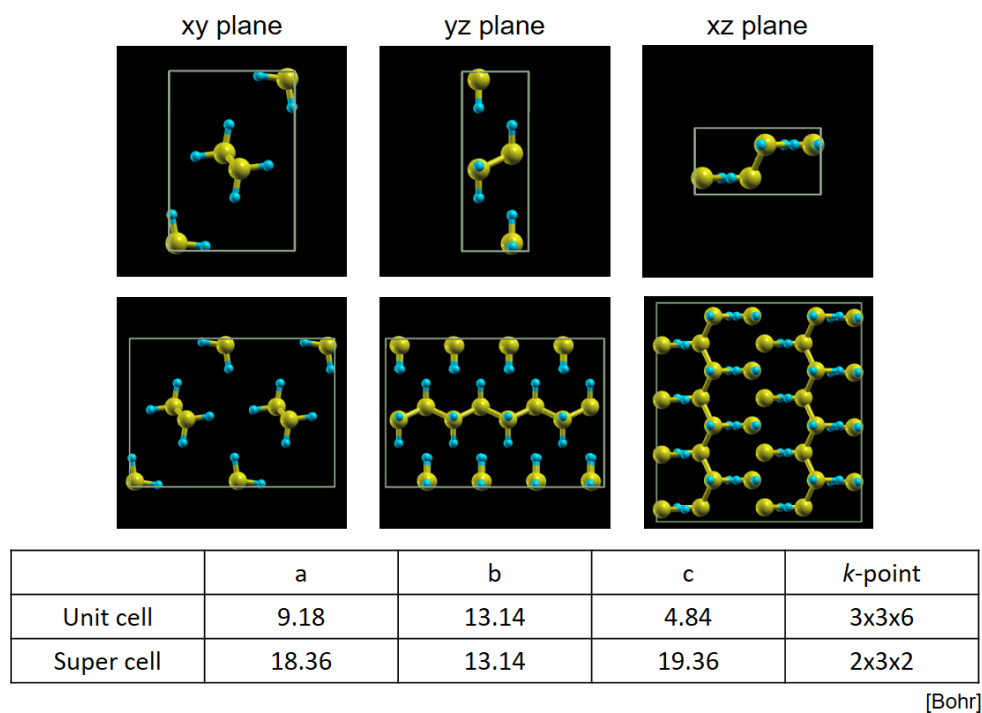


Figure A.5 – Views of the orthorhombic unit cell (above) and of the crystal supercell (below) used to simulate reactions in crystalline environment. The table gives the lattice parameters in Bohr and the k-point mesh used.

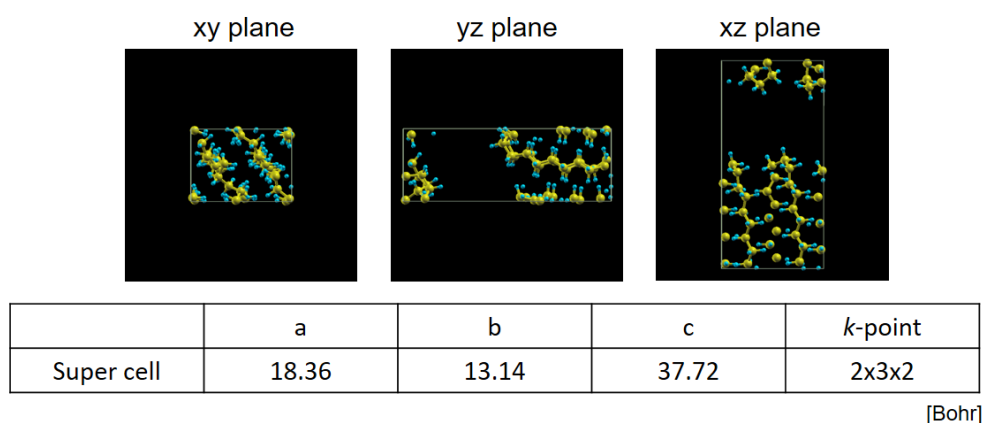


Figure A.6 – Views of the unit-cell of the lamellar model, used to simulate reactions at the crystalline/amorphous interface. The table gives the lattice parameters in Bohr.

B - Diffusion in a polymer matrix: a few case studies

After optimizing the structures, we can study the behavior of oxygen in the PE matrix. Solution, permeation, and migration energy are considered.

B.1 . Oxygen kinetics in a PE matrix

Oxygen molecules, before undergoing reactions inside the PE matrix, have to diffuse in the amorphous region, at the surface of lamellæ and possibly also inside crystalline PE regions. The reported activation energies for oxygen dissolving and diffusing into PE range from 0.35 to 0.45 eV [10]. However, in this case, this energy might be more related to the oxygen flow through an amorphous region in the polymer matrix. The calculated formation (or solution) energy of an oxygen molecule inserted between two crystalline lamellæ of our model is 0.23 eV. Although it is generally assumed that oxygen diffuses only in the amorphous region, a closer look at the mechanisms of permeation and diffusion through the amorphous and the crystal gives a better understanding of oxygen kinetics.

Firstly, we investigated solution energy of an oxygen molecule in crystalline PE as a function of the interchain distance (Fig.B.1). Compared to the amorphous region, where diffusion is supposed to take place much more easily than inside the crystal, thanks to a larger interchain space [10], the minimum of solution energy is 0.72 eV [11]. When the strain energy is removed, the curve shows similar behavior to that in amorphous silica [12] where the solution energy decreases with the increasing size of the voids, which facilitates the insertion of an oxygen molecule. This implies that oxygen can more easily diffuse into the crystal-amorphous interface where the roughness tends to be less than a nanometer [9] observed by torsional tapping atomic force microscopy (TTAFM) method. Although the surface in our lamellar surface model is very flat, the model can give insight into the details of oxygen permeation and diffusion. Fig.B.2(a) shows the activation energy of oxygen for permeation into the crystalline lamellæ. The energy barrier is 1.09 eV, which means that permeation from the amorphous region to crystalline region is not favorable. However, considering our simplified model, with no roughness and no variation in other possible microstructures, such as bent chain distance, the calculated energy would indicate the highest energy for the permeation. Once oxygen gets into crystalline PE, the energy for diffusion is 0.07 eV Fig.B.2(b). The schematic information, including initial, transition, and final state, is shown in Fig. B.3.

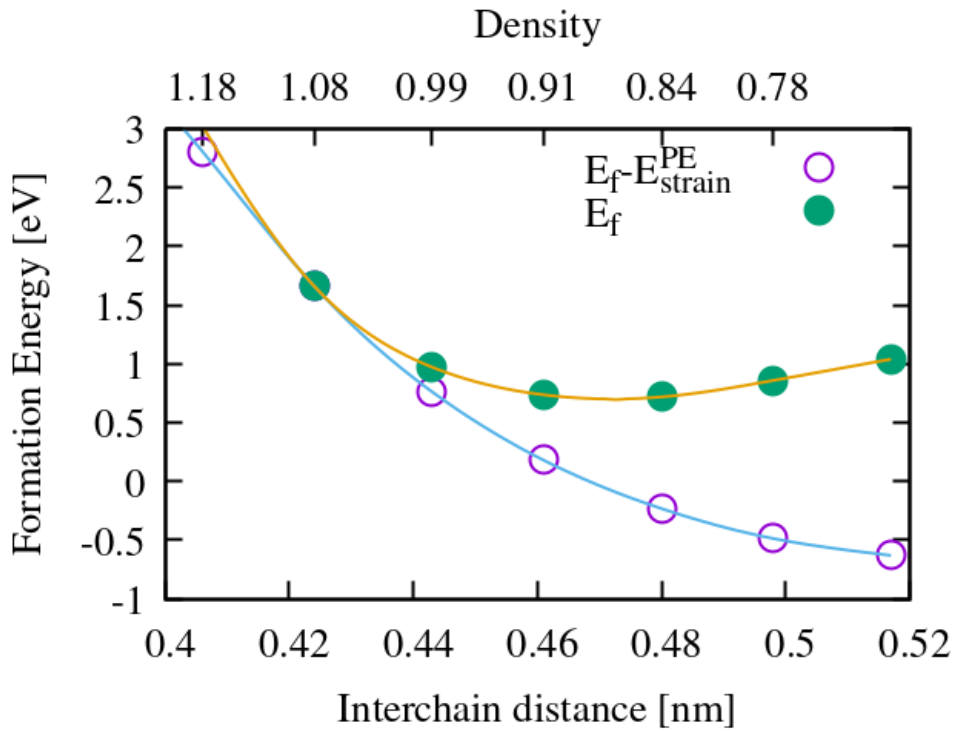


Figure B.1 – (a) Solution energy of an oxygen molecule in crystalline PE as a function of the interchain distance. For both the yellow and the blue curves, the oxygen molecule is inserted in a model of PE with scaled in plane lattice parameters to modify the interchain distance and not the dimensions along the chain. The equilibrium interchain distance is 0.424 nm; the yellow curve gives the standard solution energy (E_f), computed with respect to the equilibrium structure; the blue curve takes as a reference a PE crystal with the same scaled lattice parameters as that of the supercell hosting the molecule, that is we remove the strain energy required to dilate the PE at 0K (E_{PE}^{strain}). The oxygen chemical potential, in both cases, is the energy of an isolated O₂ molecule.

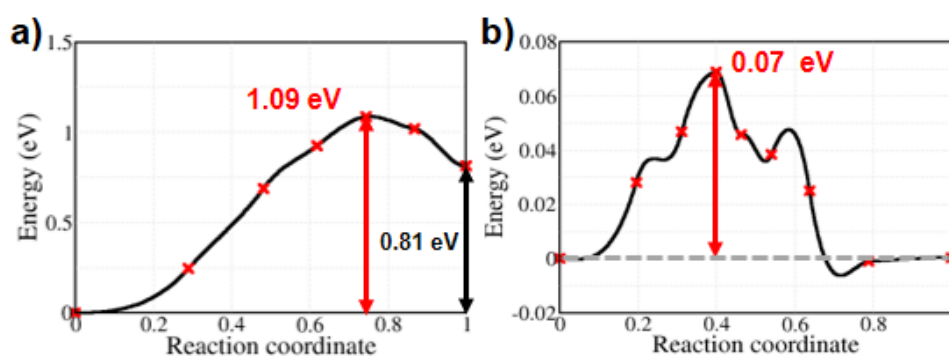


Figure B.2 – Calculated activation energies and initial and final configurations for the mechanism of oxygen permeation through crystalline lamellae. a) energy profile for oxygen permeation from the amorphous phase into the crystalline lamellae, b) energy profile for the diffusion of oxygen inside crystalline lamellae.

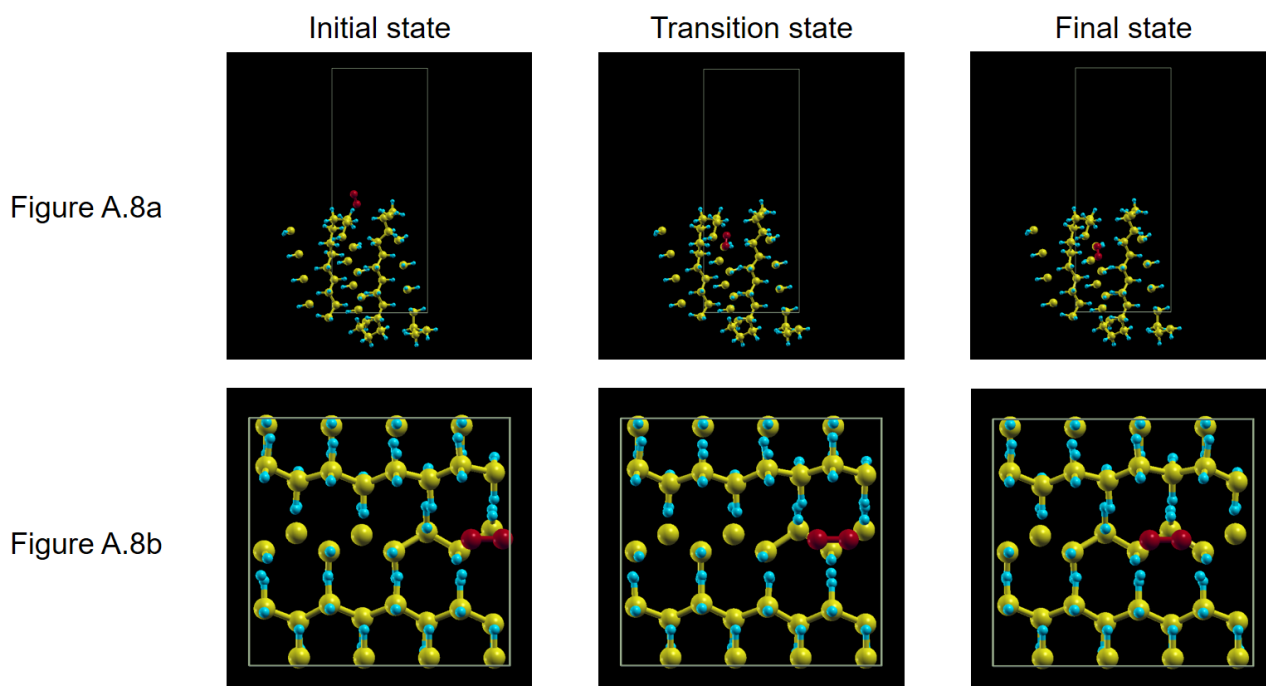


Figure B.3 – Initial, saddle point, and final structures for the permeation of an oxygen molecule from the surface to a crystalline PE (top) and for the migration in crystalline PE (bottom). The corresponding energy profiles are on Fig.B.2a and B.2b.

B.2 . Diffusion of radical species

Not only the diffusion of oxygen is important to understand oxidation kinetics, but also the kinetics of other species involved in the most relevant reactions. In particular, radicals created during the oxidation or under irradiation conditions could diffuse in the polymer matrix and cause other further reactions. In the chapter 3 and 4, we observed that the reactions, including radical species, decrease the activation energies. In this section, diffusion of alkyl radicals and double bonds, which are mainly involved in the initiation step, are discussed.

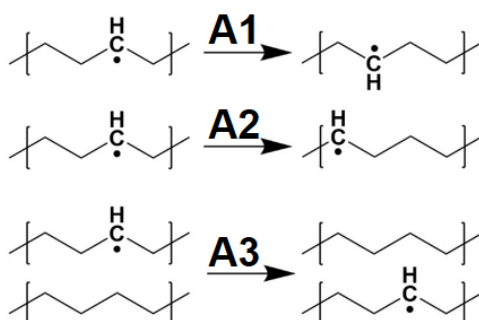


Figure B.4 – Scheme for the alkyl radical diffusion. A1: nearest neighbor, A2: second nearest neighbor (along the alkyl chain) and A3: across the chain and from a chain to a neighboring one.

Alkyl radicals can migrate by two main possible elementary migration steps: jumping along the polymer chain or from one to another (across the chains). For the migration along the chain, the nearest and second nearest hydrogen atom from an alkyl radical are considered both in the molecular and in the solid model (A1 and A2 in Fig.B.4, and B.5). For the migration across the chain, a neighboring hydrogen atom is selected and calculated in the solid and surface models.

Fig. B.5 and B.6 show calculated the activation energy for the migration of alkyl radicals. While the migration along the chain shows a high activation energy (over 1.69 eV), the migration across the chain shows reduced activation energy (1.04 eV and 0.95-1.05 eV for the solid and surface model, respectively). The results are in agreement with the study by Shimada *et. al.* [13, 14] that compared the decay rate of an alkyl radical between the urea-polyethylene complex and the solution grown crystals because the interchain motion can be controlled. The decay rate was slower in urea-polyethylene complex, despite the high mobility of the radical. This implies that the propagation across the chain is more favorable for alkyl radicals than along the chain.

For the diffusion of double bonds, also known as transvinylenes, three possible cases are considered in crystalline PE as shown in Fig B.7. The three proposed mechanisms have the same initial and final configurations, but they are obtained with different combinations of motion of the hydrogen atoms bound to the three involved carbon atoms. In Fig. B.7a, a hydrogen atom next to a double bond

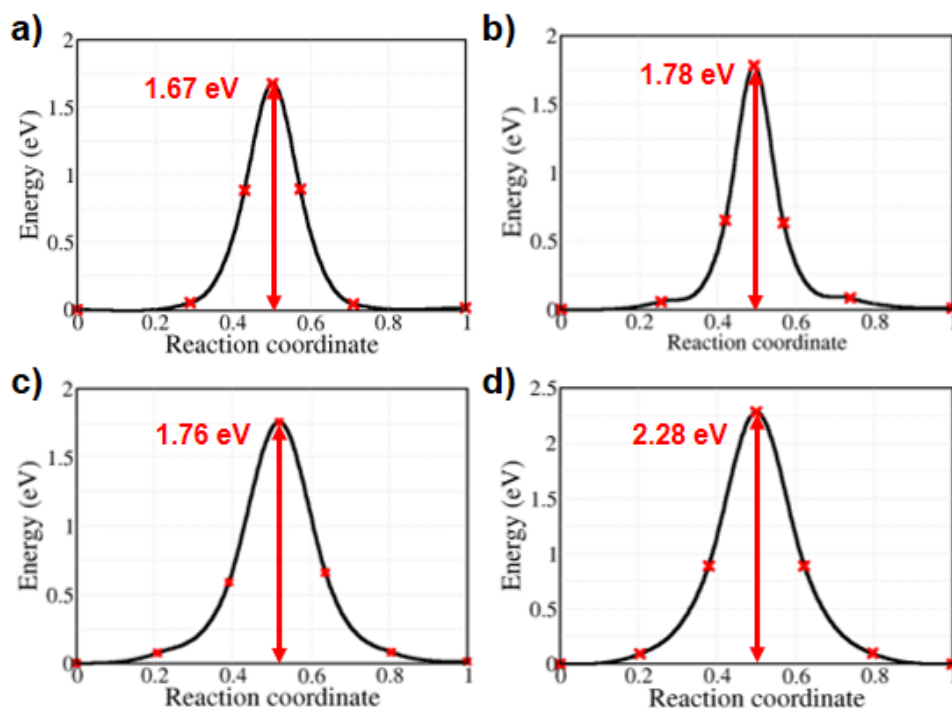


Figure B.5 – Energy profiles for the migration of an alkyl radical along the chain. Molecular model: a) nearest neighbor, b) second nearest neighbor. Solid model: c) nearest neighbor, d) second nearest neighbor.

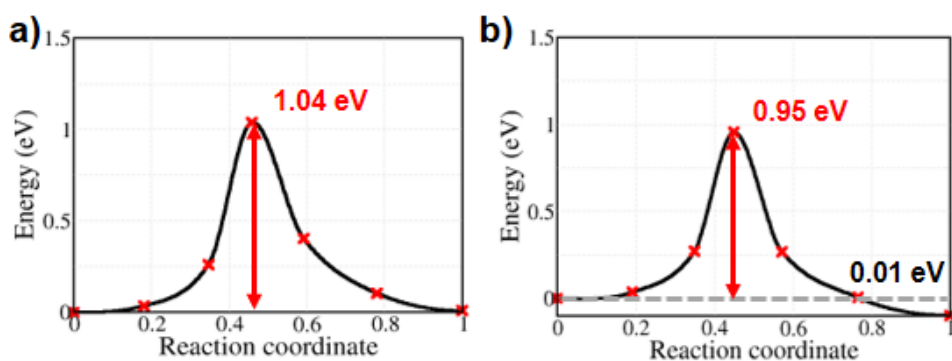


Figure B.6 – Energy profiles for the migration of an alkyl radical across the chain. a) solid model, and b) surface model.

migrates to the other side of the double bond. In Fig. B.7b, the mechanism is similar, but two hydrogen atoms are involved. In Fig. B.7c, diffusion takes place through interchain migration of a hydrogen atom. This is considered because alkyl radical migration across the chain is more favorable than that along the chain. The calculated results are shown in Fig. B.8. The overall barriers are high, which means that the reactions are unlikely to occur.

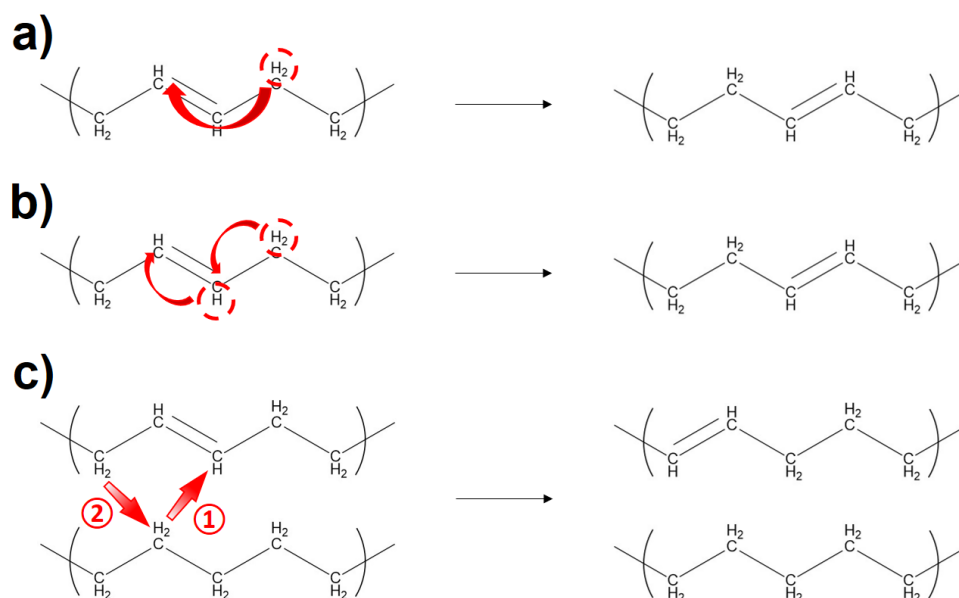


Figure B.7 – Scheme for the double bond diffusion. a) a hydrogen atom moves toward a double bond via its neighboring carbon, b) two hydrogen atoms move (through the direction of arrows), and c) double bond diffusion takes place by interchain hydrogen migration.

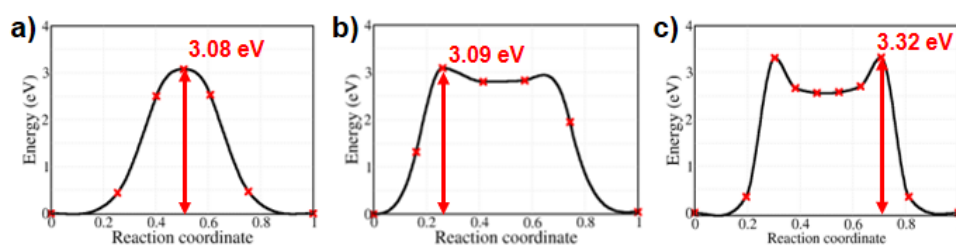
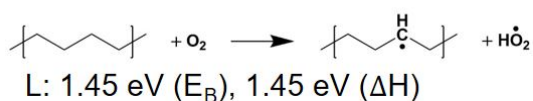
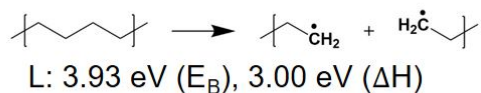
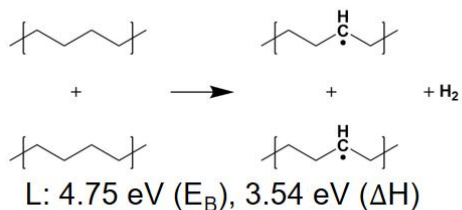


Figure B.8 – Energy profiles for the diffusion of a double bond along a polymer chain. Panels a), b) and c) correspond to the three mechanisms with corresponding labels shown in Fig.B.7.

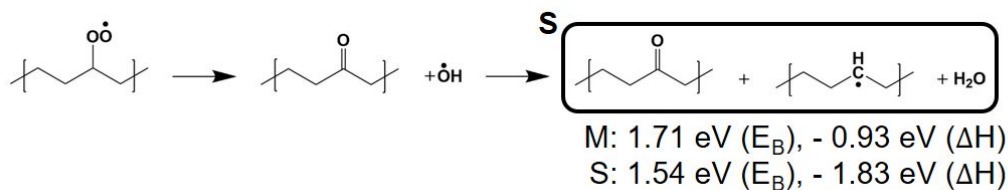
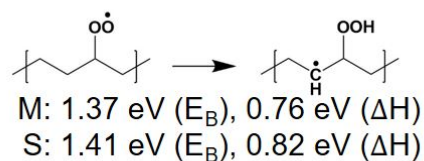
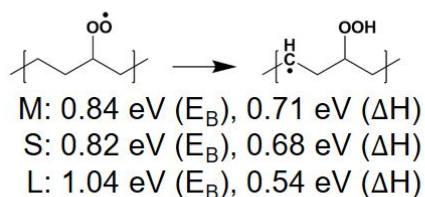
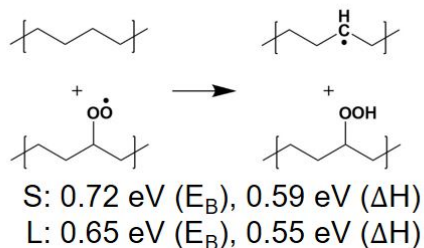
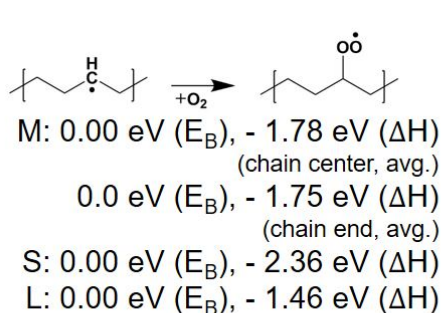
C - A list of reactions

In this section, all calculated reactions in the main chapters are summarized. M, S, and L represent molecular, solid, and lamellar surface models, respectively.

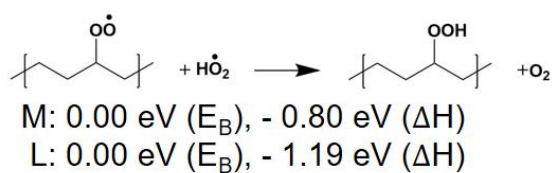
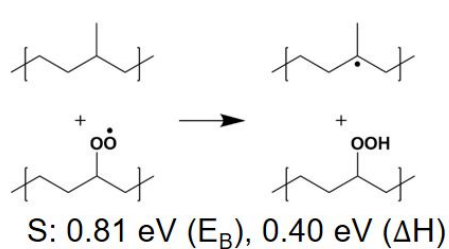
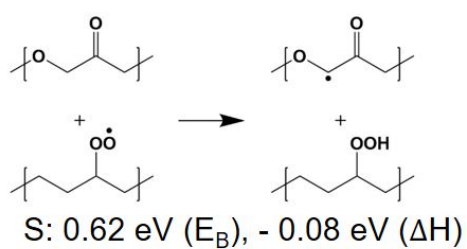
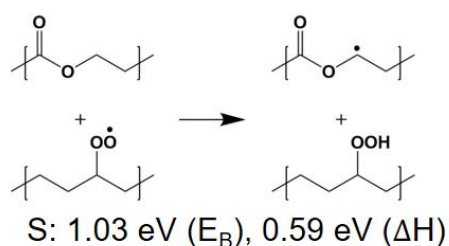
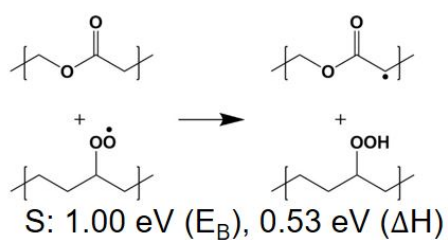
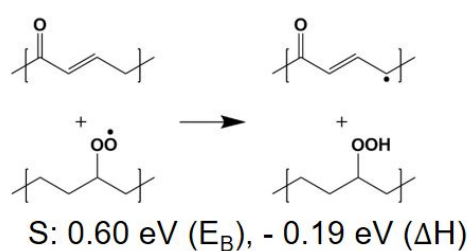
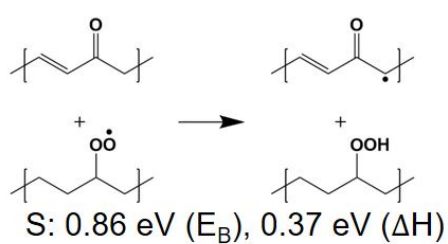
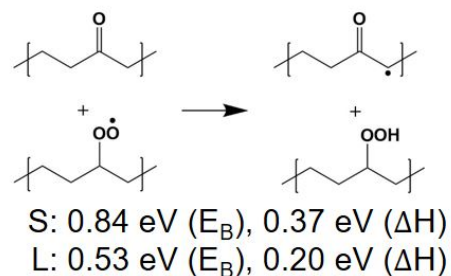
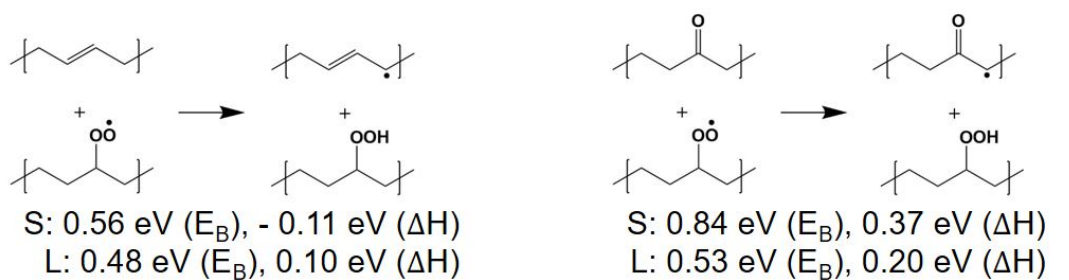
FORMATION OF ALKYL RADICALS



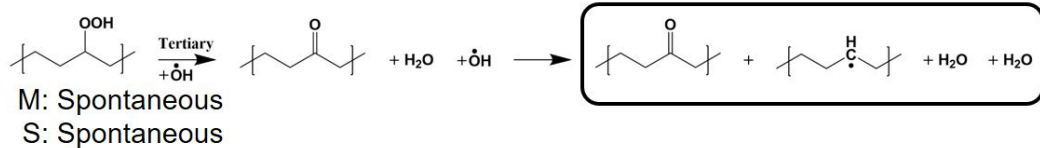
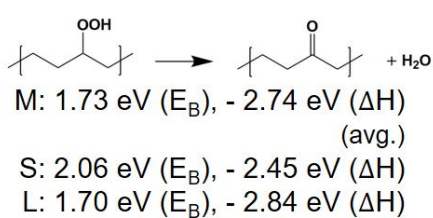
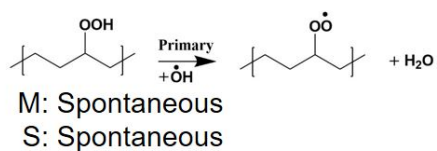
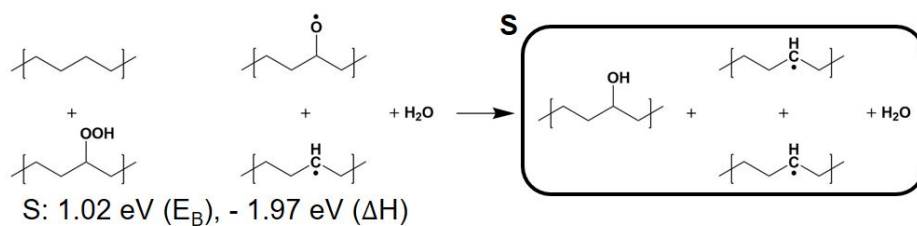
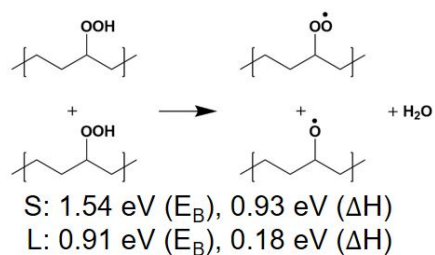
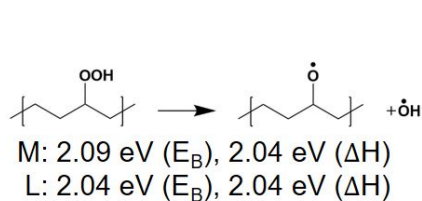
FORMATION OF PEROXY RADICALS & HYDROPEROXIDES



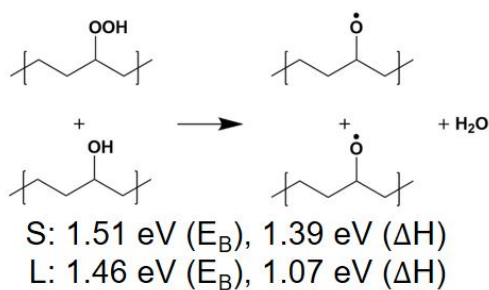
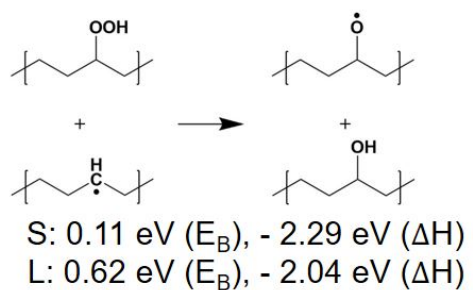
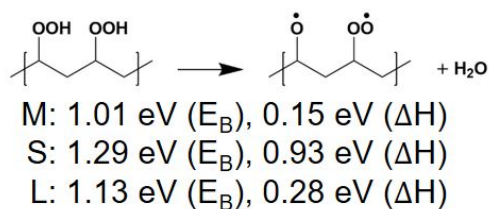
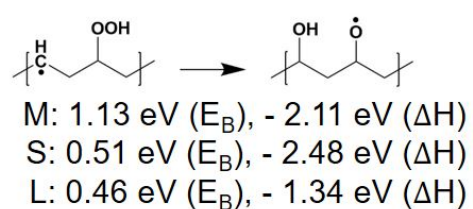
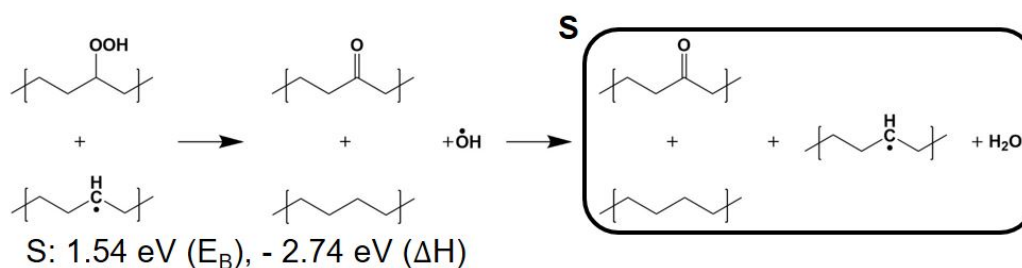
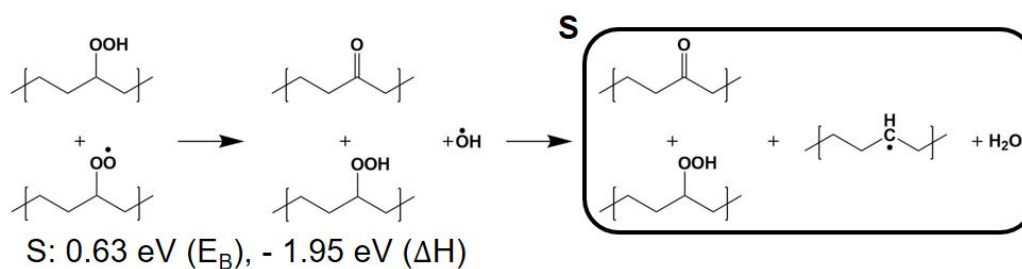
FORMATION OF PEROXY RADICALS & HYDROPEROXIDES



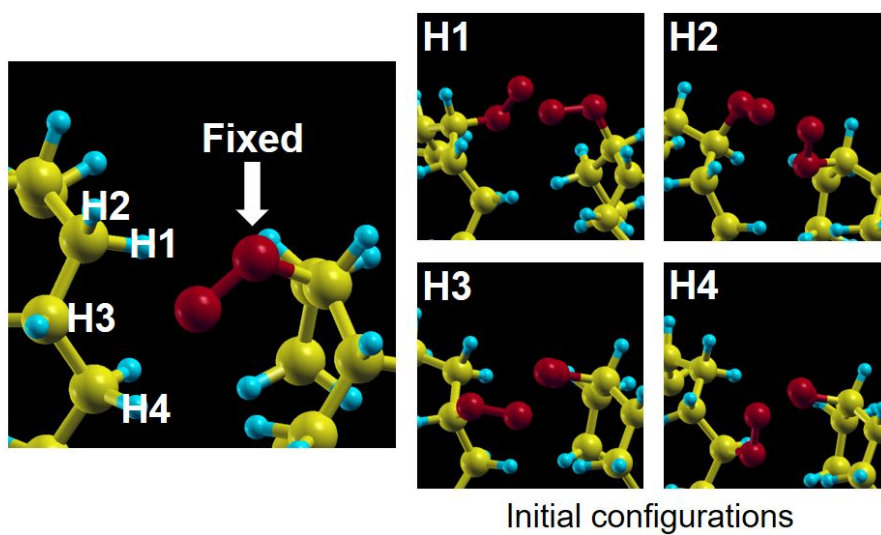
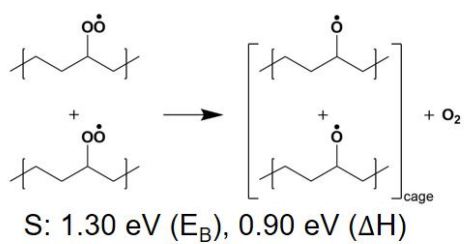
DECOMPOSITION OF HYDROPEROXIDES



DECOMPOSITION OF HYDROPEROXIDES

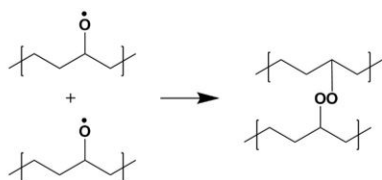


FORMATION OF ALKOXY RADICALS BY TWO PEROXY RADICALS

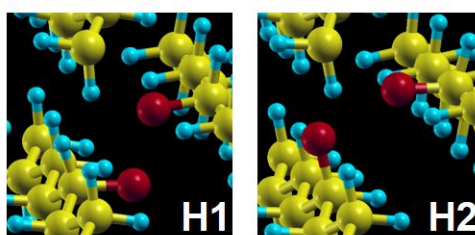


Position	E_B (eV)	ΔH (eV)
H1	0.00	- 0.27
H2	0.00	- 0.27
H3	0.05	- 0.09
H4	0.00	- 0.32

CROSSLINKING



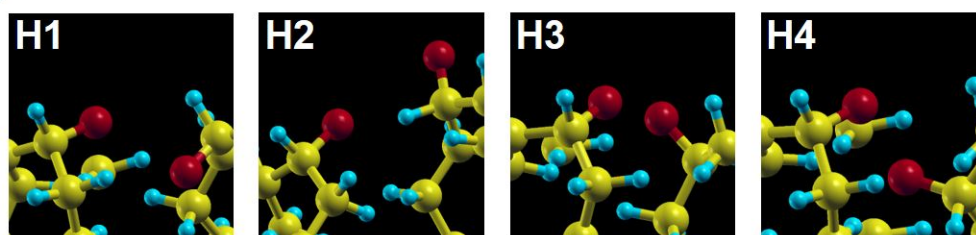
S



Initial configurations

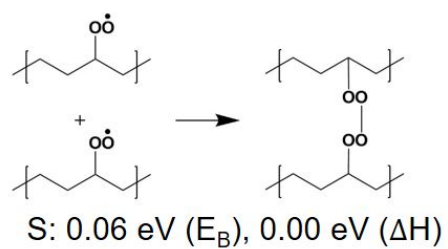
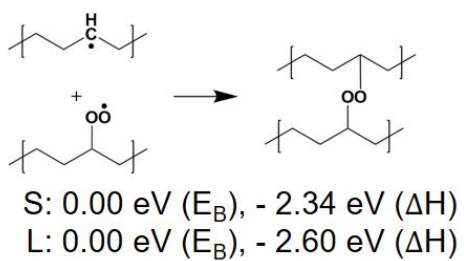
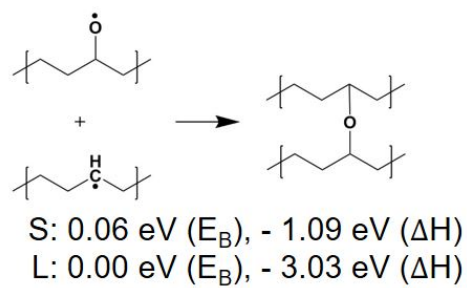
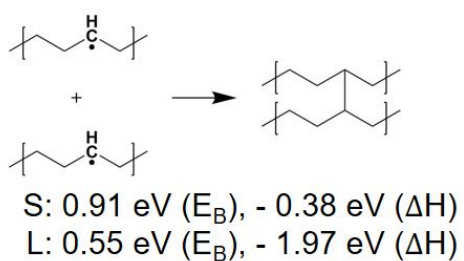
Position	E_B (eV)	ΔH (eV)
H1	0.00	- 1.12
H2	0.39	- 1.02

L

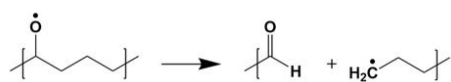
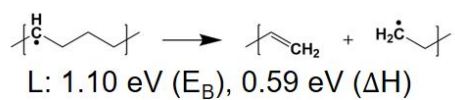


Initial configurations

Position	E_B (eV)	ΔH (eV)
H1	0.00	- 1.71
H2	0.38	- 1.39
H3	0.16	- 0.89
H4	0.00	- 1.71

CROSSLINKING

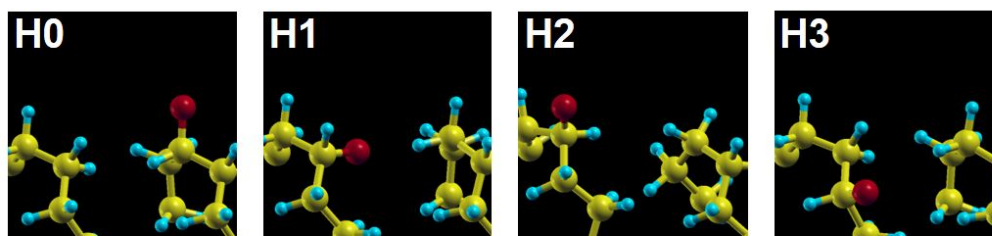
CHAIN SCISSION



M

	E_B (eV)	ΔH (eV)
$\text{C}_4\text{H}_9\text{O}$	0.39	0.28
$\text{C}_8\text{H}_{17}\text{O}$	0.44	0.36
$\text{C}_{12}\text{H}_{25}\text{O}$	0.42	0.35

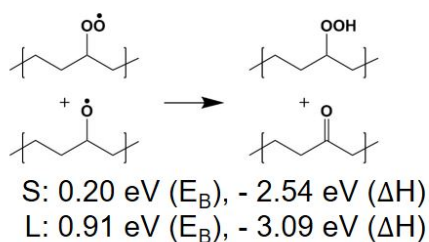
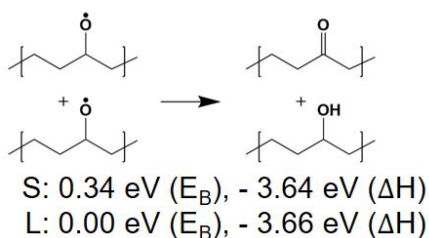
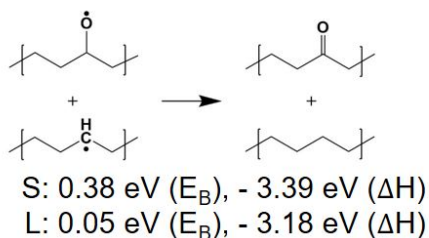
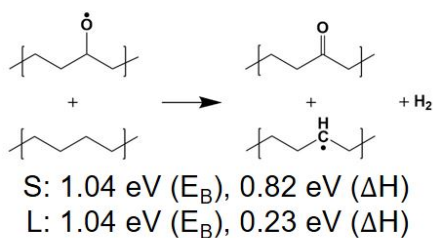
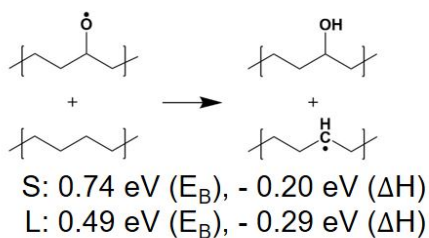
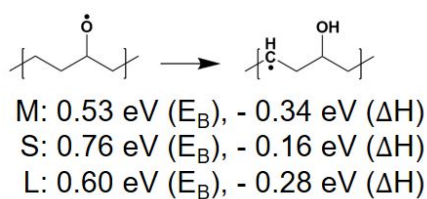
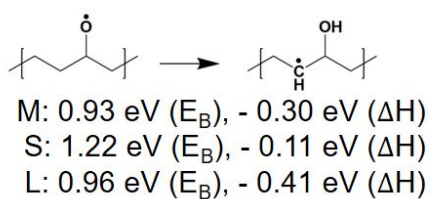
L



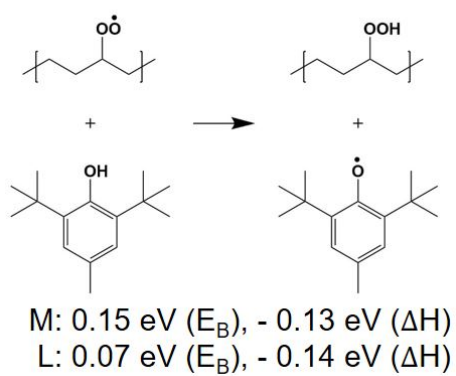
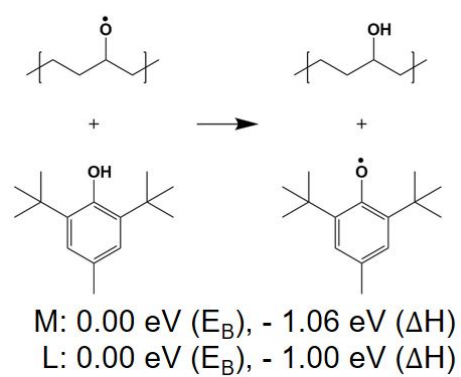
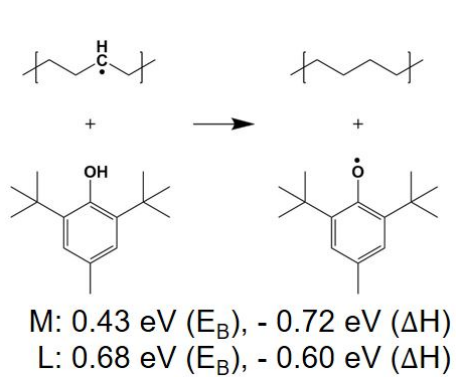
Initial configurations

Position	E_B (eV)	ΔH (eV)
H0	0.36	- 0.24
H1	0.25	- 0.31
H2	0.34	- 0.10
H3	0.27	- 0.15

FORMATION OF ALCOHOLS & KETONES BY ALKOXY RADICALS



ANTIOXIDANTS



D - Molecular dynamics: a few case studies

In this section, we present some results of ab initio molecular dynamics (Car-Parrinello molecular dynamics or CPMD, and see also Chapter 2.6). The reactions which have small or no barriers are firstly selected in order to check that they take place at room temperature (300K) based on the results of NEB calculations. Since NEB only estimates the energy barrier (ΔE , static DFT calculations at 0K), entropic contribution ($T\Delta S$) of the reactions, such as vibrational or rotational contributions to the activation free energy, are neglected. In this work, we rely on the assumption that ΔE is much larger than $T\Delta S$ because the reactions we are studying occur inside a solid or on surfaces, where rotational contributions should be negligible, and vibrational contributions are in general small. However, for small molecules in the gas phase or reactions with very small energy barriers, such contributions could be important^[15]. Therefore, analyzing trajectories of CPMD simulations, we can check that the reaction indeed takes place within a time which is of the order of magnitude of the one predicted by the ΔE calculated with NEB. If ΔS is negative and it is larger or similar to ΔE , the activation free energy is increased, and the reactions cannot take place. On the other hand, if ΔS is positive ($\Delta E - T\Delta S \ll \Delta E$), the reaction can take place at a temperature lower than expected from ΔE alone.

D.1 . Oxygen in crystalline PE

The calculated migration energy of oxygen in crystalline PE is 0.07 eV (Fig. B.2b). In the NEB calculation, the oxygen molecule was put at the same position along the alkyl chain to have the same energy at the initial and final states, and the migration was performed along the channel. Therefore, as shown in Fig.D.1, the variation of position along x and y direction is very small, and the oxygen molecule migrates along the z direction. The distance between the initial and final state along the z direction is 4.84 Bohr. This can be compared with the CPMD simulations performed starting from either the initial or the final state of the NEB path at various temperatures by counting the number of jumps (Fig.D.2). One or two jumps of the oxygen molecule along the channel are observed at temperatures between 300K and 420K over several picoseconds. Although the data is too limited to estimate the activation free energy, it is obvious that the oxygen molecule migrates along the channel at room temperature. Further analysis is needed, however, to understand the influence of the initial thermalization of the system. According to the NEB barriers, average waiting times should be 1.5 ps at 300K and 0.7 ps at 420K. The fact that the molecule sits immobile for longer times might suggest a role in the vibrational contribution to raising the free energy barrier.

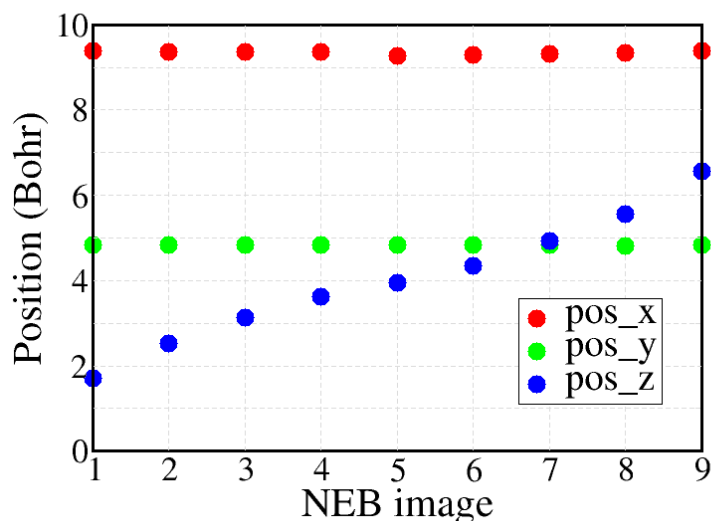


Figure D.1 – Information on the position of the oxygen molecule's center of mass in crystalline PE for each image in Fig. B.2b.

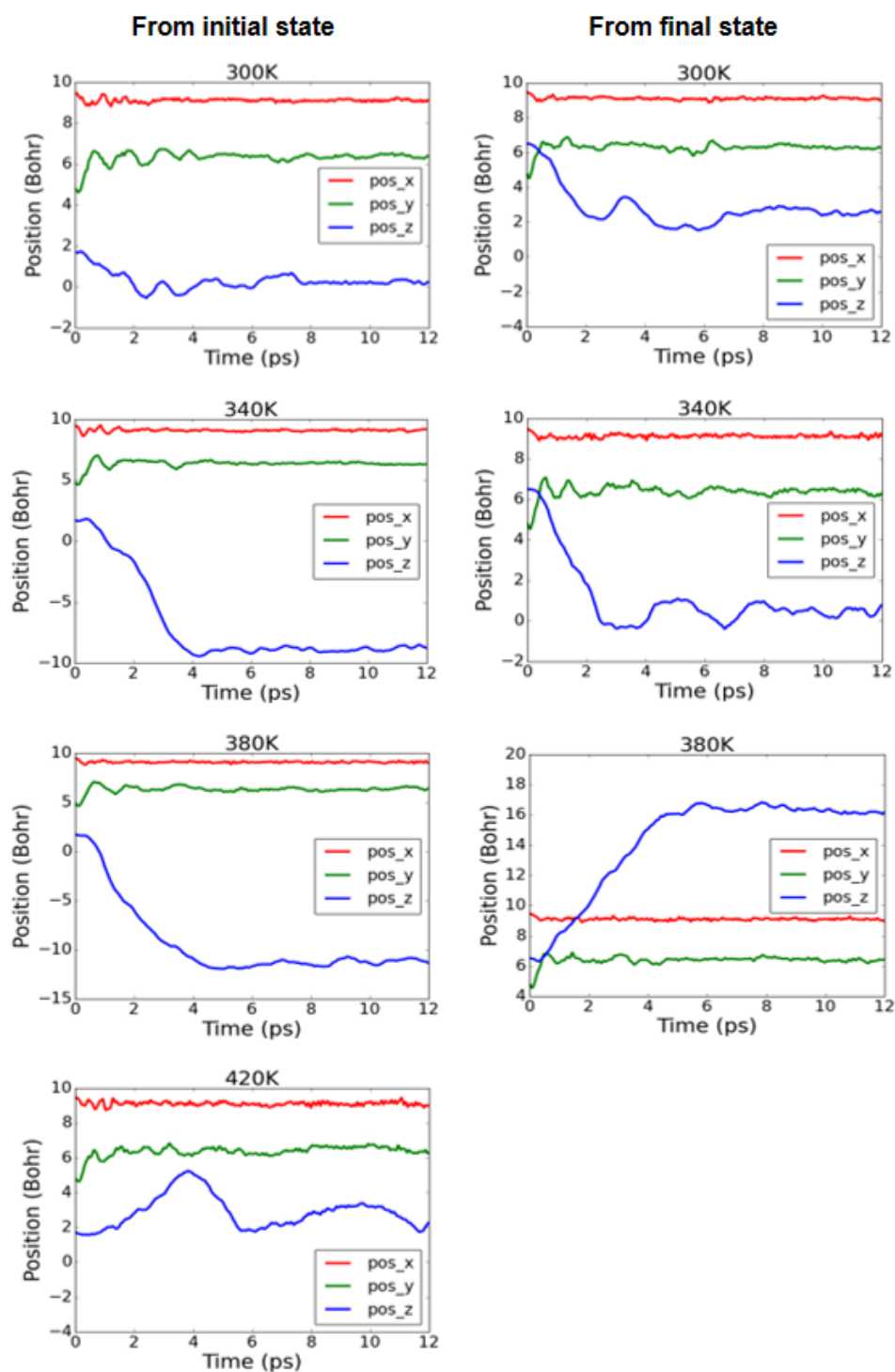


Figure D.2 – Information on the time evolution of the position of the center of mass of an oxygen molecule in crystalline PE as obtained from a CPMD simulation starting from the initial and final states of Fig. B.2b.

D.2 . Hydroperoxide decomposition by a hydroxyl radical

As discussed in Chapter 3.3 (reaction 3.15b), a hydroxyl radical is highly reactive and easily abstracts a hydrogen atom in alkyl chains. In particular, the H-abstraction reaction at the tertiary site was stressed because it leads to the formation of a ketone and a new hydroxyl radical, which participates in consecutive oxidative reactions. Because the reaction takes place during the structural relaxation, the influence of the initial distance between a hydrogen atom at the tertiary site of a hydroperoxide and an oxygen atom of a hydroxyl radical is further studied. Firstly, the total energy is calculated by varying the distance (D_4) in Fig.D.3a. When the distance is within around 4.2 Bohr, the reaction takes place during the structural relaxation (Fig.D.3b) and it is also observed during a CPMD simulation (Fig.D.3c). However, when a hydroxyl radical is put 4.7 Bohr away from a hydrogen atom at the tertiary site of a hydroperoxide, the reaction does not occur during a quasi-Newton structural optimization. Thus, starting with a hydroxyl at this distance, a CPMD simulation was performed to observe whether the reaction takes place, and the total energy was extracted in order to confirm the barrier of the reaction. Fig.D.3c shows that the reaction occurs later than when the hydroxyl is at only 3.2 Bohr from the hydroperoxide's hydrogen due to the diffusion time, but it is still very quick at room temperature (300K). This can also be confirmed by tracking the total energy of the system (Fig.D.3d).

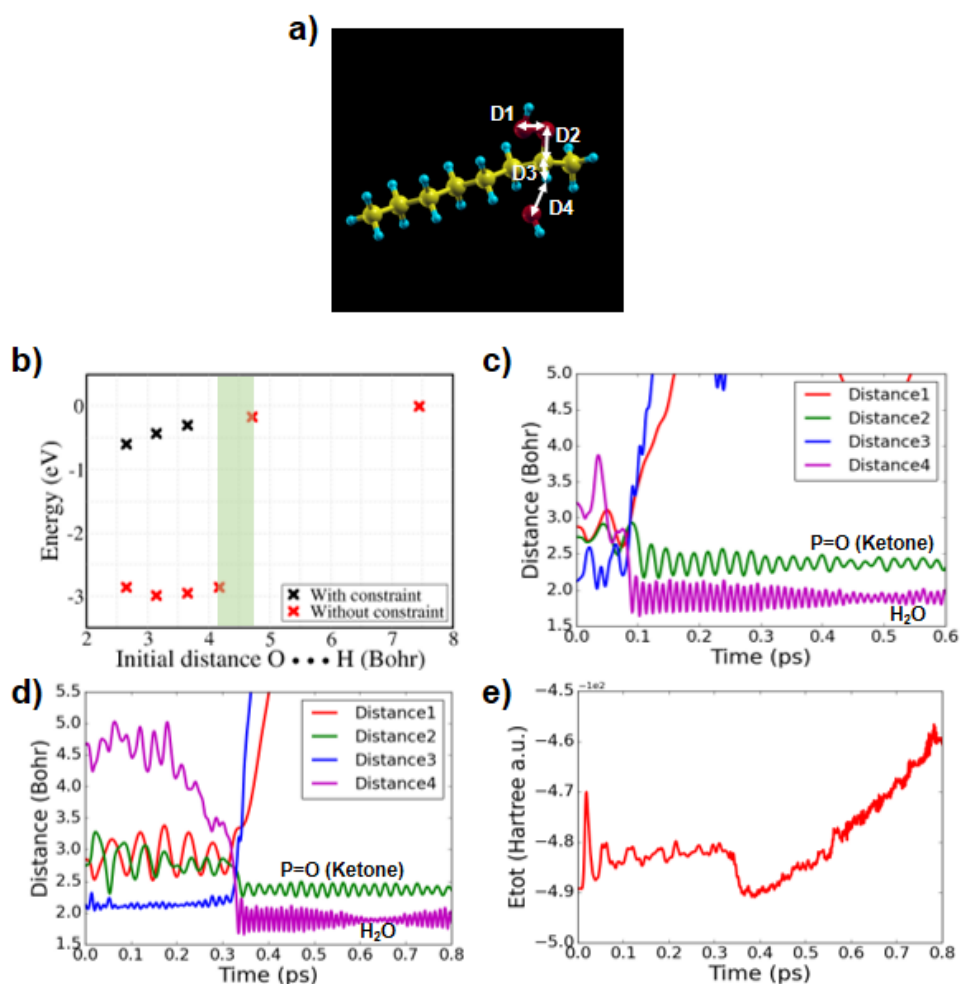


Figure D.3 – Reaction 3.15b ($\text{POOH} + \text{°OH} \rightarrow \text{P=O} + \text{H}_2\text{O} + \text{°OH}$): a) Information on the atomic distances monitored during simulations. b) Total energy obtained after a structure relaxation depending on the distance between a hydrogen atom of a hydroperoxide on a tertiary site and an oxygen atom of a hydroxyl radical w/ or wo/ distance constraints. c) Results from an MD trajectory at 300K. The starting distance is 3.2 Bohr. d) The same MD simulation but starting from a larger distance D4 (4.7 Bohr) where the reaction does not take place during the structural relaxation. e) Total energy vs time corresponding to panel (d).

D.3 . Formation of alkoxy radicals

Investigating the formation of alkoxy radicals is important to study the degradation of PE because alkoxy radicals can branch out into many oxidative reactions. In particular, reaction 4.1b (Fig.4.4) shows sufficiently low barriers for the formation of alkoxy radicals (see also chapter 4.1.2). Starting configurations of H1 and H2 positions in Fig.4.8 are studied by CPMD simulations at 300K (Fig.D.4). The reaction takes place from both positions at the given temperature. However, the oxygen molecule of the final product does not diffuse to vacuum space or rotate over several picoseconds and retains a certain distance with the alkoxy radicals. Besides, in Fig.D.4b, the oxygen molecule is dissociated for approximately 2 ps between 8 and 10 ps, which is not observed at higher temperature (360K). This could come from the barrier of the backward reaction, which is 0.27 eV, corresponding to a much longer average waiting time. The role of entropic effects could be considered, but much larger statistics should be accumulated to estimate a free energy barrier for this reaction.

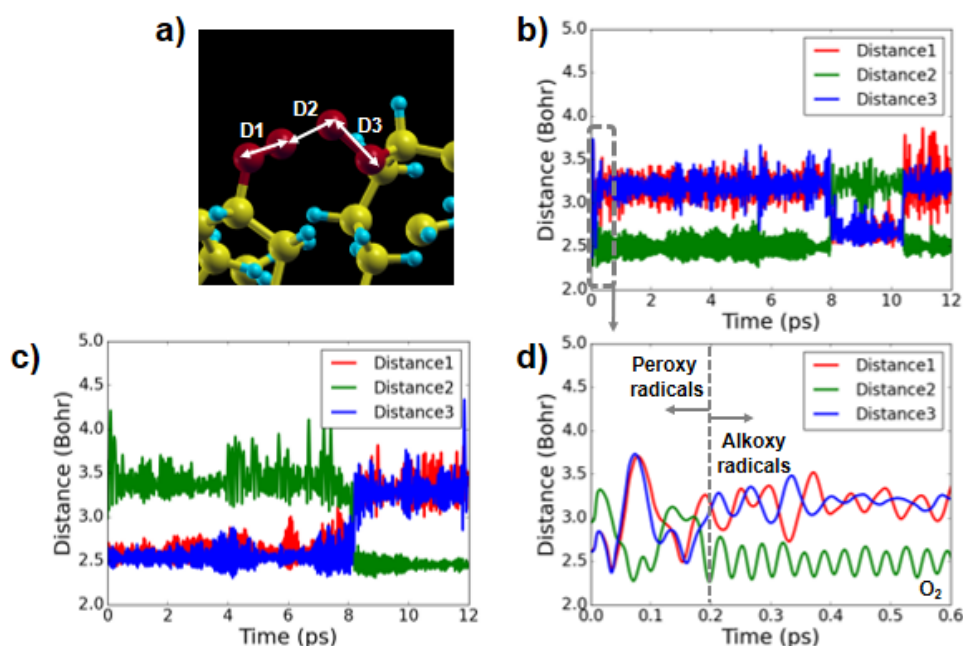


Figure D.4 – Reaction 4.4 ($2\text{POO}^\circ \rightarrow 2\text{PO}^\circ + \text{O}_2$): a) atomic distances monitored during MD simulations, b) MD results at 300K, starting from position H1 and c) MD results at 300K starting from position H2. d) a zoom on the first few ps of panel b).

D.4 . From alkoxy radicals: crosslinking from different starting configurations

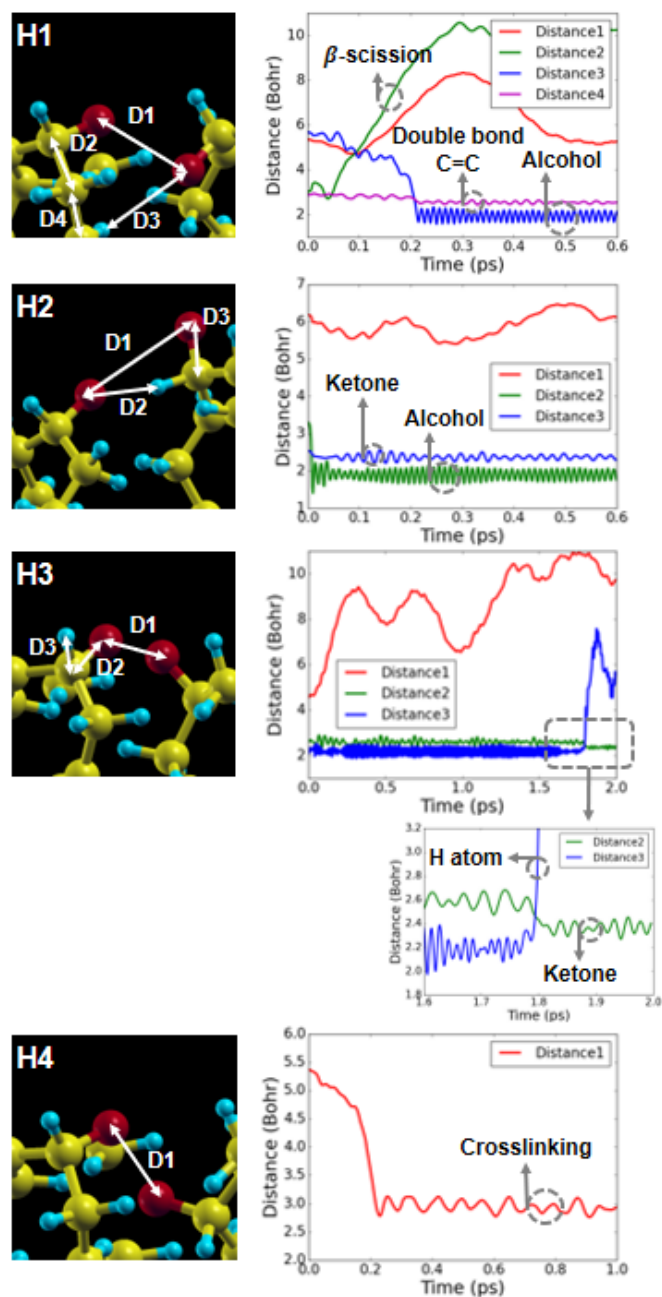


Figure D.5 – MD simulations of crosslinking from different starting configurations of two alkoxy radicals (see Reaction 4.3c and Fig.4.8).

Table D.1 – Comparison between NEB and MD calculations for reactions from two alkoxy radicals on the surface of a lamella.

Position	NEB (Final product: E_A)	MD (Final product at 300K)
H1	- Crosslinking: 0.0 eV - β -scission: 0.25 eV - Ketone&alcohol: not converged	β -scission (aldehyde), alcohol, and double bond
H2	- Crosslinking: 0.38 eV - β -scission: 0.34 eV - Ketone&alcohol: 0.0 eV	Ketone and alcohol
H3	- Crosslinking: 0.16 eV - β -scission: 0.27 eV - Ketone&alcohol: steric hindered	alkoxy radical, ketone, and hydrogen atom
H4	- Crosslinking: 0.0 eV - β -scission: not converged - Ketone&alcohol: steric hindered	crosslinking

After the formation of alkoxy radicals from two peroxy radicals, I assumed that the oxygen molecule had diffused away and, without it, I relaxed once more the structures H1 to H4 (Fig.4.8). From these structures, the activation energies of crosslinking, chain scission, and formation of ketones and/or alcohols were calculated by NEB calculations in chapter 4. The details of the four surface configurations do affect the activation energy, making them more or less likely with respect to alternative reactions. Therefore, based on each starting configuration from H1 to H4, CPMD simulations were performed, and the final products were compared with the results of NEB calculations (see Figure D.5 and Table D.1). While reactions starting from H2 and H4 produce the expected products corresponding to the calculated activation energies by NEB, H1 and H3 show quite different oxidation products. In the case of H1 position, crosslinking reaction is expected based on NEB calculations, but the final products obtained by CPMD are a double bond ($-C=C-$), an alcohol, and aldehyde (chain scission). While we did not spot any plausible reactions starting from H3 position based on our calculated activation energy, the final products by CPMD calculations are an alkoxy radical, a ketone, and a hydrogen atom, a final state that we had not considered in our NEB calculations. These differences could also come from entropic contributions, which requires further studies, but at least they imply that the oxidative reactions

can be quite complex also because of the dependence on the local environment and specific starting positions even at room temperature. Besides, as all these reactions follow from the encounter of two peroxy radicals, deactivating them or their following products (alkoxy radicals) by antioxidants can prevent, or delay, PE degradation.

Bibliography

- [1] Guido Roma, Fabien Bruneval, and Layla Martin-Samos. Optical properties of saturated and unsaturated carbonyl defects in polyethylene. *The Journal of Physical Chemistry B*, 122(6):2023–2030, 2018.
(Cited on pages 48 and 113)
- [2] Charles W Bunn. The crystal structure of long-chain normal paraffin hydrocarbons. the “shape” of the CH_2 group. *Transactions of the Faraday Society*, 35:482–491, 1939.
(Cited on page 113)
- [3] PW Teare. The crystal structure of orthorhombic hexatriacontane, $\text{C}_{36}\text{H}_{74}$. *Acta Crystallographica*, 12(4):294–300, 1959.
(Cited on page 113)
- [4] S Kavesh and JM Schultz. Lamellar and interlamellar structure in melt-crystallized polyethylene. i. degree of crystallinity, atomic positions, particle size, and lattice disorder of the first and second kinds. *Journal of Polymer Science Part A-2: Polymer Physics*, 8(2):243–276, 1970.
(Cited on page 113)
- [5] G Avitabile, R Napolitano, B Pirozzi, KD Rouse, MW Thomas, and BTM Willis. Low temperature crystal structure of polyethylene: results from a neutron diffraction study and from potential energy calculations. *Journal of Polymer Science: Polymer Letters Edition*, 13(6):351–355, 1975.
(Cited on page 113)
- [6] Jesper Kleis, Bengt I Lundqvist, David C Langreth, and Elsebeth Schröder. Towards a working density-functional theory for polymers: First-principles determination of the polyethylene crystal structure. *Physical Review B*, 76(10):100201, 2007.
(Cited on page 113)
- [7] Kristian Berland, Valentino R Cooper, Kyuho Lee, Elsebeth Schröder, T Thonhauser, Per Hyldgaard, and Bengt I Lundqvist. van der waals forces in density functional theory: a review of the vdw-df method. *Reports on Progress in Physics*, 78(6):066501, 2015.
(Cited on pages 39 and 113)
- [8] Hongyi Zhou and GL Wilkes. Comparison of lamellar thickness and its distribution determined from dsc, saxs, tem and afm for high-density polyethylene films having a stacked lamellar morphology. *Polymer*, 38(23):5735–5747, 1997.
(Cited on pages 78 and 114)

- [9] RC Savage, N Mullin, and JK Hobbs. Molecular conformation at the crystal–amorphous interface in polyethylene. *Macromolecules*, 48(17):6160–6165, 2015.
(Cited on pages 78, 114, and 117)
- [10] Alan S Michaels and Harris J Bixler. Flow of gases through polyethylene. *Journal of Polymer Science*, 50(154):413–439, 1961.
(Cited on pages 81 and 117)
- [11] Yunho Ahn, Xavier Colin, and Guido Roma. Atomic scale mechanisms controlling the oxidation of polyethylene: A first principles study. *Polymers*, 13(13):2143, 2021.
(Cited on pages 63, 77, 78, and 117)
- [12] Angelo Bongiorno and Alfredo Pasquarello. Oxygen diffusion through the disordered oxide network during silicon oxidation. *Physical review letters*, 88(12):125901, 2002.
(Cited on page 117)
- [13] Shigetaka Shimada, Yasurō Hori, and Hisatsugu Kashiwabara. Free radicals trapped in polyethylene matrix: 2. decay in single crystals and diffusion. *Polymer*, 18(1):25–31, 1977.
(Cited on page 120)
- [14] S Shimada, Y Hori, and H Kashiwabara. Relation between diffusion controlled decay of radicals and α -relaxation in polyethylene and polyoxymethylene. *Polymer*, 22(10):1377–1384, 1981.
(Cited on page 120)
- [15] Lies De Keer, Paul Van Steenberge, Marie-Françoise Reyniers, Ganna Gryn’Ova, Heather M Aitken, and Michelle L Coote. New mechanism for autoxidation of polyolefins: kinetic monte carlo modelling of the role of short-chain branches, molecular oxygen and unsaturated moieties. *Polymer Chemistry*, 13(22):3304–3314, 2022.
(Cited on pages 11, 78, 81, and 135)